THESIS

The Use of an Integrated Optimization Framework for Optimizing Noise and Fuel

by

Y. Tigchelaar

to obtain the degree of

Master of Science
in Aerospace Engineering

at the Delft University of Technology,
to be defended publicly on July 12th, 2019 at 14:30.

Student number: 1507931
Project duration: September 27, 2018 - July 12, 2019

Thesis committee:

Prof. dr. R. Curran,	TU Delft, ATO
Dr.ir. S. Hartjes,	TU Delft, ATO, supervisor
V. Ho-Huu, MSc,	TU Delft, ATO, supervisor
Ir. J. Sinke,	TU Delft, AMT

An electronic version of this thesis is available at `http://repository.tudelft.nl/`.

TU Delft Delft University of Technology

Abstract

Travelling by air has become commonplace, and more and more people can afford themselves to fly. In twelve years time, the amount of people that were carried by airlines doubled to four billion passengers in 2017. At Amsterdam Airport Schiphol, the main gateway into the Netherlands and also a large hub for connecting flights, saw a growth of 20 million passengers in four years time. The rise in air travel also has its downsides. Not only the boundaries of airport and airspace capacity are run into, noise annoyance and pollution caused by aircraft are also everyday's business. The growth in aviation and population will inevitably lead to conflicts.

Several strategies have been proposed in literature and by legislators to address this conflict. Advanced aerodynamics, aircraft engines and alternative fuels can be considered as long term solutions for this, but changing operational procedures of aircraft and airport is considered as a good solution in terms of costs and time-wise. Most research on changing operational procedures has shown significant results, however only consider a single operation while these are of influence on one another. The integration of several operational procedures into a single problem has been recognized as one of the future research topics.

In this research an integrated optimization framework is proposed that can simultaneously optimize aircraft and airport operations by allocating routes, flight procedures and runways. The framework is able to handle fuel usage, noise annoyance and capacity. Amsterdam Airport Schiphol will be used as case study airport, and a real flight departure schedule is used as reference. The framework consists of two main steps. In the first step, flights are groups according to their aircraft type, destination and departure time, and are subsequently distributed over the available runways, routes and departure procedures. This distribution is performed with a NSGA-II-II algorithm that is capable of handling non-linear, multi-objective optimization problems. In the second step, the flight distribution is apportioned over the flights in the schedule, while adhering the separation requirements. In this way it is verified if the required capacity is available, by adhering the separation at departure, a possible crossing point and the terminal point between consecutive flights. The second step is implemented with a ILP algorithm.

Results from the case study has shown that significant gains can be obtained in terms of noise annoyance. While requiring little extra fuel, up to 4%, the noise annoyance can be lowered with 31%. Not much variance is possible for flights that operate during the night hours, and so all gains are obtained on flights in the daytime. Especially the amount of people that are highly annoyed can be lowered of up to almost 50%. A further analysis of the noise contours shows that the framework

is able to shift noise in such a way that the noise levels drop below the threshold values of the noise equivalence criteria. In other words, the noise contours can decrease in size and with that the amount of people annoyed is lowered. These results are obtained by shifting flights from runway 18L to runway 24, which is more noise friendly, and by using NADP2 more frequently compared to NADP1. The model is also able to make a distinction between destinations and aircraft type, and puts heavy aircraft more frequently on shorter flight legs in order to minimize the fuel usage and the exposure to noise of residents. An examination of the entire solution set in terms of the separation requirements indicates that most of the found results are feasible. By shifting more flights to a single runway, the required capacity is at stake and adding extra flights with delay will cause an exponential growth in total required delay.

Using the integrated optimization framework leverages the potential of aircraft specific capabilities by allocating the right runway, route and procedure to each flight in such a way that an optimum noise contour is formed. Most gains can be obtained for the number of people annoyed and disturbed, and as these noise equivalence criteria are directly related to the well-being of residents around the airport and their opinion on the operation of the airport, this can only be considered as beneficial. The available capacity of a runway is deployed to alleviate noise annoyance by residents.

The framework proposed in this research can be improved at several components in future research. The addition of arrivals, extra routes and procedures would extend the applicability and value of the framework. Another improvement that can be made is the incorporation of the second step into the first step. This would eliminate infeasible solutions inside the solution set.

Preface

Luctor et Emergo

With this report, I will finalize my thesis project and this will also form the end of my time at Delft University of Technology. This thesis completes the final requirement for the degree of Master of Science in Aerospace Engineering. It has been a very long ride, during which I have been challenged with all the different courses and projects in both the Bachelor and the Master. However, the biggest challenge was something different and the ride was not only long, but bumpy as well. I have seen bad times in the last couple of years, but I managed to raise myself up and finally finish my education. I have the hope that finalizing my time at Delft University of Technology gives me the strength to keep myself up and to grow even further.

I could not have completed my time in Delft without the help of others. First of all, I would like to thank the team that supervised me during my thesis project. Sander, thank you for your time and effort, and for pushing me to dive into the matter even deeper. Furthermore, thank you for your patience given the aforementioned; your understanding of my situation helped me pull through. Vinh, I would also like to thank you for your time and effort. You helped me a lot with the direction of my research and also with the implementation of the model.

Furthermore, I would like to thank my parents for their unconditional support during my entire time in Delft. It is because of you that I was able to do what I did. I would also like to thank my friends from my rowing crew and my board. We had great times in Delft, and I could not have done it without. A special thanks to Jeroen, who helped me with my study a lot and was also there for me in bad times. I would also like to thank my fellow students of room 3.15 for the fun during the time of my thesis project.

Lastly, but most of all, I would like to thank my girlfriend Yorinde for her support, understanding, believe and motivation. You kept pushing me to continue, and you also had the believe in my abilities. Without you, I could not have finished my education in the way I did, for which I'll remain grateful forever.

Yvo Tigchelaar
Delft, June 2019

Contents

List of Figures

List of Tables

List of Acronyms

3D	3-Dimensional	4
4D	4-Dimensional	22, 23, 27, 30
AAS	Amsterdam Airport Schiphol	xi, 11–14
APP	Approach Control Center	4, 9
ATC	Air Traffic Control	4, 35, 66, 70, 71
ATD	Actual Time of Departure	31, 48, 61
BADA	Base of Aircraft Data	27
BILP	Binary Integer Linear Programming	19
CBS	Centraal Bureau voor de Statistiek	23, 28
CDA	Continuous Descent Approach	14
CTA	Control Area	4, 5
CTR	Control Zone	4
DE	Differential Evolutionary	19, 21
DME	Distance Measuring Equipment	4, 5
GA	Genetic Algorithm	19, 21, 34, 36
GIS	Geographic Information System	23, 63
GNSS	Global Navigation Satellite System	4
GPS	Global Positioning System	4
IAF	Initial Approach Fix	9
ICAO	International Civil Aviation Organization	3, 6, 10, 11
IFR	Instrument Flight Rules	3–5, 9
ILP	Integer Linear Programming	iii, 19, 21, 23, 69
ILS	Instrument Landing System	5
INM	Integrated Noise Model	14, 26
LVNL	Air Traffic Control the Netherlands	11

MRS	Minimum Radar Separation	6
MTOW	Maximum Take-off Weight	6, 15
NADP	Noise Abatement Departure Procedure	iv, ix, 11, 13, 25, 26, 35, 46, 51, 58, 59, 66, 67
NOMOS	Noise Monitoring System	14
NSGA-II	Non-Dominated Sorting Genetic Algorithm II	iii, ix, 2, 17, 18, 21, 23, 32, 34, 36, 38, 39, 41, 42, 46, 47, 51, 64, 69
PHA	People Heavily Annoyed	29
PSD	People Sleep Disturbed	29
RECAT-EU	European Wake Vortex Re-categorisation	xi, 6
RF	Radius-to-a-Fix	5, 26
RHC	Receding Horizon Control	33, 34
RNAV	Area Navigation	ix, 4, 5, 26
SEL	Sound Exposure Level	14, 24, 27
SER	Sound Exposure Ratio	27
SID	Standard Instrument Departure	ix, 9, 11, 14, 24–27, 32, 35, 48, 51, 58, 66, 71
TF	Track-to-a-Fix	5, 26
TMA	Terminal Maneuvering Area	4, 5
TWR	Airport Traffic Control Tower	4
UDP	Uniform Daylight Period	12
UTA	Upper Control Area	4
VOR	Very High Frequency (VHF) Omni-Directional Range	4, 5

Chapter 1

Introduction

The world has seen a drastic change in the last decades. It is not only possible to contact another person at the other side of the globe in matter of seconds due to digitization, travelling by air all over the globe has become commonplace while more and more people can afford themselfves to fly. Almost four billion passengers were carried by airlines in 2017, while in 2005 this number was slightly under two billion [Worldbank, 2017]. This growth rate is also foreseen for the near future. Not only is the airspace getting more and more congested, large hub airport such as Amsterdam Airport Schiphol see a massive growth in recent years. While in 2015 around 51 million passengers travelled via the airport, this amount has grown to 71 million passengers in 2018 [CBS, 2018]. To process these numbers of passengers, the available capacity in terms of infrastructure and slots is deployed at its maximum.

The last decades also saw an increase in population density. Cities are growing and uninhabited areas are getting urbanized, with the consequence that airports and cities are growing closer together. With the digital age in mind, people are getting more aware of negative environmental effects of aviation, such as noise annoyance and pollution. The growth of aviation and population will inevitably lead to conflicts. To cope with the negative effects of aviation growth, while also addressing the impact on the environment and near-airport residents, several strategies have been proposed. New regulations can be implemented, advanced aircraft engines, aerodynamics and alternative fuels can be developed and operational procedures can be changed. While the first options are costly and their benefits will only have effect on the long term, changing operational procedures of aircraft and airports seems as a good option both time-wise and in terms of costs. (Marais et al. [2013])

Research on improving operational procedures, such as new departure and arrival routes and optimized runway sequencing and allocation, have shown significant results. However, most existing research only considers a single operation, while they are part of a bigger picture and are of influence on one another. The integration of different operational procedures into one problem has been recognized but increasing complexity and computation time has resulted that research until now is scarce. Zachary et al. [2010, 2011] came up with an example how to combine several operational

procedures into one problem. Their objective was to solve for the best combination of operations to minimize the environmental impact. Although good results were found, still improvements could be made such as the use of new departure and arrival routes, multiple aircraft types and different procedures for those aircraft and the application to a larger airport with more runways and airlines.

The implicit potential of integrally optimizing runway, route and flight procedure allocation led to the start of this research. An integrated optimization framework is proposed that can simultaneously optimize aircraft and airport operations by allocating routes, flight procedures and runways to each flight in the schedule. Given the limited time window of this research, and the fact that departures are responsible for most fuel usage and noise annoyance compared to arrivals, this research only considers aircraft departing from the airport. A reference flight schedule of October 22, 2010 will be used to perform a case study on Amsterdam Airport Schiphol to show the potential of the integrated optimization framework. This particular day is suitable as reference since the runway combination used on this day is one of the most used at the airport. Around 600 flights departed, which means this specific day is an average day of operation at Schiphol. The framework will make use of the two internationally prescribed departure procedures, and the officially published Standard Instrument Departures out of the two runways that will be examined. After a literature review the non-linear, multi-objective Non-Dominated Sorting Genetic Algorithm II algorithm has been found suitable for the proposed optimization framework. This algorithm will be assisted by a Integer Linear Programming algorithm to check if the required capacity is available to perform the found flight distribution of runways, departure routes and flight procedures.

The main research question that will be answered at the end of this research in the conclusion is defined as:

What are the benefits of using a combinatorial optimization of airport and airspace operations in terms of noise annoyance, fuel usage and capacity?

This report elaborates on the research performed and is structured as follows. In this chapter the objective of the research was introduced. Chapter 2 presents all the required background information in order to form a complete view of the subject. The chapter elaborates on both safety and operational constraints of Amsterdam Airport Schiphol and also introduces the algorithms that are used in the optimization framework. The reference flight schedule that will be used in the optimization is also introduced in this chapter. With the description of the context of the research, the implementation of the proposed optimization framework is shown in Chapter 3. It explains the structure of the framework and elaborates on the data and calculations required. Chapter 4 presents all output and results of the optimization process. Two test cases will be performed that will be used for validation and verification purposes. The first test case consists of all flights to a single waypoint, while the second test case takes a look at one of the departure peaks at the airport. The actual case study comprises the entire day of departures at Amsterdam Airport Schiphol. In Chapter 5 the validation and verification of the model is performed and the results of the optimization process will be discussed. Finally, the conclusions of this research are drawn in Chapter 6, limitations of this research are indicated and recommendations for future research are stated.

Chapter 2

Background Information

In order to answer the research question, a complete view of the situation has to be formed. This chapter introduces several subjects that are required for this research and are required to understand the matter. In the first section the design and usage of the airspace will be discussed, followed by an extensive elaboration of information regarding Amsterdam Schiphol Airport in the subsequent section. This elaboration is not only done as Schiphol is used as the case study of this research, it is also used to better understand and visualize some of the information on airspace layout, routes, take-off procedures and regulations. The third and last section goes into the matter of a number of optimization algorithms which will be used in the optimization process. The information provided in this chapter will mainly be referred to later on in Chapter 3 in which the methodology will be explained.

2.1 Airspace Design and Usage

To assure safe operations, the airspace is designed and used in a specific way. (Inter)national regulations are in place to assure the high safety level which takes the technical boundaries of aircraft, surveillance and navigation systems into account. The following subsections elaborate on the design of the airspace, the creation of trajectories and separation requirements for aircraft.

2.1.1 Airspace

The airspace can be described as the area above the earth surface in which air traffic can take place. Each country can arrange their airspace based on their own needs. For this, the International Civil Aviation Organization (ICAO) classified seven categories of airspace that can either consist of controlled, uncontrolled, special use airspace or a combination of those. Controlled airspace is based on Instrument Flight Rules (IFR), where the pilots rely on their instruments in the cockpit

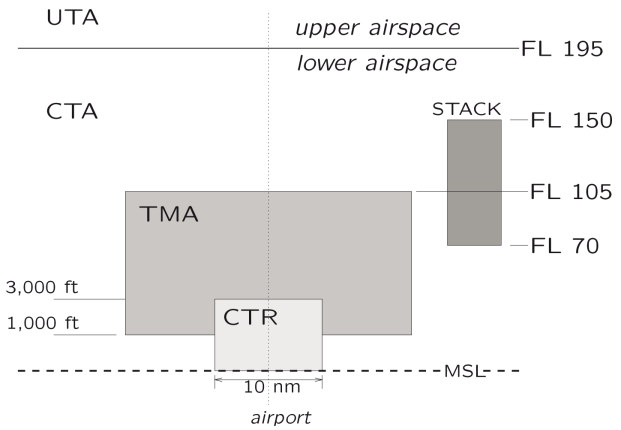

Figure 2.1: Airspace segments [Borst, 2014].

and the responsibility for separation between aircraft lies in the hand of the Air Traffic Control (ATC) controller. Almost all commercial air transport is conducted under IFR and is therefore controlled by ATC.

Figure 2.1 shows a cross section of airspace segments above and around an airport. It indicates the responsibility areas for ATC, where the tasks for the controllers vary over the different areas. For example, the air traffic controllers in the Airport Traffic Control Tower (TWR) are responsible for the control of the ground traffic at the airport and take-off and landing aircraft within the Control Zone (CTR), which is a circular area around the airport and up to 3000 feet above ground level. The Terminal Maneuvering Area (TMA) is the area that forms the connection between the CTR and the Control Area (CTA). An aircraft starts its descent or continues its take-off in this area, where the ATC responsibility is allocated to the Approach Control Center (APP). The Upper Control Area (UTA) or also called upper airspace, holds the en-route traffic.

This research only considers aircraft operations executed inside controlled airspace, in the vicinity of the airport. These operations are executed in the CTR and TMA zones.

2.1.2 Trajectories

In order to reach its destination, an aircraft will fly a certain trajectory. Traditionally these routes are established from VOR or DME to the next beacon. With the emergence of Global Navigation Satellite System (GNSS), such as GPS and later GLONASS and GALILEO, new methods of navigation are established.

Where airways and procedures formerly were generally based on the use of ground-based navigation beacons, Area Navigation (RNAV) enables the use of airways that are not based on these. In other words, it allows aircraft to fly along any track while circumventing the need to fly directly over those ground-based facilities. However, it certainly can make use of ground-based navigation aids, besides self-contained navigation aids and also a combination of those two. This results in a 3D position fix

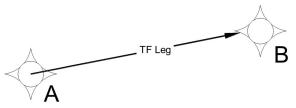

(a) Track-to-a-Fix (TF) leg

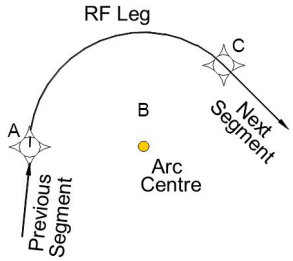

(b) Radius-to-a-Fix (RF) leg

Figure 2.2: Area Navigation (RNAV) legs

that is a much more accurate way of determining the aircraft's location, and with the utilization of new airways the available airspace can be used more efficiently. In the terminal airspace, RNAV can be used to fly new routes bypassing residential areas much more stringent that were previously not possible. RNAV routes consist of fly-by waypoints, that can either be a VOR or DME beacon or an in upfront determined latitude/longitude coordinate, connected by Track-to-a-Fix (TF) legs and Radius-to-a-Fix (RF) turns. Both are shown in schematic form in Figure 2.2.

2.1.3 Separation

An air traffic controller's most important responsibility is ensuring the safety of the aircraft flying through its sector. To ensure this, standard horizontal or vertical separation minima to keep aircraft apart are present. Usually a minimal vertical separation of 1000 feet between two aircraft is applicable under IFR, while the standard horizontal separation is five nautical miles but can vary depending on, among others, the aircraft position, type and speed. Figure 2.3 shows a visual representation of these 'separation blocks' that are formed around an aircraft. Flights are navigated in such a way that these blocks never have any overlay. In other words, if the vertical separation criterion is not met, the horizontal separation needs to be in place, or vice versa. The standard separation is shown in the block on the right side of the figure, that is applicable in the CTA. The lateral separation in the TMA is even reduced to three nautical miles (as shown in the left block in the figure), and when two aircraft perform a simultaneous parallel approach they can be closer together even more. This is only permitted while these aircraft are on their designated approach path and make use of the Instrument Landing System (ILS).

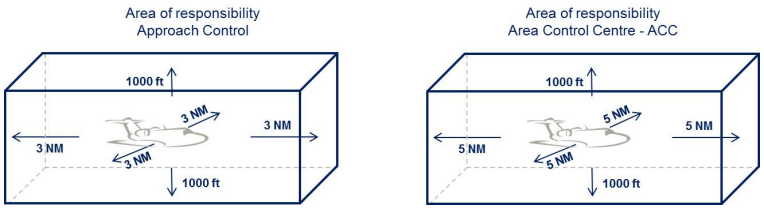

Figure 2.3: Aircraft separation [LVNL, 2019].

An important factor in determining the minimum separation distance is based on wake vortices. These vortices start at an aircraft's wingtips, and are actually two counter-rotating air masses. The difference in pressure of the upper and lower wing surface creates a roll of the air which size is depended on the size and weight of the aircraft. It can form a potential hazard towards successive aircraft as it hits the wing surface of that aircraft. The vortex keeps hanging in the air where it slowly dissolves, and therefore a certain amount of separation has to be taken into account to allow safe operations. As the size of the vortex depends on the size of the aircraft, also the amount of separation required depends on aircraft size. ICAO previously categorized all aircraft in the categories Heavy, Medium or Light. While these rules are safe, they can lead to over-conservative separation in many instances as the weight specification of each category is too broad. Besides, the impact of wake vortices is not only related to the Maximum Take-off Weight (MTOW) but also to the wingspan of the aircraft. Eurocontrol came up with a new categorization called RECAT-EU that is shown in Table 2.1 (Eurocontrol [2015]). The consequential distance-based separation minima for departure and arrivals are presented in Table 2.2. Values between brackets indicate the Minimum Radar Separation (MRS) of 2.5nm in the terminal area. Time-based separation minima on departures are presented in Table 2.3, with a MRS of 60s.

Table 2.1: RECAT-EU Wake Turbulence Categories (Eurocontrol [2015]).

Identifier	**Category**	**MTOW [kg x 1,000]**	**Wingspan [m]**	**Example aircraft**
A	Super Heavy	MTOW $\geq$ 100	$72 < b < 80$	A388, A124
B	Upper Heavy	MTOW $\geq$ 100	$60 < b < 72$	A332, B744
C	Lower Heavy	MTOW $\geq$ 100	$b < 52$	MD11, B763
D	Upper Medium	$15 <$ MTOW < 100	$b > 32$	B738, A320
E	Lower Medium	$15 <$ MTOW < 100	$b < 32$	E190, F70
F	Light	MTOW ≤ 15	-	LJ35, C650

Table 2.2: Distance-based separation minima for departures and arrivals. Values in [nm]. ((*)=2.5nm). (Eurocontrol [2015])

	Follower					
Leader	A	B	C	D	E	F
A	3	4	5	5	6	8
B	(*)	3	4	4	5	7
C	(*)	(*)	3	3	4	6
D	(*)	(*)	(*)	(*)	(*)	5
E	(*)	(*)	(*)	(*)	(*)	4
F	(*)	(*)	(*)	(*)	(*)	3

Table 2.3: Time-based separation minima for departures. Values in [s]. ((*)=60s). (Eurocontrol [2015])

	Follower					
Leader	A	B	C	D	E	F
A	(*)	100	120	140	160	180
B	(*)	(*)	(*)	100	120	140
C	(*)	(*)	(*)	80	100	120
D	(*)	(*)	(*)	(*)	(*)	120
E	(*)	(*)	(*)	(*)	(*)	100
F	(*)	(*)	(*)	(*)	(*)	80

2.2 Amsterdam Airport Schiphol

To understand the operations at Amsterdam Airport Schiphol, this section provides background information on the airport. This information is required as the optimization framework that will be proposed in this research is applied on this airport with a case study. The first subsection explains the layout of the airport, after which the process of departures at the airport is elaborated upon in the next subsection. The last subsection gives an overview of noise abatement measures that are currently in place at Schiphol.

2.2.1 Airport Layout and Location

This subsection elaborates on the location of the airport, its layout and how the layout holds with respect to its surroundings. Amsterdam Airport Schiphol is located southwest of the capital Amsterdam of the Netherlands, in the municipality Haarlemmermeer. Since the airport was founded a century ago it has grown to the international hub the airport is nowadays. Not only the airport itself grew in size, also the cities around Schiphol emerged and grew. In the direct proximity of the airport several large cities are found: Amsterdam (North-East), Amstelveen (East), Haarlem (North-West), Hoofddorp (West) and a bit further away Leiden (South-West).

An overview of all runways of Amsterdam Airport Schiphol is presented in Table 2.4 and visualized in Figure 2.4. Each of these six runways received a for this airport unique designation in order to differentiate between them. This designation is based on its orientation with respect to the magnetic north. Since three runways have the same orientation they received an extra letter to distinguish them.

The shortest runway, the 'Oostbaan', is too short to handle most of the commercial traffic Schiphol receives and is therefore mainly used for General Aviation movements. The 'Polderbaan' is the newest addition to the runway system of Schiphol, and was mainly built to alleviate noise originating from operations at the other runways. However, this runway can only be used towards or coming from the North as the city of Hoofddorp is located to the South. The same holds for 'Aalsmeerbaan' which can only be used towards or coming from the South given the proximity of the city of

Table 2.4: Runways at Amsterdam Airport Schiphol

Runway Name	**Designation**	**Dimensions [m]**
Oostbaan	04/22	2020x45
Kaagbaan	06/24	3439x45
Buitenveldertbaan	09/27	3453x45
Zwanenburgbaan	18C/36C	3300x45
Aalsmeerbaan	18L/36R	3400x45
Polderbaan	18R/36L	3800x60

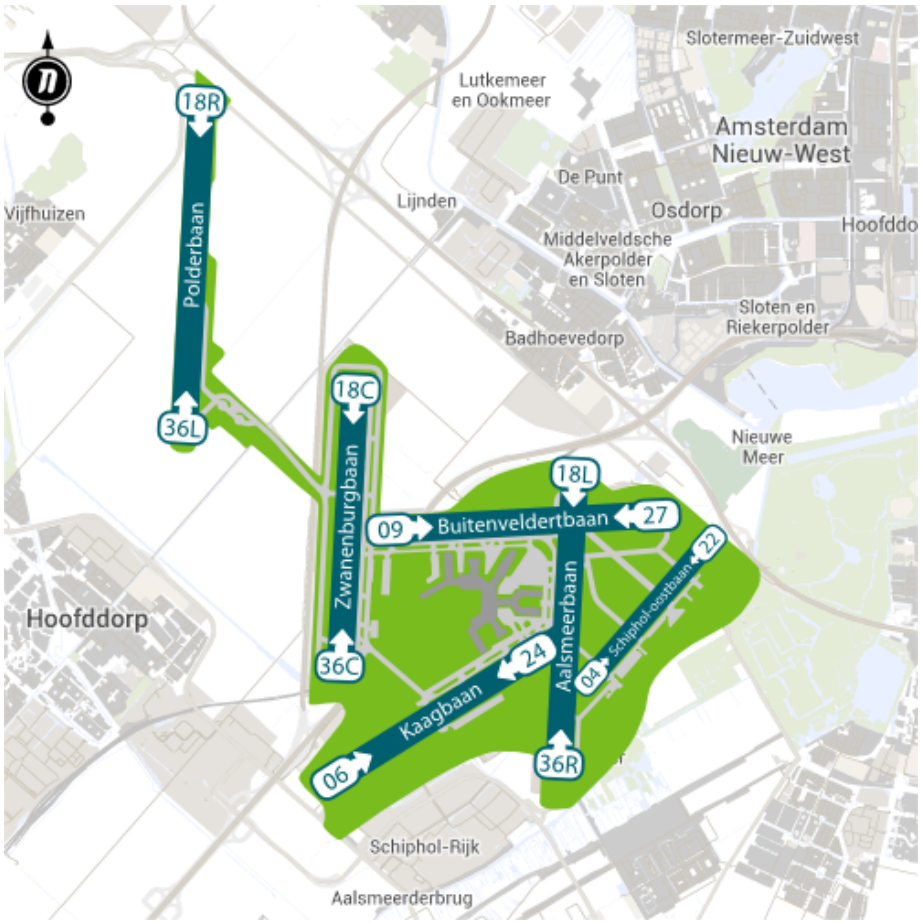

Figure 2.4: Runway layout Amsterdam Airport Schiphol [Schiphol, 2019].

Amsterdam in the North. With the configuration of the airport with crossing runways and due the fact that aircraft are required to depart and land as much as possible against the direction where the wind is coming from, not all runways are in use at the same time. Section 2.2.3 elaborates more on the preferential runway usage at Amsterdam Airport Schiphol.

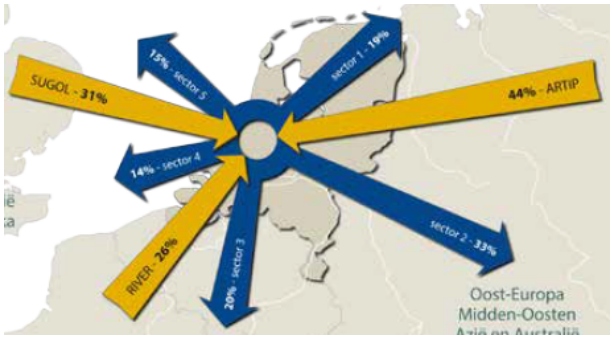

Figure 2.5: Schiphol sectors and holding stacks [Schiphol, 2014].

2.2.2 Operations

This subsection explains the (departure) operations at Amsterdam Airport Schiphol. First an overview of the flights at Schiphol will be given, after which specific routes and procedures will be elaborated upon.

In Figure 2.5 the outbound and inbound flows of Schiphol are presented. These two flows are separated already from a large distance of the airport in order to avoid any collision danger and to maintain overview of all flights. Inbound traffic is directed from the en-route airspace towards an Initial Approach Fix (IAF), and in the case of Schiphol, there are three of such locations: ARTIP, SUGOL and RIVER. At these locations a holding stack is present (see also Figure 2.1), where flights have to loiter in case the runway is occupied. Outbound traffic departs from the runway and is directed to one of the five outbound sectors dependent on their final destination, indicated in blue in Figure 2.5. This research only focuses on departures rather than arrivals, as these cause the most noise annoyance and require more fuel, whereby greater benefits can be obtained. The following part of this section therefore only includes departure operations.

For each runway at least one Standard Instrument Departure (SID) towards these sectors is established. A SID is an officially published IFR procedure for the transition between the terminal and the en-route airspace. They are established to simplify the clearance delivery by the APP controller, noise abatement, separation of incoming and outgoing air traffic and obstacle and terrain clearance. Which specific SID is assigned to the aircraft depends on the destination of the aircraft as well as what other runways and SIDs are in use to prevent interference with other aircraft.

An example of a SID can be found in Appendix A, and as can be seen is defined as a ground track of a trajectory in the horizontal plane from the runway towards a departure fix. At certain intermediate points along the SID-path, the expected altitude of the aircraft is defined. These

intermediate points are waypoints, and are used to indicate a change in direction, speed, or altitude along the desired path. The expected altitude at such a point can be a minimum, a maximum or exact altitude the aircraft has to comply with at that specific location. A departure procedure is the vertical component of the departure trajectory, and prescribes guidelines for the thrust and climb rate in order to reach a certain altitude on time. Although different aircraft make use of the same departure procedure, differences exist in the vertical profile due to differences in atmospheric conditions, aircraft type and take-off weight. The next subsection elaborates more on the departure procedures and runway usage for departures.

2.2.3 Noise Abatement

The communities in the vicinity of airports suffer from the noise implied by operating aircraft. This noise causes annoyance, can result in health problems both physically and mentally and has an impact on the value of property. It is therefore important to mitigate noise as much as possible. This subsection examines possible noise abatement measures and elaborates on the steps taken at Amsterdam Airport Schiphol and what those measures entail for the day-to-day operation.

Earlier policies on noise mitigation focused on solely reducing noise at the source. Growth in commercial air traffic urged the global community to find more ways to alleviate the nuisance of aircraft noise. The International Civil Aviation Organization (ICAO) defined a balanced approach to aircraft noise management that consists of four elements: [ICAO, 2018]

1. Reduction of noise at source
2. Land-use planning and management
3. Noise abatement operational procedures
4. Operating restrictions

Reduction of Noise at Source

This element considers the reduction of noise originated from the aircraft itself. It involves optimization of both engines and airframe and legislation is in place to ensure that the latest available noise reduction technology is applied on the aircraft. For example, it is not allowed in the Netherlands to operate noisy aircraft of the ‘Chapter 2’-category, as these aircraft would entail too much annoyance.

Land-Use Planning and Management

The main goal of the second element is to minimize the people affected by aircraft noise by introducing land-use zoning around the airport. It is also used to ensure that gains achieved by the

reduction of noise due to the latest technology (element 1) are not offset by further (residential) developments. An example that also falls under this element was the construction of the 'Polderbaan' at Schiphol, which was not only needed for extra capacity but was also built to alleviate noise at other areas in the vicinity of the airport.

Noise Abatement Operational Procedures

Operational procedures for noise abatement include procedures for take-off and landing and a preferential use of certain runways and air routes. At Amsterdam Airport Schiphol for example a stringent preference list of the runways usage exists, as presented in Table 2.5. Runway usage is based on the weather conditions and the required capacity on that time of the day, where preference is given to runways that avoid noise sensitive (residential) areas. Night time operations are heavily bounded and only specific airways and runways are allowed to be used. Table 2.6 shows the preference list for night time operations. The combination of preferred runways is composed based on agreements made by the *Alderstafel Schiphol*, named after chairman Hans Alders, which is a jointly attempt of all different stakeholders such as the Dutch government, Schiphol Group, Air Traffic Control the Netherlands (LVNL) and local residents to collaborate on the use and development of Amsterdam Airport Schiphol.

As already mentioned in the previous subsection, one of the benefits of using SIDs is that it can mitigate noise exposure to citizens. SIDs provide a ground track that avoids highly populated areas. With this, they form the horizontal component of a departure trajectory. The vertical component of these trajectories are established as a departure procedure.

In the departure phase of a flight, an aircraft accelerates and climbs out from the runway towards the cruise phase. To achieve this acceleration the engines of the aircraft are in a high thrust setting. This high thrust setting comes with a lot of noise, which results in annoyance among residents living around the airport. Since aircraft in the departure phase actually cause the most annoyance among residents, also a lot of research is put into the development of noise mitigating departure procedures. In ICAO [2006] two commonly used Noise Abatement Departure Procedures NADP are described.

The first procedure, NADP 1, is a departure procedure alleviating noise close to the aerodrome. It involves a power reduction at 800 ft altitude and maintains the flaps and slats in the take-off configuration until at least an altitude of 3000 ft is reached. From this altitude, a positive rate of climb is maintained while the flaps and slats are retracted and the airplane accelerates smoothly to an en-route climb speed. A schematic representation of NADP 1 is presented in Figure 2.6.

On the other hand, the second procedure designed by ICAO (NADP 2) can be used to alleviate noise more distant from the aerodrome. From an altitude of 800 ft, the flaps and slats are to be retracted while maintaining a positive rate of climb. As the high lift devices are retracted, the power setting is reduced and the aircraft smoothly accelerates towards an en-route climb speed. NADP 2 is shown in Figure 2.7. Until recently NADP 1 was the preferred departure procedure at Amsterdam Airport Schiphol, this however changed to NADP 2.

Table 2.5: Preferred runway usage at AAS (06:00 - 23:00) [Schiphol, 2014].

Visibility	**Preference**	**Arr. 1**	**Arr. 2**	**Dep. 1**	**Dep. 2**
Good:					
Visibility > 5000 m	1	06	(36R)	36L	(36C)
Cloud base > 1000 ft	2	18R	(18C)	24	(18L)
Within UDP	3	06	(36R)	09	(36L)
	4	27	(18R)	24	(18L)
Good:					
Visibility > 5000 m	5a	36R	(36C)	36L	(36C)
Cloud base > 1000 ft	5b	18R	(18C)	18L	(18C)
Good or marginal:					
Visibility > 1500 m	6a	36R	(36C)	36L	(09)
Cloud base > 300 ft	6b	18R	(18C)	18L	(24)

Table 2.6: Preferred runway usage at AAS (23:00 - 06:00) [Schiphol, 2014].

Preference	**Arrivals**	**Departures**
1	06	36L
2	18R	24
3	36C	36L
4	18R	18C

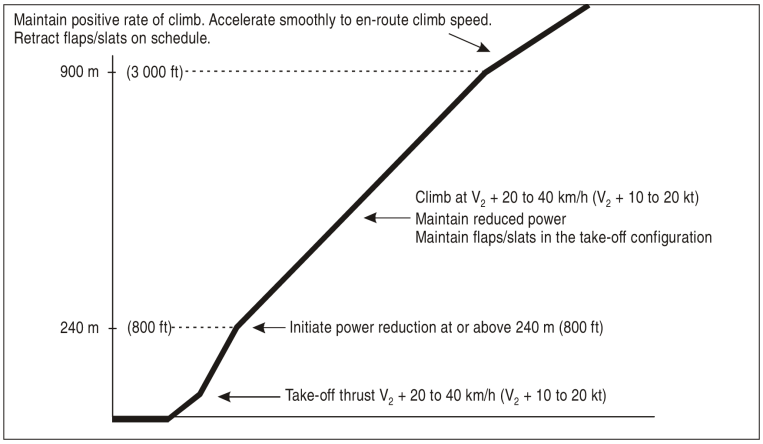

Figure 2.6: Noise Abatement Departure Procedure 1 [ICAO, 2006].

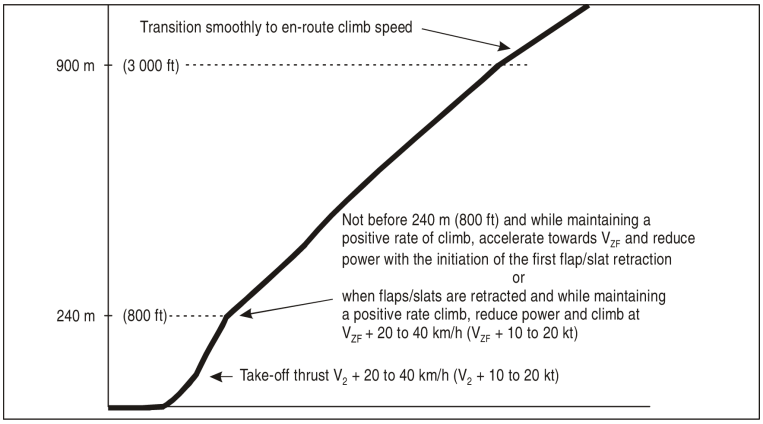

Figure 2.7: Noise Abatement Departure Procedure 2 [ICAO, 2006].

Operating Restrictions

Apart from (technological) improvements in the design of aircraft, airports and the airspace, operating restrictions are also a good instrument of a government or authority to counteract annoyance of residents that originates from aircraft noise. Examples are operating quotas, noise charges and curfews.

The maximum amount of operations allowed at Dutch airports until 2020 is currently set at 580,000 commercial flights (take-off or landings). Of this number, 510,000 operations are allocated to Amsterdam Airport Schiphol while the remaining 70,000 are distributed over the other commercial airport in the Netherlands. To set a more stringent limit regarding the noise impact, cumulative noise measurements are used. For Amsterdam Airport Schiphol the L_{DEN} and L_{night} are used, where *DEN* stands for day, evening and night. These numbers consists of the accumulation of the

Table 2.7: Equivalence Noise Criteria [Schiphol, 2014]

Noise Criterion	**Max. Amount**	**Prognosis 2019**
Houses within contour of $L_{DEN} \geq 58$ dB(A)	12,200	9,400
Inhabitants highly annoyed caused by $L_{DEN} \geq 48$ dB(A)	180,000	125,000
Houses within contour of $L_{night} \geq 48$ dB(A)	11,100	6,600
Inhabitants experiencing sleep disturbance caused by $L_{night} \geq 40$ dB(A)	49,500	20,000

single event Sound Exposure Level (SEL) of each overflying aircraft. The earlier mentioned Alderstafel established equivalence noise criteria regarding both L_{DEN} and L_{night}, which are presented in Table 2.7.

Every year Amsterdam Airport Schiphol sets a traffic forecast that also elaborates on the expected noise annoyance (prognosis for 2019 shown in the last column of Table 2.7). To calculate the impact of aircraft noise on the ground the Integrated Noise Model (INM) is used. The noise forecast made uses a contour to show the areas exposed to a certain noise level. In this way the earlier mentioned benchmarks can be checked upon in the forecast. To check if these benchmarks are met at the end of the year, the actual noise on the ground is also monitored. This is done with the Noise Monitoring System (NOMOS) which uses 31 noise monitoring points in the vicinity of Schiphol. The results of these measurements are used in new negotiations at the Alderstafel.

Night operations at Schiphol are very much restricted. They do not only count ten times as heavy in the cumulative L_{DEN}-calculations, there is also a limit of 32,000 operations during night hours. Arrivals during the night are obliged to perform a CDA to mitigate sleep disturbance as much as possible, while only specific airways and runways are allowed to be used.

2.2.4 Flight Schedule

Amsterdam Airport Schiphol receives almost half a million flight movements per year, which is on average around 1400 a day. All flights have to comply with the regulations presented earlier and have to fit in the airspace and configuration of the airport. An example of a flight schedule is presented here, and this schedule of October 22th 2010 will also be used in the case studies. The actuel distribution of aircraft over the different SIDs can be found in Appendix B. In Table B.1 these flights are subdivided over flights during the day, evening and night.

During this day, inbound traffic was directed to land from the north, while outbound traffic departed towards the south. Out of the 611 departures, 406 took off from the 'Kaagbaan (24)', 193 from the 'Aalsmeerbaan (18L)' and only 12 from the 'Oostbaan (22)'. As the traffic on the latter only included small aircraft, such as Cessna Citations, these aircraft will not be included later on. The runway combination of runway 24 and runway 18L is one of the most preferred runway combinations which makes this flight schedule an interesting test case for this research. Besides, the prognosis for

2019 is that 80.900 flights will take-off from runway 24 and 60.200 from runway 18L, by which these runways together account for 57 percent of the total amount of take-offs. Schiphol is a hub airport where different aircraft arrive and depart around the same time in order to make the journey of transfer passengers more convenient. This behaviour results in several banks during the day, which can clearly be seen in the distribution of flights over the day in Figure 2.8. On this specific day, runway 24 was available the entire day while runway 18L assists the operation during peak hours when extra departure capacity was required.

A total of 49 different type of aircraft were used during this day. The fleet of this day ranges from small Fokker F100s, to medium sized Boeing 737-400s and Airbus A320s up to heavy Boeing B747-400s and McDonnel Douglas MD-11 aircraft, among others. These aircraft type have been grouped to form a fleet composition of five different aircraft type, of which the distribution is shown in Table 2.8. The grouping has been done in order to minimize modelling time, manage the flight schedule in a clear manner but not loose to much data quality with too little variation. The classification of the aircraft has been done based on MTOW, wingspan and number of engines. As a result every main aircraft type identification class is present, while category B is present with two different aircraft. The reason for this is to make a distinction between aircraft with two and four engines, as the latter results in a lot more noise annoyance and have a higher fuel consumption. Some of the grouped aircraft type are more common at Schiphol. This fleet mix is presented in Figure 2.9.

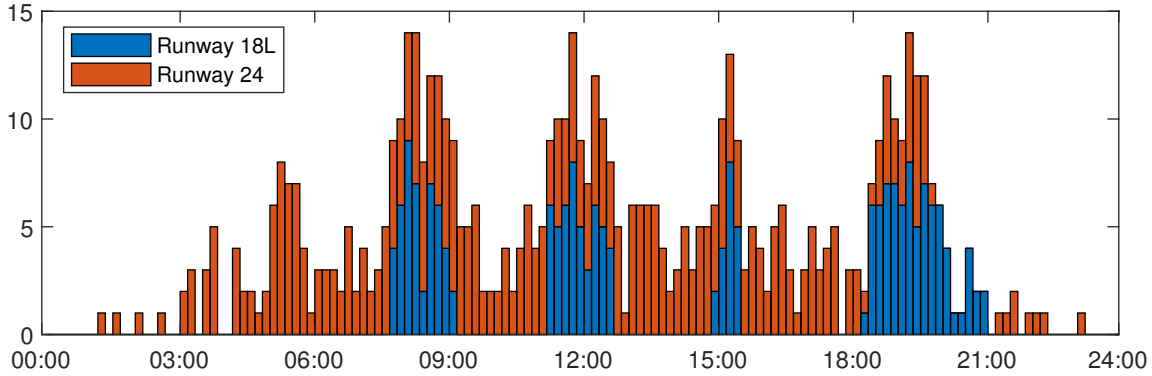

Figure 2.8: Distribution of flights over the day

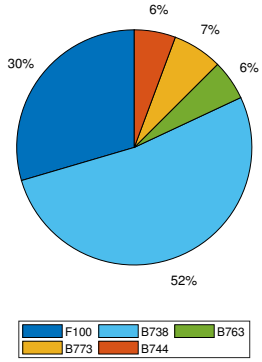

Figure 2.9: Different aircraft in the schedule

Reference Aircraft	**Identifier**	**Original Aircraft Type**
Fokker F100	E	B462, CRJ2/7/9, DH8D, E145/70/90, F70/100, MD82, RJ85
Boeing 737-800	D	A318/19/20/21, B733/4/5/6/7/8/9
Boeing 767-300	C	A306/10, B752, B763/4, MD11
Boeing 777-300	B	A332/3, B772/W
Boeing 747-400	B	A343, B742/4

Table 2.8: Fleet Composition

2.3 Optimization Algorithms

The integrated optimization framework that is presented in this research makes use of a combination of several optimization algorithms. These algorithms were chosen after an extensive literature review of available optimization strategies. This section elaborates on the basics of the chosen methods.

2.3.1 NSGA-II

For a right implementation of the proposed optimization framework, evolutionary algorithms seem capable of dealing with such a problem. The Non-Dominated Sorting Genetic Algorithm II [Deb et al., 2002, Deb and Sundar, 2006] is one of the most powerful methods for this, and is also capable of handling multi-objective optimizations. Furthermore this method can handle non-linearity which is required for the problem as noise levels are compared to one another. Noise levels are presented in decibels, which is a logarithmic (non-linear) scale.

The Non-Dominated Sorting Genetic Algorithm II algorithm is a form of a Genetic Algorithm, and in this form is implemented by Song Lin into Matlab [Lin, 2011]. The theory behind Genetic Algorithms is loosely based on Darwinian evolution, that makes use of the survival of the fittest principle. The process of natural selection is used to find a better solution. A population of candidate solutions, each having a set of properties (chromosomes), evolve and mutate towards a better result. In between two generations, a part of the earlier generation is selected to turn into a new generation. Fitter solutions are more likely to be chosen for this. With the selected portions of the earlier generation two processes are performed: crossover and mutation.

Crossover

The crossover process is used to combine the genetic information of two parents to generate two children. In the NSGA-II algorithm the so called intermediate crossover is implemented, which is a form of crossover that linearly combines genes of two parents to produce two new offspring. Equations 2.1 and 2.2 present this process. Two parameters have to be determined in the algorithm. The crossover fraction determines the fraction of the variables in a population to do crossover. The crossover ratio, named R in the equations, controls which part of a gene of two parents end up in the gene of the two children. A random number is also introduced in the formulas to add some variety in the formation of the genes.

$$C_1 = P_1 + rand \cdot R \cdot (P_2 - P_1) \tag{2.1}$$

$$C_2 = P_2 - rand \cdot R \cdot (P_2 - P_1) \tag{2.2}$$

Mutation

The NSGA-II algorithm supports Gaussian mutation. In the mutation process a gene is altered by means of a Gaussian distributed number in order to find a solution outside the previous solution. Equations 2.3 and 2.4 present the formation of a new child out of a parent. Three parameters control the behaviour of the mutation process. The mutation fraction determines the fraction of the variables in a population to mutate. The scale parameter determines the standard deviation of the random number generated, and the shrink controls the decrease in the scale of mutation as the optimization progress goes forward. In Equation 2.4 this is indicated as the ratio between the current generation of the process ($G_{current}$) and the maximum number of generations (G_{max}).

$$C = P + S \cdot randn \cdot (ub - lb) \tag{2.3}$$

$$S = scale \cdot \left(1 - shrink \cdot \frac{G_{current}}{G_{max}}\right) \tag{2.4}$$

Settings

As said, the NSGA-II algorithm is a multi-objective algorithm. Any amount of objectives can be chosen from two and above, although the algorithm has a problem to find good results in case a large amount of conflicting objectives is implemented. To find a solution, whatever the amount of objectives, a number of decision variables need to be in place. For all variables a lower bound and upper bound have to be set. These numbers bound the search space for that particular decision variable. Two type of decision variables can be implemented, as the algorithm is able to handle both continuous (real) and integer variables.

At the beginning of a generation, the composition of the chromosomes of each population is determined using the crossover and mutation methods. As the subsequent calculations of the objective (or fitness) function of each population within the same generation are not related to the calculations of the other populations, these can be performed in parallel. The parallel process will speed up the calculations of the entire optimization.

Constraints

The NSGA-II algorithm has a constraint handling technique at its disposal called binary tournament selection. Two solutions from the population are picked and the solution that scores higher is chosen. A solution α constrained-dominates solution β (and therefore scores higher), if any of the following three conditions is true:

1. Solution α is feasible and solution β is not.
2. Both solutions are feasible, but solution α dominates solution β.

3. Both solutions are infeasible, but solution α has a smaller overall constraint violation.

While a solution is infeasible, it is not desirable to maintain this solution in the populations. Although eventually it is required to remove this solution, this process is only initiated from generation 30. This has been chosen to build a wide enough spectrum for the populations in the beginning of the optimization process, with the intention to not end up in a local optimum.

2.3.2 Differential Evolutionary Algorithm

Differential Evolutionary algorithms are part of the meta-heuristics and try to find an optimal solution for a problem by iteratively improving a (candidate) solution with regard to a given measure of quality. As long as this measure of quality is not achieved in a certain iteration the optimization will continue. The optimization will nonetheless stop when the maximum allowed number of iterations is reached.

A Differential Evolutionary algorithm looks a lot like a Genetic Algorithm (GA), they are both part of the family of Evolutionary Algorithms. However the selection process between two successive generations works a little differently. Instead of the crossover and mutation processes, a DE makes use of a formulae that consists of a crossover probability and a differential weight factor.

2.3.3 Integer Linear Programming

In a standard form of Integer Linear Programming (ILP) a linear function is formulated that needs to be maximized, as shown in Equation 2.5. This function is subjected to a series of constraints and results in an exact solution. The function is often solved with a standard solver, such as IBM ILOG CPLEX Optimization Studio (CPLEX for short), that can be integrated with other programming languages. An example of this is the implementation of CPLEX within the software package Matlab, which is developed by Mathworks.

$$\begin{aligned} \text{maximize} \quad & c^T x \\ \text{subject to} \quad & Ax \leq b \\ & x \geq 0 \\ \text{where} \quad & x \in Z^n \end{aligned} \tag{2.5}$$

As the name suggests, the decision variables of an ILP consist only out of integers. Normally these variables can have any value, as long as they are integers and within the bounds set for that variable. It can also be chosen to implement the variables as binaries, meaning they will be either 0 or 1. When all variables are set to be binary, the optimization method is called Binary Integer Linear Programming (BILP). The constraints imposed to the decision variables and objective function can consist of both equality and inequality constraints.

2.4 Conclusion

This chapter introduced several subjects that together form the basis for this research. First the design of the airspace was discussed and the formation of trajectories and separation requirements for aircraft flying through this airspace. Amsterdam Airport Schiphol is chosen as case study airport, and the subsequent section elaborated on the layout and operations of the airport and specific noise abatement regulations such as preferential runway usage and the use of specific departure procedures. A flight schedule of October 22th 2010 has been explained which will be used as reference in the optimization process. The framework for this optimization will make use of three different algorithms that were introduced in the last section of this chapter. These algorithms were chosen due to their specific capabilities that are required for the optimization framework. The information of this chapter will be used in the following chapter, which explains the methodology of this research in detail.

Chapter 3

Methodology

In the introduction of this research, an integrated optimization framework has been proposed. After considering all the required background information in the previous chapter, this chapter explains the proposed method in detail. In the first section an overview of the framework will be explained. All the different steps required for this framework are clarified in more detail in the subsequent sections. In the last section conclusions are drawn.

3.1 The Model

As explained, the model should be able to allocate take-off runways, departure routes and departure procedures to flights in a flight schedule in order to optimize for noise and fuel. After an extensive research, it was chosen to make use of a GA implementation to use as optimization algorithm. In this way a large set of optimal solutions can be obtained. In total, three different algorithms will be implemented. Besides the GA, a Differential Evolutionary (DE) algorithm and an Integer Linear Programming (ILP) algorithm will be used in order to perform all the required tasks for the optimization framework.

Figure 3.1 presents the flow diagram that shows the working principle of the integrated optimization framework. The model starts with an initial solution, which is generated by a DE algorithm. This initial solution is required to guide the optimization process of the next step. The second step consists of a genetic optimization process, implemented via a NSGA-II algorithm. In a Genetic Algorithm a population breeds for a certain amount of generations. First, the population is processed in order to obtain the right kind of variables to work with, namely the distribution of flights over the different runway, route and procedure combinations. Of this flight distribution the required fuel and the noise equivalence criteria are calculated subsequently, which result in a number for the objective values. If the maximum amount of generations is not yet reached, the population starts to breed to obtain a new population. The selection for the new population consists of the crossover and mutation processes. When this iteration is finished, the final set of solutions is passed

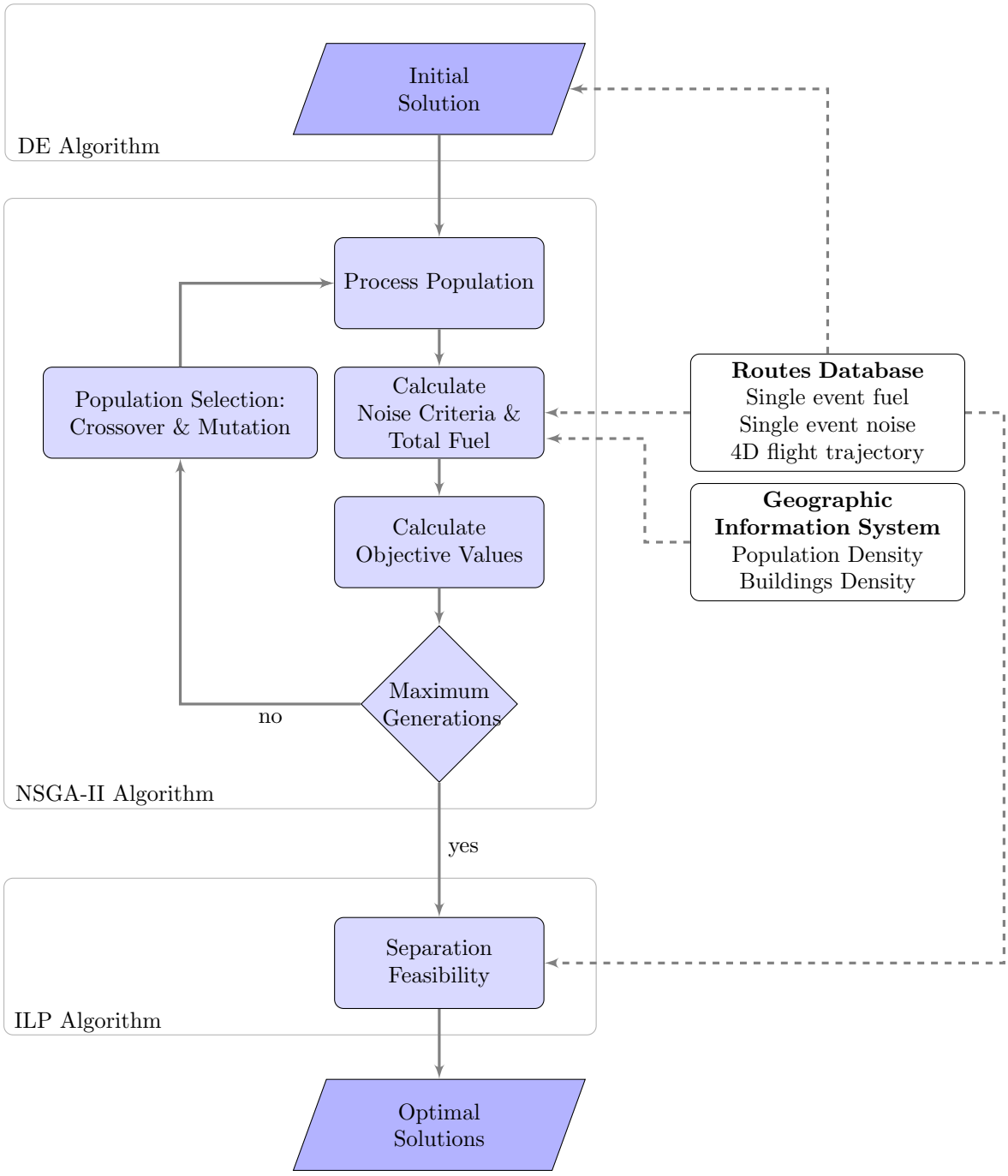

Figure 3.1: Flow diagram of integrated optimization framework

to the next step. By making use of an ILP algorithm the feasibility of the solutions with respect to separation requirements is checked. The set of solutions that show to be feasible form the set of optimal solutions.

For this model to work a lot of pre-processed data is required, so that the model itself is mainly used to connect different sets of data and only has to do few calculations itself. A database has to be formed that consists of all possible runway, route and procedure combinations for each implemented aircraft type. Of these combinations, the amount of fuel and single event noise load of that flight are required. Furthermore the 4D trajectory (x,y,z position in time) of each flight is required in order to comply with separation requirements later on.

In the following sections all parts of the framework presented in Figure 3.1 are explained. First the Geographic Information System that will be used throughout the framework will be introduced. Second the modelling of the Standard Instrument Departure routes that are in use at Amsterdam Airport Schiphol is elaborated upon. The single event noise and fuel of these routes are required for the calculations of the noise equivalence criteria and the total fuel calculations. The ILP algorithm that is used for the feasibility check for separation is explained thereafter. All these parts are combined in Section 3.7 where the implementation of the model into the NSGA-II algorithm is presented.

3.2 Geographic Information System

In order to unambiguously represent all routes, flight paths and the noise contours, the same Geographic Information System (GIS) is used throughout the framework. The specific GIS used is the 'Rijksdriehoeksstelsel' of the Kadaster (Dutch land registry) [Kadaster, 2019]. This Cartesian coordinate system, with the units in meter, has a x-coordinate from West to East and a y-coordinate from South to North. The origin of the system lies to the South of the French capital Paris, although this particular place is irrelevant for the system. This origin has been chosen such that all x- and y-coordinates have a positive value while the smallest value for y is always greater than the largest possible value for x. This results in an unambiguous geographic reference system, where x-coordinates and y-coordinates cannot be mixed up.

The area that is taken into consideration in the framework lies between the x-coordinates $x = [0.45e5, 1.70e5]m$, and the y-coordinates $y = [4.33e5, 5.35e5]m$. The area has been chosen such that all the terminal points of the departure routes fall within this rectangular area. Demographic data acquired from Centraal Bureau voor de Statistiek (CBS) is used throughout the framework, and consists of both population density as the density of buildings. Figure 3.2 shows the population density of the considered area on a 500x500m grid. In the centre of the figure the six runways of Amsterdam Airport Schiphol are indicated in blue.

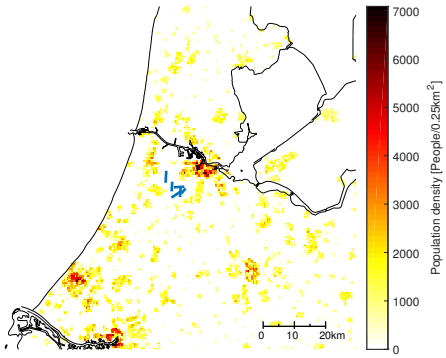

Figure 3.2: Population density for the area around Schiphol under consideration.

3.3 Routes Modelling

The routes that will be used in the optimization framework are the Standard Instrument Departure (SID) routes, explained in Section 2.2.2. These routes have been modelled for each of two departure runways, five different aircraft type, two departure procedures and the seven terminal points. This subsection elaborates on the modelling of these routes, from which a dataset is built that consists of the noise metrics on ground level per grid-coordinate, the so called single event Sound Exposure Level (SEL), the fuel required for that flight and the flight path of the aircraft from take-off to the terminal point in x-, y- and z-coordinates per unit of time. This section explains the modelling of the routes.

In order to model the routes, an aircraft performance model and the flight trajectory have to be modelled. To simplify the modelling of the aircraft, a number of assumptions are made and listed below.

- No wind vector present
- A non-rotating and flat Earth
- Aircraft performs a coordinated flight
- Flight path angle is small ($0° < \gamma < 15°$)
- Aircraft weight remains constant

An intermediate point-mass model [Ho-Huu et al., 2017, Hartjes and Visser, 2017] is used to represent an aircraft in flight, in which it is assumed that there is an equilibrium of forces normal to the flight path. The equations of motion of this point-mass model can be written as presented in Equation 3.1 till 3.5, in which the time derivatives of the true airspeed, x- and y-distance flown, altitude

and aircraft weight are shown. The other variables present indicate the gravitational constant g_0, thrust T, drag D, flight path angle γ and the fuel mass flow $\dot{m}_f$.

$$\dot{V}_{TAS} = g_0 \cdot \left(\frac{T - D}{W} - \sin\gamma \right) \tag{3.1}$$

$$\dot{x} = V_{TAS} \cdot \cos\gamma \cdot \sin\chi \tag{3.2}$$

$$\dot{y} = V_{TAS} \cdot \cos\gamma \cdot \cos\chi \tag{3.3}$$

$$\dot{h} = V_{TAS} \cdot \sin\gamma \tag{3.4}$$

$$\dot{W} = -\dot{m}_f \cdot g_0 \tag{3.5}$$

An airline pilot gets the indicated airspeed V_{IAS} presented in its cockpit, which is subsequently used to adhere the airspeed with the speeds prescribed in the NADPs. Although the indicated airspeed is desirable to use in the equations, the equivalent airspeed V_{EAS} can serve as a proxy for V_{IAS} at low altitudes and airspeeds, which is easier to calculate. The relationship between V_{EAS} and V_{TAS} is presented in Equation 3.6, and is dependent on the ambient air density ρ and the air density at sea level ρ_0.

$$V_{EAS} = V_{TAS} \cdot \sqrt{\rho/\rho_0} \tag{3.6}$$

Equation 3.6 can be combined with the equations of motion. Furthermore, the time derivatives of the x- and y-distance flown can be combined to form the time derivative of the flight path distance flown $\dot{s}$. The equations of motion can be rewritten as shown in Equations 3.7 till 3.10. With these equations the point-mass model consists out of four state variables $[V_{EAS}, h, s, W]$ and two control variables $[\gamma, T]$.

$$\dot{V}_{EAS} = \left[g_0 \cdot \left(\frac{T - D}{W} - \sin\gamma + \frac{1}{2\rho} \cdot \frac{\delta\rho}{\delta h} \cdot V_{TAS}^2 \cdot \sin\gamma \right) \right] \cdot \sqrt{\rho/\rho_0} \tag{3.7}$$

$$\dot{s} = V_{EAS} \cdot \sqrt{\rho/\rho_0} \cdot \cos\gamma \tag{3.8}$$

$$\dot{h} = V_{EAS} \cdot \sqrt{\rho/\rho_0} \cdot \sin\gamma \tag{3.9}$$

$$\dot{W} = -\dot{m}_f \cdot g_0 \tag{3.10}$$

For the flight path that the aircraft will follow a trajectory parameterization technique is used [Hartjes and Visser, 2017]. The flight path is decomposed into a horizontal ground track and a vertical path. The ground track of the flight path, which will coincide with the published SID, is

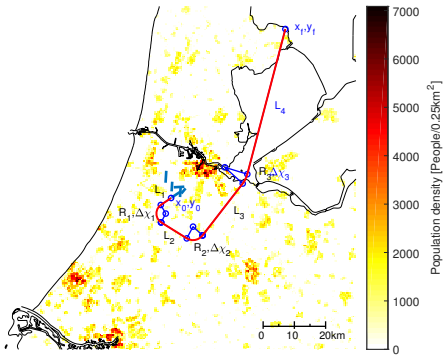

Figure 3.3: Ground track parameterization of SID ANDIK 1S

built up as a RNAV route. As explained in Section 2.2.2, a route can be modelled as a start point followed by a series of straight (Track-to-a-Fix) and curved (Radius-to-a-Fix) segments. A straight leg is defined by one parameter, namely length L of the segment, and a curved segment is defined by two parameters: turn radius R and heading change $\Delta\chi$. A ground track can be built up from any number of Track-to-a-Fix and Radius-to-a-Fix segments, and from geometry it follows that the value of two parameters can be calculated with the values of the others. An example of this is given in Figure 3.3 for the SID 'ANDIK 1S', departing from runway 24 towards terminal point Andik, consisting of four straight segments and three turns. In this case length L_4 and heading change $\Delta\chi_3$ follow from geometry with the other parameters. An overview of all modelled SIDs for the two departure runways is presented in Figure 3.4. It has to be noted that the names that are indicated in this figure not necessarily correspond to the official published name of that waypoint. The SIDs are named after their endpoint, and some of these endpoints fall outside of the area that is under consideration. It has been chosen to stick to the names of the SIDs rather than the names of some intermediate waypoints. From the figure it can be seen that each of the two runways is connected to all seven waypoints with a single SID, except for runway 24 that has a second possible route towards the waypoint called 'Andik'. In total runway 24 therefore has eight possible departure routes, while runway 18L has seven.

For the vertical path, it is not allowed throughout the departure phase to descend and/or decelerate. The profile is divided into a number of segments based on the two NADPs. For each of these segments the control parameters γ and T are kept constant, so these can only change when there is a change of segment. The values of these parameters are based on the requirements for the two NADPs.

The x-, y- and z-coordinates of the flight path, together with the airspeed V and thrust T are required to calculate the noise of the flight. For the calculations the amount of data points of the flight path are reduced in the last part of the flight in order to save computation time. These noise calculations are executed with INMTM [Hartjes, 2010], which is a noise model replication of the in-flight noise assessment model that is integrated in the widely used Integrated Noise Model (INM). The noise calculations are based on empirically determined noise-power-distance tables,

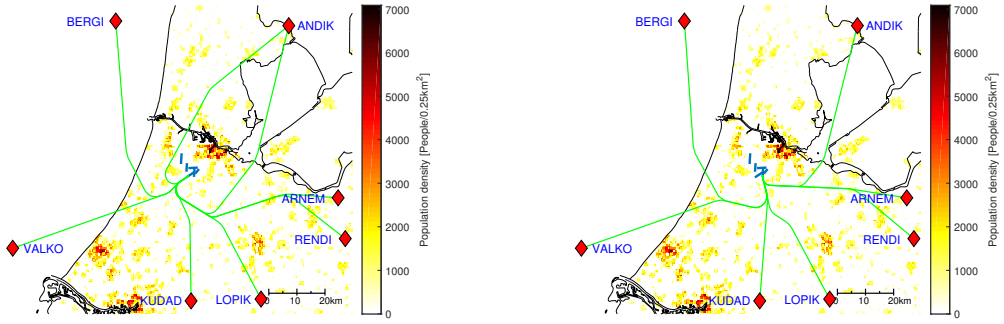

(a) Runway 24

(b) Runway 18L

Figure 3.4: Modelled Standard Instrument Departure (SID)

which depends on thrust level and the distance between a location on a grid (the observer) and the flight segment of the aircraft. Although this noise model consists of noise metrics for most modern commercial airliners, other data that is required in the modelling of the routes comes from BADA. The Base of Aircraft Data (BADA) is an aircraft performance model developed by Eurocontrol. This database gives information about aircraft weight, engines, high-lift device settings and required and maximum velocities. The noise calculations result in the single event Sound Exposure Level (SEL), presented per grid coordinate. The unit is dB(A), where the A represents a sound filter that reduces the loudness of specific frequencies which are less disturbing to the human ear.

The output of the routes modelling consists of the 4D flight trajectory, the fuel burned and the single event Sound Exposure Level of the departure of one aircraft. The 4D flight trajectory is a combination of the x-, y- and z- position of an aircraft over time. To generate this data, the flight path is interpolated such that a data point is given at every second of flight. The fuel burned is a single value that represents the amount of fuel used by the aircraft to fly from the end of a specific runway to the respective terminal point, following a predefined ground track and following one of two departure procedures. The noise metric represents the noise coming from the aircraft performing the before mentioned respective flight, as experienced on the ground, and is presented per grid-coordinate. Given the fact that the SEL-values follow a logarithmic scale, these values are therefore transformed to the Sound Exposure Ratio (SER), which is more convenient to use in calculations of the total noise of multiple flights. This transformation is shown in Equation 3.11.

$$SER_{(x,y)} = 10^{\left(\frac{SEL_{(x,y)}}{10}\right)} \tag{3.11}$$

Period		Penalty
Day	07:00 - 19:00	1
Evening	19:00 - 23:00	$\sqrt{10}$
Night	23:00 - 07:00	10

Table 3.1: Noise penalties

3.4 Noise Calculations

In accordance with regulations, the cumulative noise load of multiple flights during a day is expressed in L_{DEN}, where DEN stands for day, evening and night. Equation 3.12 presents the calculation for L_{DEN} for multiple flights. As stated in the previous section, the noise load of a single aircraft is stored in the database as a SER-value. In the L_{DEN}-expression, these values can be easily added up for each grid-coordinate. There is also a penalty factor included for flights in the evening and for flights during the night. Table 3.1 gives an overview of the penalties that are used at Amsterdam Airport Schiphol. The last term in the expression is a correction factor for the average noise load on an entire day.

$$L_{DEN}^{(x,y)} = 10 \cdot \log_{10}\left(\sum\left(SER_k^{(x,y)} \cdot penalty_k\right)\right) - 10 \cdot \log_{10}\left(24 \cdot 60 \cdot 60\right) \tag{3.12}$$

In line with L_{DEN}, another important noise criteria is L_{night}. For this expression, that is presented in Equation 3.13, only flights between 23:00 and 07:00 are included, and the penalty factor is left out. The correction factor at the end of the expression is altered to only count for the eight hours during the night period.

$$L_{night}^{(x,y)} = 10 \cdot \log_{10}\left(\sum\left(SER_k^{(x,y)}\right)\right) - 10 \cdot \log_{10}\left(8 \cdot 60 \cdot 60\right) \tag{3.13}$$

With the values of L_{DEN} and L_{night} known, the four equivalence noise criteria that were introduced in Section 2.2.3 can be calculated. These criteria comprise the amount of buildings and amount of people annoyed inside specific L_{DEN} and L_{night} contours. By making use of demographic data acquired from *Centraal Bureau voor de Statistiek (CBS)*, it can be determined if the cumulative noise load complies with the regulatory values of the various equivalence noise criteria. The demographic data contains the amount of inhabitants and houses per grid-coordinate.

Two of the noise equivalence criteria consider a maximum value for the allowed number of houses that experience a certain threshold noise value. By counting the number of houses within the noise contour formed by this threshold noise value, it can be shown that the series of flights during a day comply with the regulatory constraints. The other two criteria analyze the maximum amount of inhabitants that are heavily annoyed or disturbed during their sleep. For this, a so called dose-response relationship is used, which is based on statistical analysis of people experiencing aircraft noise (J.A.J. van Engelen [2006]). The relationship between the ratio of people heavily annoyed and the L_{DEN}-level is presented in Equation 3.14, and is only valid for L_{DEN}-levels between 39

and 65 dB(A). The noise equivalence criteria that is related to this topic is only applicable from $L_{DEN} = 48dB(A)$ and above, so that areas with a noise value below this number will receive a $PeopleHeavilyAnnoyed(PHA)$-value of zero. The formula is extrapolated linearly above 65 dB(A) until the ratio reaches one.

$$\%PHA = \left(\frac{e^{-8.11001+0.1333 \cdot L_{DEN}}}{1 + e^{-8.11001+0.1333 \cdot L_{DEN}}} \right) \tag{3.14}$$

Multiplying the ratio of people heavily annoyed at a specific grid-coordinate with the amount of people living at that location results in the amount of people heavily annoyed at point on the grid. By summing these values for all grid points the total amount of people heavily annoyed can be computed. This summation is shown in Equation 3.15

$$PHA = \sum_{x=1}^{x} \sum_{y=1}^{y} \%PHA_{(x,y)} \cdot People_{(x,y)} \tag{3.15}$$

Similar to the calculations for the amount of people heavily annoyed during the entire day, there is also a dose-response relationship between the amount of people that are disturbed while sleeping and the level of L_{night} (J.A.J. van Engelen [2006]). This relationship is presented in Equation 3.16 and is only valid between L_{night}-levels of 29 and 57 dB(A). For noise levels above this range the relationship is linearly extrapolated. As the noise equivalence criterion for people that are disturbed during their sleep is only applicable above a L_{night} value of 40 dB(A), it is not necessary to extrapolate the relationship below 29 dB(A). However noise values below 40 dB(A) will receive a $PeopleSleepDisturbed(PSD)$-value of zero. Similar to the calculations of the amount of people heavily annoyed, the amount of people disturbed while sleeping can be computed with Equation 3.17.

$$\%PSD = \left(\frac{e^{-6.642+0.1046 \cdot L_{night}}}{1 + e^{-6.642+0.1046 \cdot L_{night}}} \right) \tag{3.16}$$

$$PSD = \sum_{x=1}^{x} \sum_{y=1}^{y} \%PSD_{(x,y)} \cdot People_{(x,y)} \tag{3.17}$$

3.5 Fuel Calculations

The amount of fuel that a single aircraft uses to fly from its take-off runway to its terminal point is stored in a database. This amount depends on aircraft type, departure runway, route flown and procedure followed. To obtain the total amount of fuel used by all the aircraft during the day, the

single values of each aircraft in the schedule are simply added up. This summation is shown in Equation 3.18.

$$\text{Fuel}_{\text{total}} = \sum_{i=1}^{\text{No. flights}} f_{(\text{runway,route,procedure,aircraft})}(i) \tag{3.18}$$

3.6 Separation Feasibility

The integrated optimization framework has the goal to find a suitable composition of departure runway, route and procedure for all departing flights in a day that among others results in less noise annoyance. For flexibility reasons and in order to save computation time, the flights that use the same aircraft type during a daily period are treated together as a group. For this group it is then decided which part of the group flies a certain route and procedure. Although a result will be found much quicker compared to treating each flight in the schedule individually, it is not known if this distribution of aircraft groups can be divided over the flight schedule in such a way that the schedule is feasible in terms of separation requirements.

A linear model is implemented to distribute the different aircraft groups over the flights in the schedule. In order to mitigate any collision possibilities, the schedule is implemented such that it has to meet the separation standards at the take-off runway, a crossing point where two routes cross(over) each other and at the terminal point of the routes. If none of the possible route distributions comply with the separation regulations, a (positive) time delay will be imposed to a flight at the take-off time. In this way the separation in 4D will be guaranteed.

The model will be set up using Matlab, with an implementation of CPLEX to solve the linear model. Section 2.3.3 already discussed the basics of Linear Programming, and this section will built on that information. The following paragraphs introduce the objective function and decision variables of the model. Subsequently the constraints imposed to the decision variables are discussed.

3.6.1 Decision Variables and Objective Function

The goal of the model is to minimize the total delay. In order to model the flight schedule and to impose delay, two sets of decision variables are necessary:

$x_{f,r}$: flight f flies route r
d_f: take-off delay flight f

For every flight f there are six or four decision variables $x_{f,r}$ in place, dependant on if the flight heads to waypoint 'Andik' or one of the other waypoints respectively, as was already stated in Section 3.3. These variables are binary, and the model can therefore either chose the variable to be one (the flight flies that route and procedure combination) or zero (the flight does not fly that

route and procedure combination). If α is the amount of flights heading towards 'Andik' and β the total amount of flights, then the total amount of decision variables $x_{f,r}$ is $(\alpha \cdot 6 + (\beta - \alpha) \cdot 4)$. Each flight in the schedule can be given a positive delay at the time of take-off, resulting the flight to depart that amount of time later. Each d_f can take an integer value equal or larger than zero. The total amount of decision variables d_f is equal to the amount of flights f inside flight schedule F. The objective function of the model is to minimize the total delay, as presented in Equation 3.19.

$$\text{Minimize Delay} = \sum_{f=1}^{F} d_f \qquad \in f \in F \tag{3.19}$$

Besides the decision variables and objective function, several data sets are required to solve the problem:

F:	set of flights in schedule
R:	set of routes
A:	set of aircraft type
t_f:	take-off time of flight f
$t_{sep}(a_k, a_i)$:	required separation time between leading aircraft a_i and follower a_k
$FT_f^{a,r}$:	flight time of flight f to waypoint flying route r with aircraft a
$CT_f^{a,r}$:	flight time of flight f to crossing flying route r with aircraft a
$FD_{r,a}$:	input flight distribution with the amount of aircraft a flying route r

Table 3.2: Fictitious Flight Schedule

Flight	**Waypoint**	**ATD**	**A/c Type**	**Arnem Route Combinations**				**Bergi Route Combinations**			
1	Arnem	07:30	B738	$x_{1,1}$	$x_{1,2}$	$x_{1,3}$	$x_{1,4}$				
2	Bergi	07:35	F100					$x_{2,5}$	$x_{2,6}$	$x_{2,7}$	$x_{2,8}$
3	Bergi	07:40	B744					$x_{3,5}$	$x_{3,6}$	$x_{3,7}$	$x_{3,8}$
4	Arnem	07:45	F100	$x_{4,1}$	$x_{4,2}$	$x_{4,3}$	$x_{4,4}$				
5	Arnem	07:50	F100	$x_{5,1}$	$x_{5,2}$	$x_{5,3}$	$x_{5,4}$				
6	Bergi	07:55	B738					$x_{6,5}$	$x_{6,6}$	$x_{6,7}$	$x_{6,8}$
7	Bergi	08:00	B738					$x_{7,5}$	$x_{7,6}$	$x_{7,7}$	$x_{7,8}$
8	Arnem	08:05	B744	$x_{8,1}$	$x_{8,2}$	$x_{8,3}$	$x_{8,4}$				
9	Arnem	08:10	B744	$x_{9,1}$	$x_{9,2}$	$x_{9,3}$	$x_{9,4}$				
10	Arnem	08:15	B738	$x_{10,1}$	$x_{10,2}$	$x_{10,3}$	$x_{10,4}$				
...	...	...	...	...	...	...	...	...	...	...	...

Table 3.3: Fictitious Flight Distribution

A/c Type	**Arnem Route Combinations**				**Bergi Route Combinations**			
F100	0	0	2	0	0	0	0	1
B738	0	0	0	2	0	1	1	0
B744	0	0	1	1	0	0	0	1

3.6.2 Constraints

The objective function is subject to six constraints in order to satisfy the flight distribution and comply with the separation requirements. The first three constraints are used to assign aircraft coming from the distribution of aircraft to specific flights. For example, each flight has to fly one and only one route and procedure combination. The other three constraints are used to meet the separation requirements at the take-off runway, a crossing point and at the terminal point of a route. If the separation requirements are met at any of these three points, the separation is also adhered along the way of their flight path, since in that case overtaking is not possible and flights cannot deviate from their flight path. Hereafter these six constraints are explained in detail, and in order to better understand the constraints use is made of the fictitious flight schedule presented in Table 3.2 and a fictitious flight distribution presented in Table 3.3. Such a flight distribution is the output of the NSGA-II algorithm and would be the input of this separation feasibility model. This fictitious set-up only consists of two possible waypoints and three different aircraft type. Both waypoints have four possible route combinations, consisting of a composition of two SIDs and two departure procedures. The exact composition however is irrelevant for this example.

Constraint 1: Each flight in the flight schedule has four or six binary decision variables depending on the heading of the aircraft. These variables each stand for a specific departure route and procedure combination. As a flight can only fly one of these combinations, the sum of the decision variables for each flight has to be equal to one. This constraint is only feasible in the case that one decision variable equals one and the others are equal to zero. Indicated in the fictive flight schedule in blue, the variables that represent the second flight in the schedule ($x_{2,5}$ till $x_{2,8}$) should add up to one.

$$\sum_{j=1}^{n(R)} x_{f,j} = 1 \quad \forall\, f \in F \tag{3.20}$$

Constraint 2: Each flight in the schedule can fly a certain route. In the flight distribution resulting from the optimization framework, a total amount of flights performing a specific route and procedure combination has been defined. To match this number, the sum of all flights performing that route (irrespective of aircraft type) has to be equal to the amount specified in the flight distribution table. An example is given in the fictive flight schedule of Table 3.2, where the variables that represent route 3 are indicated in red. These variables should add up to $2+0+1=3$, as shown in Table 3.3.

$$\sum_{i=1}^{n(F)} x_{i,r} = FD_r \quad \forall\, r \in R \tag{3.21}$$

Constraint 3: The flight distribution table specifically states an aircraft type to be operated a certain amount of times during day, evening and night. To match this number, the sum of all flights operated by a certain aircraft type flying to a specific terminal point has to be equal to the flight distribution. It is possible however that there are more flights operated to that terminal point than specified in the flight distribution. The model has to assign these flights to other routes, so that other constraints are satisfied. Indicated in green in Tables 3.2 and 3.3, flights six and seven are both heading towards 'Bergi', and are operated by a Boeing 737-800. As can be seen from the

flight distribution of this example, only one of those two flights can use this runway, route and procedure combination.

$$\sum^{i=r,m=a} x_{i,m} = FD_{i,m} \quad \forall\, r \in R, a \in A \tag{3.22}$$

Constraint 4: Two flights departing from the same runway have to take wake turbulence separation requirements into account, as introduced in Section 2.1.3. If the departure time between two flights does not offer enough time separation, a departure delay can be introduced to the successive flight in order to comply with the separation requirements. Since it is not yet known how the distribution of flights will be executed, the separation constraint has to be in place for each of the two runways, and for all flights k that follow after flight i. To implement this, a large number M is introduced. If two flights i and k are chosen to take-off from the same runway, these terms will disappear and the take-off times of these flights are checked against the required separation time between the aircraft type of flight i and k. In the case that two flights are not scheduled by the model on the same runway, the large number M will not disappear and the constraint is always satisfied.

To reduce computation time and the amount of constraints, a Receding Horizon Control (RHC) strategy is implemented. When leading flight i is checked against all upcoming flights k, this would result in a lot of constraints. It was chosen to only check flight i against the next ten flights. This method is valid since the take-off time of the tenth aircraft after flight i is always far more than the largest possible separation requirements between two aircraft type.

$$(t_k + d_k) - (t_i + d_i) - M \cdot x_k - M \cdot x_i \geq t_{sep}(a_k, a_i) - 2 \cdot M \quad \forall\, i \in F, k \subseteq i \tag{3.23}$$

Constraint 5: Two successive flights that head to the same waypoint have to have enough time separation when arriving each at this location. A comparable constraint as to constraint four has been implemented to meet this requirement. In this case the flight time (FT) of flights i and k is added to obtain their arrival time at the waypoint. This flight time depends on the chosen route, procedure and take-off runway and the aircraft type of that flight. Again the same RHC strategy is implemented to reduce computation time and the amount of constraints.

$$\begin{aligned}(t_k + FT_k^{a,r} + d_k) - (t_i + FT_i^{a,r} + d_i) - M \cdot x_k - M \cdot x_i \\ \geq t_{sep}^{waypoint}(a_k, a_i) - 2 \cdot M \quad \forall\, i \in F, k \subseteq i\end{aligned} \tag{3.24}$$

Constraint 6: The flight paths of two successive flights, that not necessarily departed from the same runway or are heading towards the same waypoint, can have a crossing at a certain moment. If these flight paths not have enough vertical separation, there could be a potential collision danger at this location. In order to avoid this, the take-off delay can be used to avoid the aircraft from arriving at the crossing point at the same moment. Again, a comparable constraint as to constraint five is introduced, although this time the flight time is interchanged with the crossing time (CT). CT is the time a flight arrives at a specific crossing point, and is dependent on the chosen route,

procedure, take-off runway and the used aircraft of flights i and k. Also in this constraint the RHC strategy is implemented.

$$(t_k + CT_k^{a,r} + d_k) - (t_i + CT_i^{a,r} + d_i) - M \cdot x_k - M \cdot x_i \geq t_{sep}^{crossing}(a_k, a_i) - 2 \cdot M \quad \forall\, i \in F, k \subseteq i \tag{3.25}$$

3.7 Model Implementation

The optimization process has been modelled in a NSGA-II algorithm, which is an implementation of a GA in Matlab. This algorithm is widely applicable and can be altered to ones own insight. It is a multi-objective algorithm, which gives the opportunity to take several contradictory objectives into consideration. The following paragraphs present the implementation of the proposed framework into this algorithm.

3.7.1 Objectives

The goal of the research is to find a combination of runways, routes and procedures that is better in terms of noise and fuel than the reference solution. Furthermore the proposed solution must comply with the separation requirements. The separation requirements will be met by introducing a delay to several departures, in order to avoid any collision danger. It is the goal to have as little delay as possible. Although the algorithm can be used to implement two or more objectives, evaluation of the algorithm has shown that by having only two objectives the model can find solutions much faster. During several trials it has been found that the implementation of the separation feasibility model into the NSGA-II algorithm did not end in results that were satisfactory. It is therefore chosen to implement this model after the NSGA-II algorithm, and let this model check if the final results are feasible in terms of separation requirements or not. The imposed delay to check for feasibility is calculated as described in Section 3.6.

Given the aforementioned, the objectives have been implemented as follows. The first objective of the NSGA-II algorithm, presented in Equation 3.26 will be the total fuel. The sum of the amount of fuel that every flight uses for their route and procedure combination is normalized with respect to the reference solution. The objective is multiplied by four in order to match the values for objective 2.

$$\text{Min. Obj. } 1 = 4 \cdot \frac{\text{Fuel}_{total}}{\text{Fuel}_{total}^{reference}} \tag{3.26}$$

The second objective of the algorithm, presented in Equation 3.27, will consist of the noise equivalence criteria. The four noise equivalence criteria will be normalized with respect to the reference

solution so that each criteria will have a value of one if the solution is equal to the reference solution. These four values will be added up with equal weights to form the first objective. The 'H' in the equation stands for houses, in relation to the respective noise equivalence criteria. A solution that outperforms the reference solution will therefore have a value lower than four. The reference solution is explained in more detail in Subsection 3.7.2, and scores four in both objectives.

$$\text{Min. Obj. } 2 = \frac{H_{L_{DEN}(\geq 58)}}{H^{reference}_{L_{DEN}(\geq 58)}} + \frac{PHA_{L_{DEN}(\geq 48)}}{PHA^{reference}_{L_{DEN}(\geq 48)}} + \frac{H_{L_{night}(\geq 48)}}{H^{reference}_{L_{night}(\geq 48)}} + \frac{PSD_{L_{night}(\geq 40)}}{PSD^{reference}_{L_{night}(\geq 40)}} \tag{3.27}$$

3.7.2 Reference Solution

In order to normalize the solutions that are found in the optimization, the values for fuel and noise are divided by the values of a reference. This procedure is convenient as it immediately shows the performance of a solution that is found with respect to the real situation. The reference solution consists of the actual flights that flew on October 22th 2010, of which the flight schedule is used in this research project. Although it is desirable that aircraft follow their designated Standard Instrument Departure, in reality flights are vectored by ATC in a diverging manner in order to adhere the separation requirements. The reference solution that is used as benchmark will therefore be based on radar data rather than a modelling of the SIDs which would be an approximation.

In line with the modelling of routes explained in Section 3.3, the flights of the reference solution are modelled in a similar way. However, in this case the radar tracks are used to form the horizontal part of the trajectory, compared to the SIDs used in Section 3.3. Although a SID would consist of a combination of multiple turns and straight segments, it is not known from the radar tracks exactly where turns are initiated and what their radius and length is. In order to shorten the processing time, it is assumed that the radar tracks consist of a series of short straight segments. The downside of this assumption is that the bank angle of possible turns is not included, which has an effect on load factor, thrust required and noise produced. As the entire flight path is interpolated linearly over a series of 100 pieces, which results in very short (straight) segments, it is therefore assumed that this downside is only marginal and can be neglected. With the horizontal flight path modelled, the vertical component can be added. As Schiphol currently forces aircraft to use Noise Abatement Departure Procedure 2, the flights are modelled with this departure procedure.

The reference solution that is based on radar data is used as the main benchmark, and the fuel and noise values resulting from this reference are used in Equations 3.26 and 3.27. Besides this reference solution, the actual flights of the reference day are also modelled using the official SIDs. The shape and destination of the radar tracks are compared to the official SIDs, and matching routes are stored. The entire flight schedule is subsequently modelled according to these modelled trajectories. This so-called modelled reference solution will be used to compare the modelled solution set in more detail with the reference solution based on the radar tracks.

Variable		Value
Crossover	Fraction	0.8
	Ratio	0.9
Mutation	Fraction	0.5
	Scale	0.5
	Shrink	1.0

Table 3.4: Crossover and mutation settings

3.7.3 Settings

In order for the algorithm to work properly, several settings have to be made and adjusted. As explained, aircraft can depart in seven directions. Each runway is connected with these seven waypoints with a SID, except for runway 24 that has a second possible route towards 'Andik'. In other words, there are two possible routes towards each waypoint, apart from waypoint 'Andik' that has three. With two possible departure procedures, for each waypoint there are four (or six in case of 'Andik') route and procedure combinations possible, which leads to a total of $1 \times 6 + 6 \times 4 = 30$ route and procedure options for each aircraft type at each part of the day. Since there are three day parts and five different aircraft type, the model has $5 \times 3 \times 30 = 450$ decision variables. These variables are continuous values with a lower bound of 0 and an upper bound of 1. For aircraft type that have no flights during a certain day part, the upper bound of the related decision variables will be 0. Although these variables could also be removed from the algorithm, these empty decision variables will not capture that much computation time while this leaves the model to be more flexible for different schedules.

A GA requires a population size that breeds for a certain amount of generations. For both of these numbers there is no golden rule. In an optimization with a small amount of decision variables, the population size has a rule of thumb to be twice the amount of decision variables. Since this implementation requires a large amount of decision variables, this rule is not applicable. For the test cases it is chosen to set the size of the population to be 50, while the case study will make use of a population of 100. The NSGA-II implementation of the algorithm has no stopping condition to its disposal. Therefore the optimization in any way has to run to its set value for the maximum amount of generations. After several iterations it is decided that the test cases will run for 250 generations, while the case study will continue for 500 generations.

Section 2.3.1 elaborated on the selection process for a following population that makes use of crossover and mutation. For both of these processes a number of settings have to be applied. A small iterative study, in which one of the settings was altered while keeping the others equal, resulted in the settings presented in Table 3.4.

3.7.4 popMaker

The previous paragraph elaborated on the decision variables of the optimization algorithm. Each variable stands for a specific aircraft, runway, route and procedure combination. A series of four

or six of these variables depicts all the runway, route and procedure combinations with a certain aircraft type to a specific terminal point. Each series subsequently has to represent all the aircraft in the flight schedule of that type towards that terminal point. It has been chosen to use continuous variables between 0 and 1 for this in order to avoid an unnecessary amount of constraints and to let the schedule be feasible at all times. To convert the continuous decision variables to an integer amount of aircraft, a function called 'popMaker' ('population maker') has been created and implemented. In the flow diagram of the integrated optimization framework in Figure 3.1 this has been depicted as the 'Process Population' step.

This function works as follows. First the values for the series of decision variables are added up, resulting in a value between 0 and 4 (or 0 and 6). Second the required amount of aircraft coming from the flight schedule is divided by this number. The resulting value is subsequently multiplied by each decision variable individually. As an amount of aircraft has to be an integer value, these numbers are rounded to the nearest integer. A check is installed in order to verify if the required amount of aircraft is matched, considering the rounding. If the required amount is not met, the value that is closest by receives an extra aircraft or one less. The check is performed again until the schedule is satisfied.

3.7.5 Constraints

As mentioned in Section 2.2.3, Amsterdam Airport Schiphol is limited in the use of several runways in the evening and during the night. From 21:30 till 05:30 runway 18L (Aalsmeerbaan) is not allowed to be used for departures, resulting all departures to take-off from runway 24 (Kaagbaan), given the flight schedule used in this research. It has to be noted that this period partially falls in the evening period as well as in the night period. To impose a constraint on this for the model, the number of take-offs that fall in evening and night period during the closure of runway 18L have been counted. The difference between these numbers and the total amount of departures in the evening and the night period are the maximum allowed numbers of departures on runway 18L in these periods. In case the population resulting from the *popMaker*, described in the previous paragraph, not complies with these numbers a violation constraint is introduced.

In order to guide the optimization algorithm and to find solutions faster, a constraint has also been introduced to the noise and fuel metrics resulting from each of the populations. It is the intention to find a solution that outshines the reference solution, however it might be possible that a small loss in the total fuel used can gain a large profit in the noise metrics. Therefore the model is allowed to use at maximum five percent more fuel with regard to the reference solution. A violation constraint is introduced in case the population in consideration results in a larger amount of fuel used.

As said, the goal is to find a better solution than the reference solution. Since the noise objective is composed out of the four noise equivalence criteria, a small loss in one of those might waste the entire population while the other criteria show good results. A constraint relaxation has been implemented in order to widen the horizon of the optimization process and to hold on to promising populations. The four equivalence criteria are each normalized with respect to their reference value. However the model is allowed to have up to 20% above the reference value for each of the single noise equivalence criteria. The objective of the model is still to find a overall solution better than the

reference solution. A constraint is imposed when one of the normalized noise equivalence criteria is above 1.2 times their reference value.

In case a population has a violation of one or more of the constraints, the population cannot be used in the optimization process. If the population is thrown out immediately from the beginning the genetic process might result in a too narrow search space. Populations with a violated constraint will therefore only be discarded after generation 30, in order for the model to built up a wide enough spectrum of populations from the beginning to continue the optimization process.

3.7.6 Initial population

In a genetic algorithm the initial population is generated randomly, which results in a wide range of solutions inside the entire search space. Given the amount of decision variables this lets the algorithm to search in directions were probably no optimal solutions will be found. In order to find better solutions and also improve computation time, the initial solution is seeded with populations that (partially) might result in optimal solutions. For this it has been chosen to find the solution that results in minimum fuel or the optimal solution for the noise objective that combines the four noise equivalence criteria. As the aforementioned NSGA-II algorithm is multi-objective, the same method has been implemented in a single-objective Differential Evolutionary algorithm. The optimal solutions for each of the single objectives form the basis of the initial solution of the integrated optimization framework.

3.8 Conclusion

In this chapter the methodology of the proposed integrated optimization framework was explained. In a flow diagram the entire structure of this framework was presented, after which each part of the model was explained in detail. The last section elaborated on the implementation of the model, that combines all previously explained parts. The next chapter presents the results that follow from running the integrated optimization framework.

Chapter 4

Results

In the previous chapter a method was proposed for an integrated optimization framework to benefit from the implicit potential of the combinatorial optimization of runway, route and procedure allocation in order to minimize noise and fuel. This method has been composed and the results coming from the framework are presented in this chapter.

The first two sections present the results for two test cases. First the results of a test case consisting of all flights towards a single waypoint is shown. In the second section the results of a test case consisting of a small part of the flight schedule is presented. These two test cases will be used for validation and verification purposes in Chapter 5. Subsequently, a full day of departures at Amsterdam Airport Schiphol will be considered. Here the entire flight schedule will be used for the combinatorial optimized allocation of runways, routes and procedures for the same day. The last section ends the chapter with a short conclusion.

4.1 Test Case 1: A single waypoint

For this test case all the flights in the schedule that are heading towards the ANDIK waypoint are considered. The area that is overflown by the routes towards ANDIK include both heavily populated and uninhabited areas. As there are three possible routes towards this waypoint (ANDIK 1S, ANDIK 2E, SPIJKERBOOR 3K), the optimization framework has multiple options while the small subset of only 75 flights gives the possibility to process the results in a clear manner. This test case will mainly be used to validate the NSGA-II optimization model. For the noise calculations, the flights are corrected for a full 24 hours, as stated in Equation 3.12. Given the confined amount of flights in this test case, the flights will be multiplied by a factor of eight in order to match the amount of flights in the full schedule. Since the flights towards ANDIK are spread over the day, the departure times of the flights are far apart. The separation feasibility model will therefore not be used for this test case as all solutions are assumed to be feasible.

Table 4.1: Test Case 1: Total fuel and noise of reference solution and initial population

Criterion	Reference Radar data	Reference Modelled	Min. Fuel	Min. Noise
Total fuel used [lb]	440424	450260	441935	476148
Houses within contour of $L_{DEN} \geq 58$ dB(A)	1870	5375	3485	2110
Houses within contour of $L_{night} \geq 48$ dB(A)	2870	3695	3590	3695
People highly annoyed ($L_{DEN} \geq 48$ dB(A))	56189	60019	62986	36723
People sleep disturbed ($L_{night} \geq 40$ dB(A))	6842	6476	10723	6503

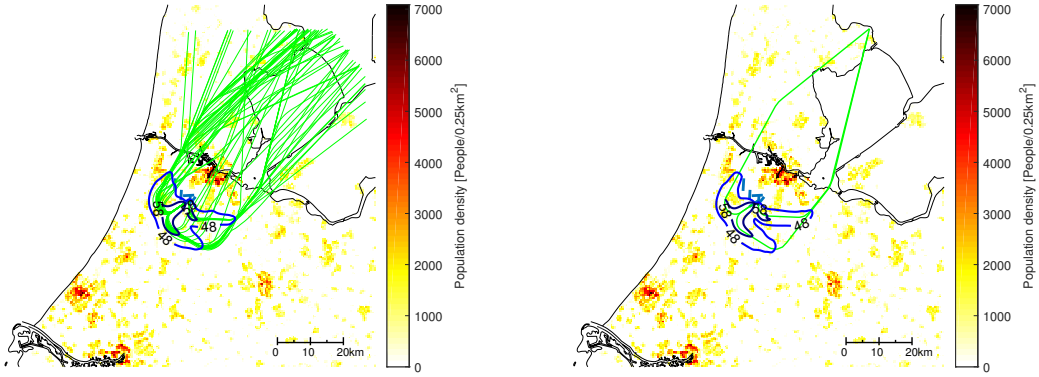

(a) Based on radar data (b) Modelled

Figure 4.1: Test Case 1: Noise contours L_{DEN} in dB(A) of reference solutions.

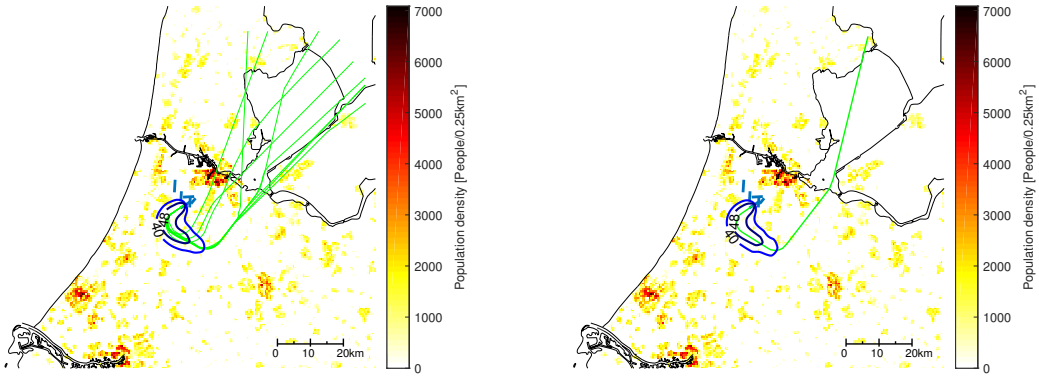

(a) Based on radar data (b) Modelled

Figure 4.2: Test Case 1: Noise contours L_{night} in dB(A) of reference solutions.

4.1.1 Reference Solution and Initial Population

In order to compare the solutions for each of the case studies, the actual amount of fuel used and the actual amount of noise annoyance on that day has to be known. As already explained in Section 3.7.2, the reference solution based on radar data is used for this as a benchmark. The modelled reference solution is subsequently used to put both the solutions that are found and the reference solution based on radar data into perspective. The total fuel used and the calculated values for the four noise criteria of both reference solutions are presented in Table 4.1, and the L_{DEN} and L_{night} noise contours of both reference solutions are shown per grid coordinate in Figures 4.1 and 4.2.

As already discussed in the previous chapter, an initial population is required for the NSGA-II algorithm in order to search in the right direction. This initial population is composed out of the populations that represent the minimum fuel and the minimum noise solutions, and these two will form the most extreme points of the search space. The values of the initial population are also presented in the same table.

4.1.2 Fuel vs. Noise

With the reference solution known, and the two most extreme possible solutions, the NSGA-II can be set up and put to work. Since this optimization will be used as a test case, the size of each of the populations and the length of the optimization will be decreased with respect to the full case study. A population of 50 and an evolution of 250 generations is chosen for this case study.

This subsection only shows the end result, meaning the last generation of the optimization process. Appendix C gives an overview of the optimization, beginning with generation 1 with increments of 50 until the last generation. In Figure 4.3 the final generation is plotted with objective 1 (fuel) on the x-axis and objective 2 (combined noise criteria) on the y-axis. The two stars indicate the reference solutions. The red star indicates the reference solution based on radar data, the green star the reference solution based on the modelled routes. All solutions dominate at least one other solution and therefore the Pareto front is formed by all solutions. As can be seen from the figure, not a single solution dominates the radar data based reference solution, which was already clear from the initial population in Table 4.1. This can be explained due to the fact that the flights in the radar based reference solution are vectored in a diverging manner, and since the flight schedule has few flights, these have not enough noise load in several grid-coordinates to come above the threshold values of the noise equivalence criteria. There is however a solution that scores more or less equal on the fuel objective, and on the other side of the spectrum a solution that scores more or less equal on the noise objective. The modelled reference solution is dominated by several solutions. It should be noted that the optimization has not yet converged, and the amount of generations of 250 can be considered to small. As this test case is only used for validation and verification of the model, the results can still be used for this purpose. In the following paragraphs the solutions are reviewed a little more in-depth.

Figure 4.4 presents the difference that each solution of the optimization has with respect to both reference solutions. These differences are plotted for fuel and each of the four noise equivalence criteria. From left to right the solutions are sorted from least fuel use to the solution with the

largest fuel requirement. As can be seen from the plot on top, the fuel varies almost linearly from 0% difference towards a maximum of 8% increment.

The two subsequent plots represent the equivalence criteria regarding houses within a certain contour. Not a single solution is able to achieve a gain in these two criteria with respect to the radar data reference solution. The modelled reference solution shows a different pattern. For the L_{DEN} noise contour both a gain as a loss can be obtained with respect to this reference. The L_{night} noise contour however shows no possible gain.

Approximately twelve solutions score worse on the amount of people that feel highly annoyed, but the other solutions score better with a maximum gain of more than 30%. The amount of people that are disturbed in their sleep shows a little gain for most of the solutions, although this gain is equal to the value of the modelled reference solution.

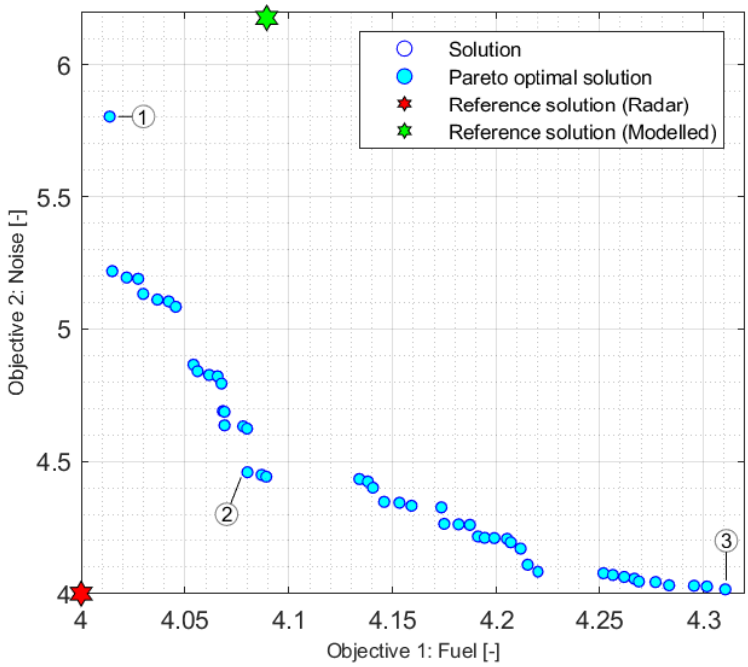

Figure 4.3: Test Case 1: NSGA-II optimization result generation 250/250

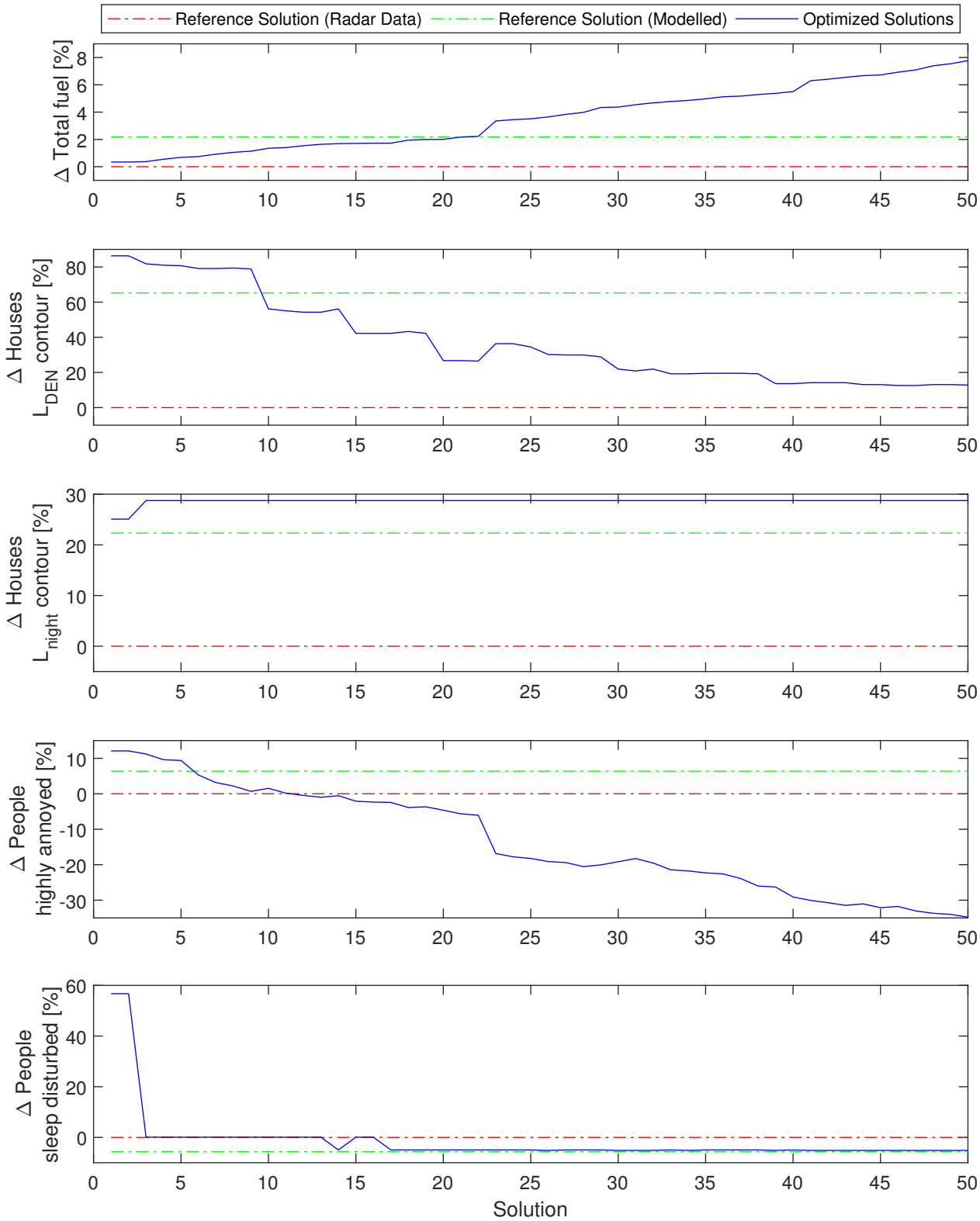

Figure 4.4: Test Case 1: Fuel and Noise difference of different populations

Analysis of noise contours

In these paragraphs the noise contours of the solutions that were found are reviewed in-depth. Since the optimization consists out of 50 optimal solutions, it has been chosen to only elaborate on a few of those solutions. Three solutions have been chosen for this, and are numbered in Figure 4.3. Solution 1 is the fuel-optimal solution and solution 3 is the noise-optimal solution. Both of them score almost equal in terms of the fuel and noise objectives respectively compared to the reference solution based on radar data. Solution 2 is a solution that falls in between solutions 1 and 3; it shows a good balance between the two objectives.

The analysis of the noise contours is based on the L_{DEN} and L_{night} noise levels that can be experienced on a specific grid-coordinate. These noise levels are grouped in several noise level ranges, and are plotted against the number of buildings and the number of people heavily annoyed or sleep disturbed. In this way the four noise equivalence criteria are covered. Figures 4.5 and 4.6 show this analysis, and present a comparison between the two reference solutions and the three chosen solutions from the Pareto front. Two things have to be noted from these figures. First, for each of the figures the two left most groups fall outside the considered noise levels for the respective noise equivalence criteria. Including these groups in the figures makes a broader analysis possible. Second, the noise level ranges in Figure 4.5 have a different distribution in comparison with the noise level ranges in Figure 4.6. The reason for this is the difference between the respective noise equivalence criteria threshold level and the maximum experienced noise level. For example, the noise equivalence criteria for the amount of people heavily annoyed includes the inhabitants experiencing a L_{DEN} value of 48 dB(A) or above, while the noise equivalence criteria for the amount of buildings only starts from L_{DEN} values of 58 dB(A).

A first thing that can be observed from the distribution of noise is that for the more noise optimal solution, relatively more noise is experienced by people living in areas below the threshold noise values, offset by a smaller group of people that would have been highly annoyed with higher noise levels. This tendency is at the cost of the people living really close by the airport, who experience a higher noise level. The plots in Figure 4.5 that consider the noise equivalence criteria for the amount of buildings show the same tendency, although the threshold value for the noise equivalence criteria is higher whereby not only the highest noise level group grew in terms of the amount of buildings but also the second and third highest.

It is also possible to compare the plots between the L_{DEN} based noise equivalence criteria and the L_{night} based ones. As can be noted from the plot, not much variance for the L_{night} based criteria in the amount of buildings or amount of people that are disturbed while sleeping is possible over the different noise level ranges. This can be explained due to the few amount of flights that operate at night and that those are already quasi-optimal in terms of noise annoyance. The L_{DEN} based noise equivalence criteria show a much more varied pattern which indicates that there is a lot of deviation possible within the entire solution set.

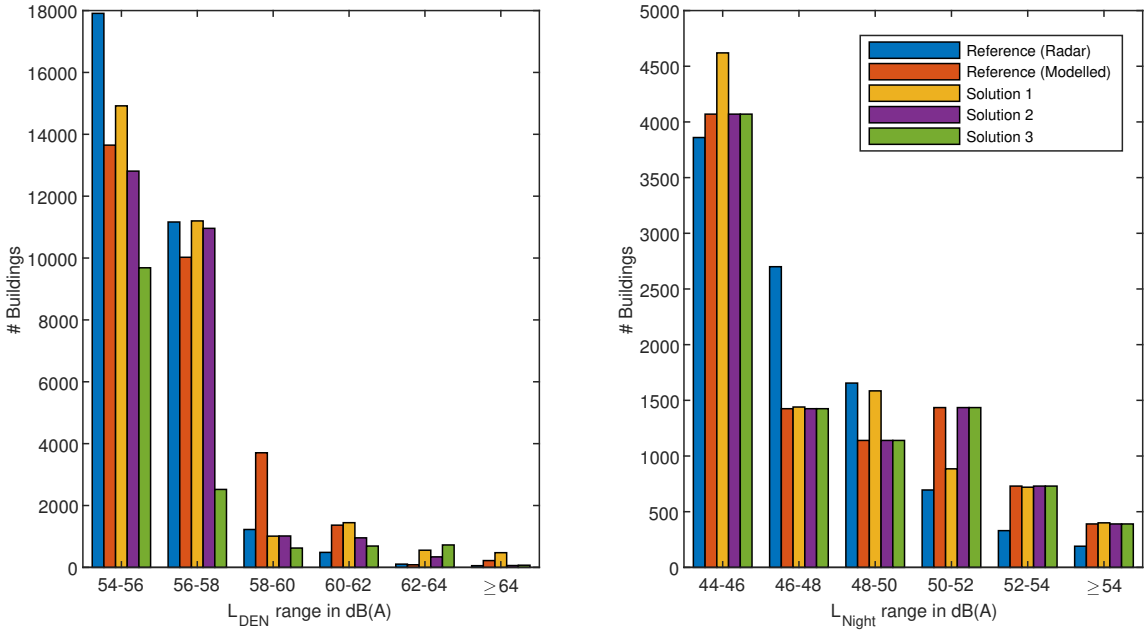

Figure 4.5: Test Case 1: Distribution of buildings over different noise level ranges.

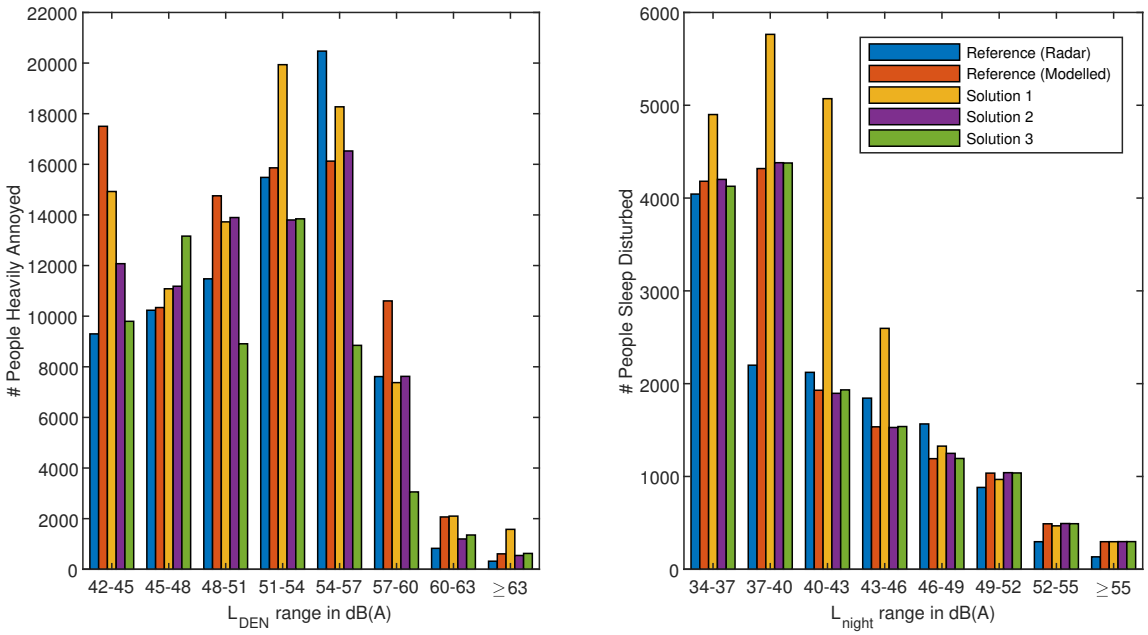

Figure 4.6: Test Case 1: Distribution of people heavily annoyed and sleep disturbed over different noise level ranges.

Table 4.2: Test Case 2: Total fuel and noise of reference solution and initial population

Criterion	Reference Radar data	Reference Modelled	Min. Fuel	Min. Noise
Total fuel used [lb]	95589	95149	94286	100345
Houses within contour of $L_{DEN} \geq 58$ dB(A)	3870	4265	5755	1675
People highly annoyed ($L_{DEN} \geq 48$ dB(A))	49410	52624	48328	24793

4.2 Test Case 2: A single bank

Amsterdam Airport Schiphol operates as a hub airport. Aircraft arrive and depart in short periods of time such that a transfer from one flight to a subsequent flight is convenient for passengers. A clustering of flights (a so-called 'bank') of the reference flight schedule, between 07:30 and 10:00, is chosen for this test case. This period, which consists of 124 departures, already proved to be a peak during the day in Figure 2.8. The results of this test case study will mainly be used to validate the separation feasibility and delay model in the next chapter. It is also because of this intention that the solutions found in the NSGA-II optimization process will not be investigated in-depth for this test case.

In comparison with test case 1, the flights in this test case will not be multiplied by a certain factor in order to have enough impact. Since the flights are operated within a confined period of time, the last term in the calculations of L_{DEN} (Equation 3.12) will be altered to correspond with this time span of the departure peak of 2.5 hours. As one might have noticed, since all flights are operated during the day-period, the penalty term in this equation will be equal to one for all flights.

4.2.1 Reference Solution and Initial Population

In line with the method for test case 1, radar data is used to provide a reference solution in order to compare the results of the optimization algorithm. The flights in the flight schedule between 07:30 and 10:00 have been modelled according to their respective radar tracks while performing flight procedure NADP2. As no flights in the night period are included, the L_{night} noise metric and two of the noise equivalence criteria are left out. The resulting noise loads for L_{DEN} are shown per grid-coordinate in Figure 4.7, and the amount of fuel used and the two remaining noise equivalence criteria are presented in Table 4.2. The table is augmented with the data of the reference solution based on modelled routes. The initial population is formed by the minimal fuel and minimal noise solution, and the numbers of these solutions can also be found in the same table.

4.2.2 Fuel vs. Noise

Similar to test case 1, the NSGA-II optimization for test case 2 consists of a population of 50 which evolves over 250 generations. With the solutions that represent the minimum fuel and minimum noise annoyance solutions as starting point, the optimization process is initiated. The resulting final

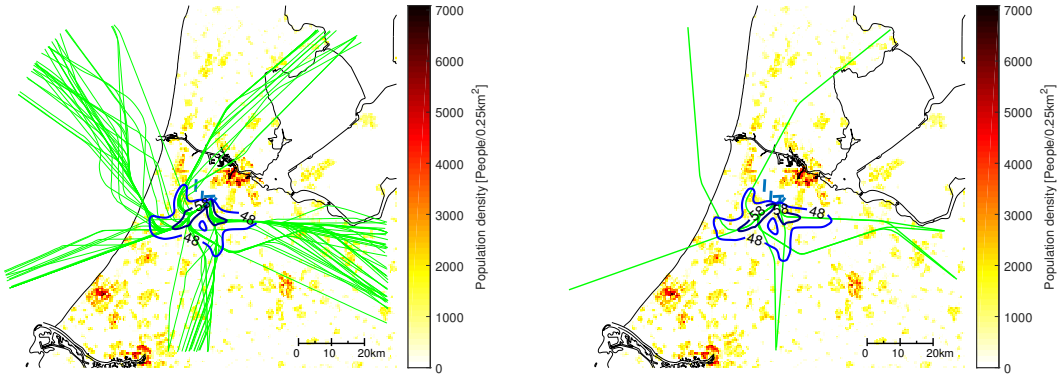

(a) Based on Radar Data

(b) Modelled

Figure 4.7: Test Case 2: Noise contours L_{DEN} in dB(A) of reference solution.

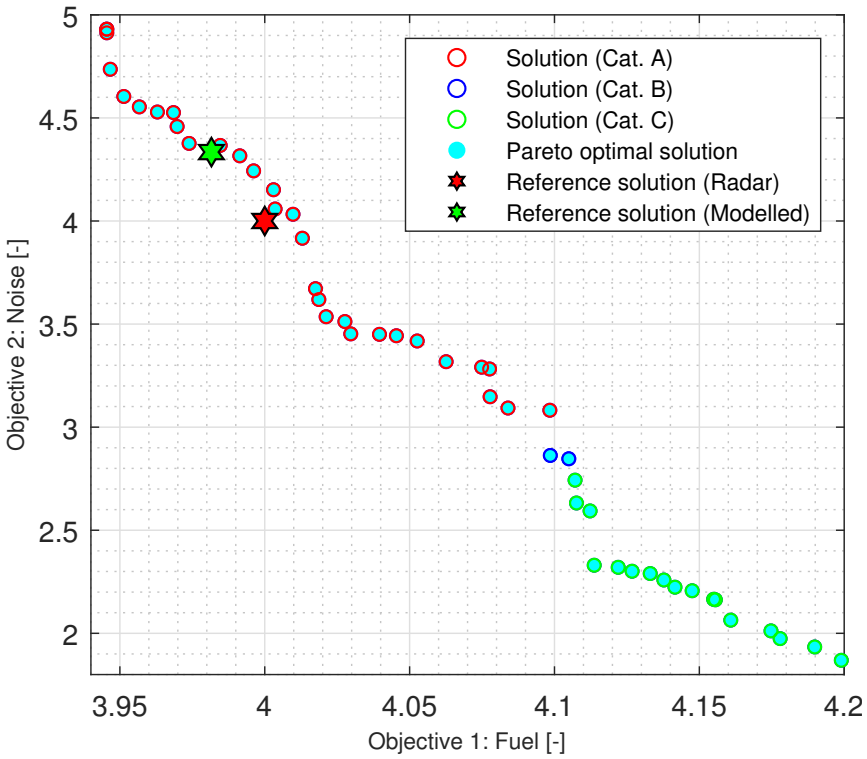

Figure 4.8: Test Case 2: NSGA-II optimization result generation 250/250

generation is presented in Figure 4.8, of which all solutions are dominant and therefore together form the Pareto front. Both reference solutions more or less lay on this front, and cannot yet be considered as one of the optimal solutions. With respect to the reference solution based on radar data, a maximum gain of 1.38% can be obtained by allowing 18.9% extra noise annoyance. On the other side of the Pareto front, the maximum reduction of noise annoyance can be 53% which comes at a cost of 5% extra fuel required. The development of the populations over the generations can be seen in Appendix C.2. It should be noted that also in this test case, in line with test case 1, the optimization has not yet converged. Given the purpose of this test case, to use it for validation and verification, the result is however found to be appropriate.

Table 4.3: Test Case 2: Overview of imposed delay.

	Delay Range [s]	**Number of Solutions**	**Average Flights with Delay**
A	106 - 1718	31	33
B	5849 - 7501	2	85
C	19972 - 55702	17	104

4.2.3 Delay

In the last subsections the results of a test case study were presented. This test case comprises a single bank taken from the flight schedule of Amsterdam Airport Schiphol. The solutions presented some interesting results, such as a possible gain of 50% in terms of the noise equivalence criteria, at a small cost of only 5% more fuel that is required for the flights. It is however not yet clear if the flight distributions that were found (each solution represents a flight distribution) are even possible if one looks at the take-off runways and flight paths of those flights. Enough time separation needs to be in place in order to assure safe operation. As described in Section 3.6, a model has been developed that adheres the separation requirements and imposes a take-off delay if this is not satisfied. The flight distribution is divided over the scheduled flights so that the required amount of flights are operated by the right aircraft, runway, route and procedure combination.

It is assumed that the reference solution based on radar data is performed without any delay. This assumption is made as the Actual Time of Departure (ATD) is used as departure time of the modelling. In the ATD probable delays are already taken into account, and therefore the radar tracks as flown can be considered to be operated without any delay. Furthermore, the radar tracks follow a diverging pattern from which separation between different aircraft is maintained. The modelled reference solution however follows the prescribed SIDs, and is therefore analyzed with the separation feasibility model as well. It has been found that in total 49 seconds of delay is required for the 124 flights in the schedule. Out of these 124 flights, only five require a delay, which in total add up to 49 seconds.

In Table 4.3 a small overview is presented of the delay results found for test case 2. Three categories can be identified: flights with a relative small delay, a very large delay and a couple of solutions that fall in between. For the first category, 31 solutions fall within this delay range and on average 33 flights within those solutions require a delay in order to satisfy the separation requirements. On

the other side of the spectrum, 17 solutions fall within the largest possible delay range. 104 flights on average out of the 124 require a delay in order to meet the requirements. The three categories that are indicated in this table are also color-coded in Figure 4.8. As one can see the categories are not scattered across the figure, but are nicely grouped together. For the entire solution set, the relation between the total delay and the amount of flights with delay is presented in Figure 4.9. In this figure the reference solutions are also included. The three solution categories are grouped, and follow an almost exponential pattern. Adding an extra flight with delay causes a lot of extra delay. It can also be seen that none of the solutions score as good as the reference solutions in terms of delay, although category A comes close.

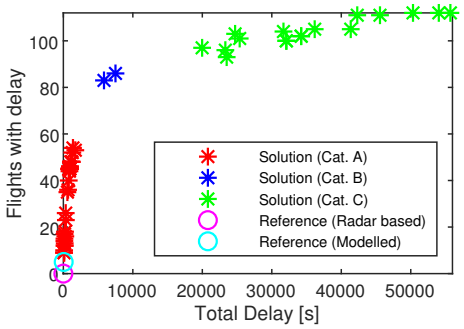

Figure 4.9: Test Case 2: Relation between total delay and number of flights with delay.

To know if the separation requirements are satisfied, three locations along each of the flight paths are investigated. Two aircraft that consecutively depart from the same runway require enough time separation between each of their departures. Figure 4.10 shows three box plots of the delay that has been imposed at departure. The left most plot (a) contains the amount of flights that require a take-off delay based on their scheduled take-off time. The 'scheduled+propagation' plot in the middle (b) shows the same flights, but only those that require a delay resulting from an earlier imposed delay as well. The right plot (c) presents the amount of flights that need a take-off delay that originates from an earlier delay. The number of flights that are presented in this figure is larger than the number of flights in the flight schedule, which results from the fact that these flights are checked upon the 10 earlier flights and thus shows the total amount of conflicting departure times.

There is a possibility that the flight paths of tho flights cross at a certain point in the airspace. In Figure 4.11 the delay that is required at the crossing point is presented. It has to be noted that this actually is the delay that is added to the departure time, in order to have enough separation at the crossing point. The plots are presented equal to the plots in Figure 4.10. The left plot shows the amount of flights for which a delay was required based on their scheduled departure time, and the plot in the middle shows if these flights also required a delay that originates from an earlier flight. The plot on the right shows flights that require a delay only because of delay that has propagated from earlier flights.

Figure 4.12 shows delay that is required for flights that have the same terminal point. When these flights arrive at this location enough time separation has to be in place. A delay to enforce this is added to the departure time, in order to end up at the terminal point with sufficient time separation. The plots present the same data as for Figures 4.10 and 4.11.

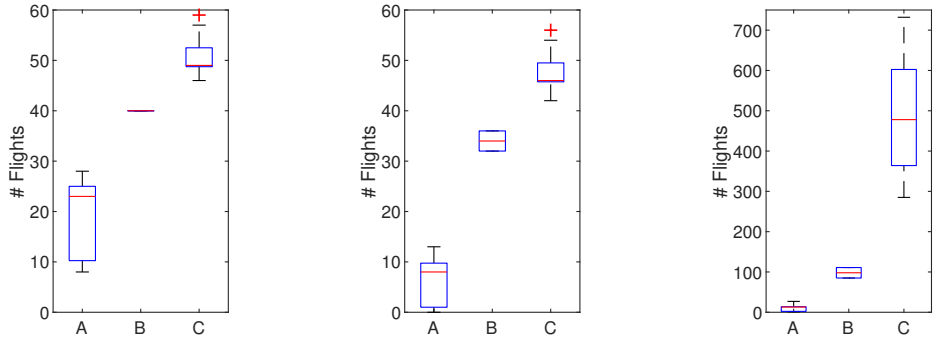

(a) Scheduled (b) Scheduled + Propagation (c) Only Propagation

Figure 4.10: Box plot of delay required at take-off presented per delay range.

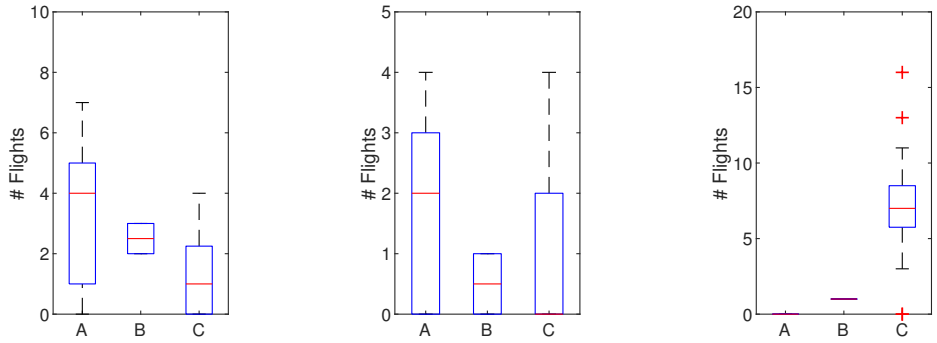

(a) Scheduled (b) Scheduled + Propagation (c) Only Propagation

Figure 4.11: Box plot of delay required at crossing presented per delay range.

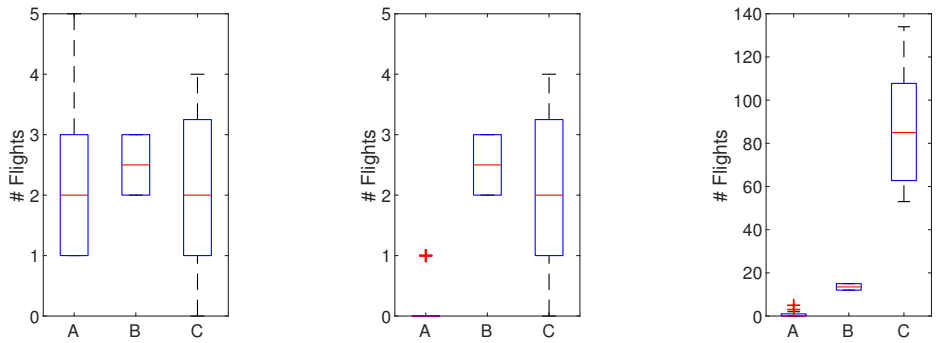

(a) Scheduled (b) Scheduled + Propagation (c) Only Propagation

Figure 4.12: Box plot of delay required at waypoint presented per delay range.

4.3 Case Study: A full day at Schiphol

Although much effort is already put into fuel reducing measures and noise annoyance mitigation at Schiphol, there might be a more optimal combination of runways, routes and procedures given that these are not designed and allocated combinatorial. In this section a case study is presented for the integrated optimization of the allocation of runways, routes and procedures of a full day at Amsterdam Airport Schiphol. The section starts with the reference solution, which is the total amount of fuel and values for the noise equivalence criteria of the reference flight schedule of October 22, 2010. The framework will optimize with respect to these numbers. The second subsection presents the initial solution and population, which is required as stated in Section 3.7.6. The flight schedule will be optimized with respect to fuel and noise subsequently, after which the final generation of this optimization will be used as input to test if these schedules are feasible.

4.3.1 Reference Solution and Initial Population

As already discussed for the two test case studies, a reference solution is required in order to verify the quality of the found solutions. The reference solution that is used as benchmark is based on radar data of the flights that flew on October 22th 2010, modelled according to the method described in Subsection 3.7.2. A second reference solution is based on their official designated SIDs, and both reference solutions are modelled with NADP2. A visual representation of the noise contours L_{DEN} and L_{night} of both are shown in Figures 4.13 and 4.14 respectively. The corresponding values of the reference solutions for total fuel and the four noise equivalence criteria are presented in Table 4.4.

Two populations will be composed and together with the reference solution these three will be added to the initial population of the NSGA-II optimization. The first population that will be calculated is the population that represents the minimum required fuel flight distribution while taking all the constraints into account. The second population represents the second objective of the optimization, the combined noise criteria. The values found for the minimum fuel and minimum noise solution are presented in the same table as the reference solution.

4.3.2 Fuel vs. Noise

The initial solution, consisting out of the two most extreme solutions in terms of fuel and noise, forms the basis of the optimization process. The reference solution will be used to compare the found solutions of the optimization. For this case study a population of 100 is chosen while the evolution runs for 500 generations. This results in 500.000 iterations that consists of the formation of a flight distribution and the calculations of the amount of fuel and noise equivalence criteria.

The entire population of the final generation is presented in Figure 4.15. An overview of intermediate generations can be found in Appendix C. The x-axis in the figure represents objective 1 (fuel) and the y-axis represents objective 2 (noise). Again the reference solutions are indicated with the red and green stars. Although the entire population is plotted in the figure, not all solutions are

Table 4.4: Total fuel and noise of reference solution and initial population

Criterion	Reference Radar data	Reference Modelled	Min. Fuel	Min. Noise
Total fuel used [lb]	423072	423894	409802	442410
Houses within contour of $L_{DEN} \geq 58$ dB(A)	3370	4285	8625	2385
Houses within contour of $L_{night} \geq 48$ dB(A)	4525	4900	9905	4785
People highly annoyed ($L_{DEN} \geq 48$ dB(A))	43918	44500	48541	22462
People sleep disturbed ($L_{night} \geq 40$ dB(A))	11891	9717	22726	9810

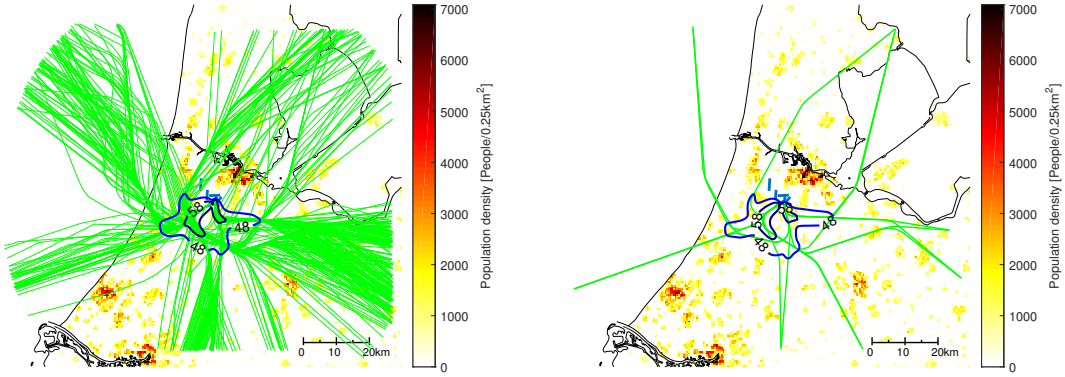

(a) Based on radar data (b) Modelled

Figure 4.13: Noise contours L_{DEN} in dB(A) of reference solutions.

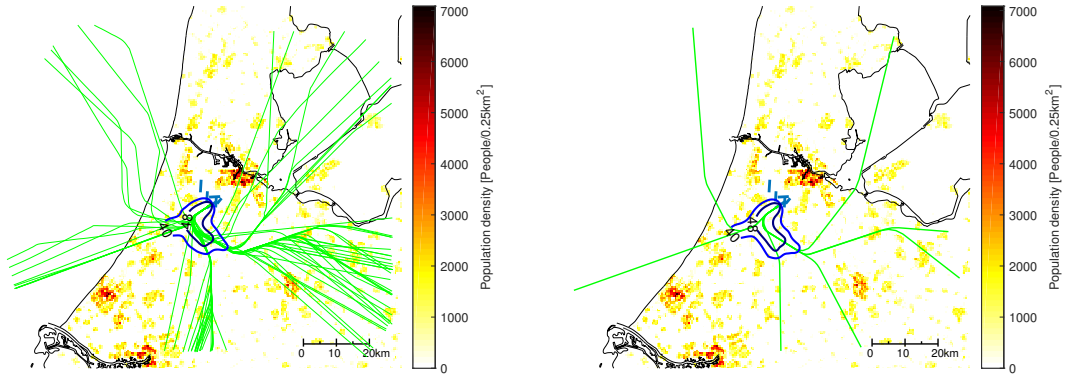

(a) Based on radar data (b) Modelled

Figure 4.14: Noise contours L_{night} in dB(A) of reference solutions.

dominant. The Pareto optimal solutions, the solutions that dominate the other solutions in at least one of the objectives, are indicated as the filled circles in the color cyan. These 91 solutions together form the Pareto front. Since it is not yet known of any of the solutions found are feasible regarding separation requirements, the entire population is maintained for the time being.

Looking at the figure it can be noted that both reference solutions are actually located on the Pareto front. Given its location on the figure the reference solution can also be considered as optimal. The Pareto front bends at the location of the reference solution from almost vertical on the left side of the figure into a diagonal pattern. It also has to be noted that only a marginal gain can be maid in terms of fuel use. This marginal gain comes at a cost of 13% loss with respect to objective 2, the noise equivalence criteria. The most optimal solution regarding the latter shows a 31% profit. This profit however comes at a cost of approximately 4% in the total required fuel. If the modelled reference solution is considered, indicated in green, the found solutions show a slightly better performance. Nonetheless it has to noted that only small gains in the total amount of fuel can be realized while gains in noise annoyance can be significant.

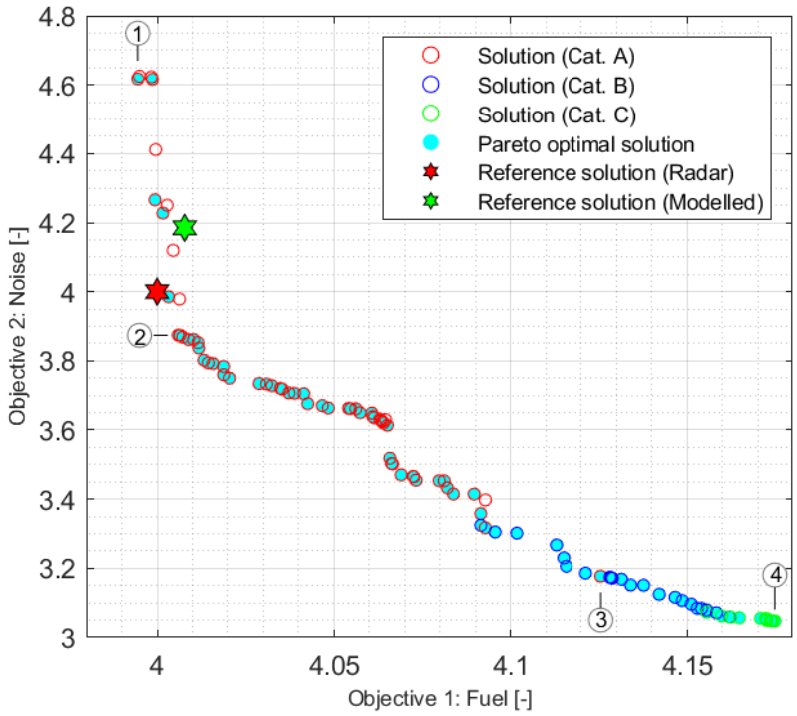

Figure 4.15: NSGA-II optimization result generation 500/500

The Pareto front discussed in the previous paragraphs presents a global overview of the found solutions. Each point on the grid stands for a specific solution that contains a certain flight distribution. This is a distribution of aircraft type over the different routes and procedure combinations, for day, evening as well as the night period. Such a flight distribution subsequently represent a total amount

of fuel and a value for each of the four noise equivalence criteria. Figure 4.16 presents the difference of these five values with respect to the reference solution and indicates the alteration of these over the different populations of the final generation. All 100 solutions are included and are sorted in line with Figure 4.15. In other words, populations that score less on objective 1 (fuel) are placed more to the right of the figure. The five plots that the figure contains are sorted accordingly such that one can compare the results of a single solution vertically over the different plots. Each plot also contains a red and green dashed line, representing the reference solutions based on radar data and modelled routes respectively. The following paragraphs explain the different plots globally. A more thorough analysis and discussion of the result can be found in the next chapter.

The plot on the upper side of the figure contains the result of the total fuel used. As can be seen almost all solution score worse on this objective than both the reference solution based on radar data as the modelled reference solution. Only six solutions score more or less equal to both of them. All other populations score worse, with a maximum increment of 17.5%.

The second plot shows an erratic pattern of the amount of houses within the $L_{DEN} \geq 58dB(A)$ contour. Almost half the solution score worse, where the amount of houses affected can be up to 60% higher. The best solution scores almost 30% better with respect to the reference solution. Looking at the modelled reference solution, indicated with a green horizontal line, almost 90% of the solutions have a better result regarding the houses in the L_{DEN} contour.

In the center of the figure the plot presents the difference for noise equivalence criteria two, the amount of houses within the $L_{night} \geq 48dB(A)$ contour. None of the solutions score better, in fact most of them score almost 6% worse. Meanwhile these solutions score 2% better with respect to the modelled reference solution.

The fourth plot contains the difference in the amount of people that are highly annoyed within the $L_{DEN} \geq 48dB(A)$ contour. All solutions score better than both reference solutions, ranging from a small gain of 2% to almost 50%.

On the bottom of the figure the last plot presents the difference of people that are disturbed in their sleep that live within the $L_{night} \geq 40dB(A)$ contour. Most solutions perform better, with a maximum possible gain of 17.5%. The highest loss is around 4%.

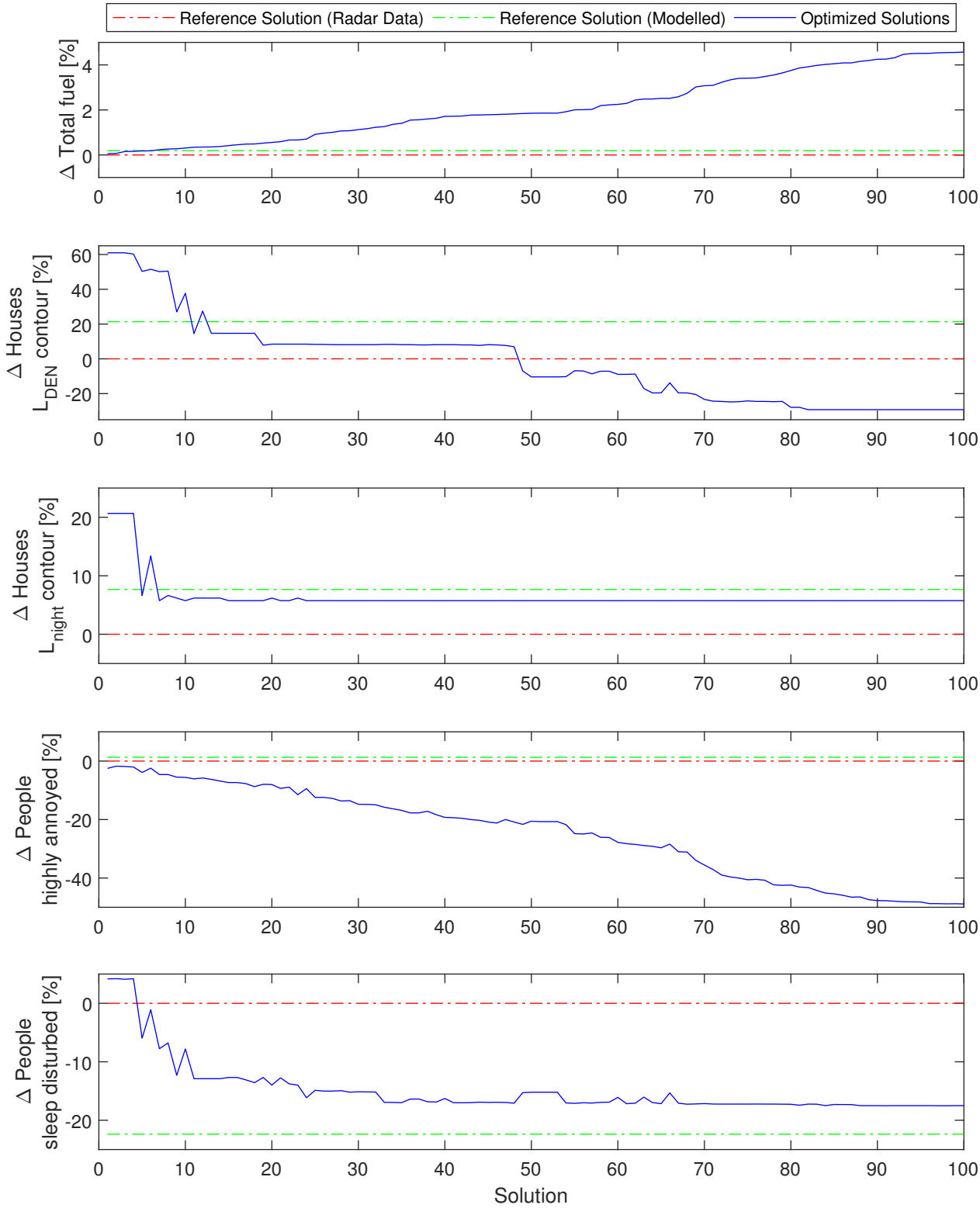

Figure 4.16: Fuel and Noise difference of different populations

Analysis of noise contours

The entire final population of the optimization was presented in the previous paragraphs. Besides analyzing these solutions based on their objective values, they can also be analyzed according to the L_{DEN} and L_{night} contours. This process has already been presented for Test Case 1, therefore this part will only present the related plots and a short explanation. An extensive elaboration is added in the discussion in Chapter 5.

Figure 4.17 presents the amount of buildings that fall within a specific noise level range, and Figure 4.18 shows the amount of people that are heavily annoyed or sleep disturbed within a specific noise level range. Both figures differentiate between L_{DEN} and L_{night} noise levels, and in this way the four noise equivalence criteria are treated. The plots consists of six data sets, consisting out of the two reference solutions and four solutions that where picked from the entire spectrum of solutions from Figure 4.15. Solutions 1 and 4 are the fuel-optimal and noise-optimal solutions, respectively. Solution 2 is a solution that has a good balance between the two objectives, and is located on the Pareto front where the more vertical and diagonal part intersect. Solution 3 is included as it is the noise-optimal solution of solution category A. These categories will be introduced further in the elaboration of possible imposed delay in Section 4.3.3.

As can be seen from the left plot in Figure 4.18, the amount of people heavily annoyed is considerably less comparing the reference solution with the four solutions for the noise levels between 48 and 57 dB(A), even for the fuel-optimal solution 1. The model tends to shift noise below the threshold value at the benefit of the people that live inside the considered noise contours. In the areas close by the airport, where not so many people live but the noise levels are higher, the noise is concentrated even more. This same pattern can be seen in the right plot of the Figure, that considers the L_{night} noise contours.

In Figure 4.17 the amount of buildings that fall within a specific noise level range are shown, and the respective noise equivalence criteria have a higher threshold value than the criteria for the amount of people heavily annoyed and sleep disturbed. As noise is concentrated in the area in the direct vicinity of the airport, this has a direct effect on the amount of buildings affected. The higher noise level ranges score worse with respect to the reference solution, and only the lower noise level ranges (58 till 62 dB(A)) perform better.

Comparing the plots that consider the L_{DEN} noise contours and the plots that consider the L_{night} noise contour, it can be observed that not much variance is obtained in the L_{night} noise level ranges. This is due to the lower amount of departures during the night and the fact that these are already restricted in their operations. Most of the gains have to come from the flights that operate during the day and evening period.

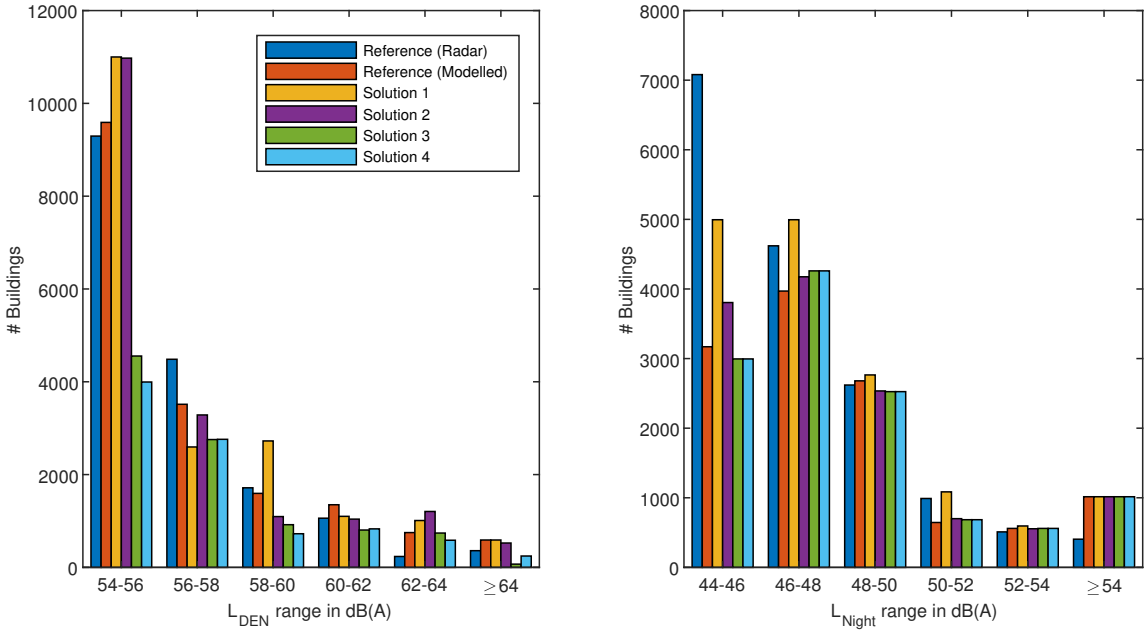

Figure 4.17: Distribution of buildings over different noise level ranges.

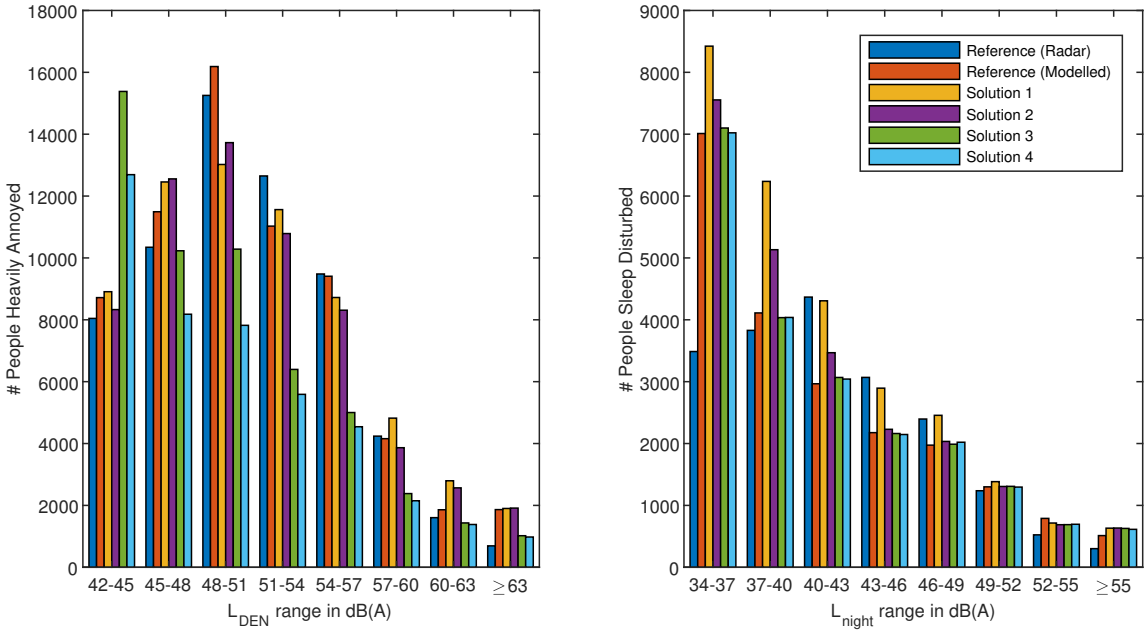

Figure 4.18: Distribution of people heavily annoyed and sleep disturbed over different noise level ranges.

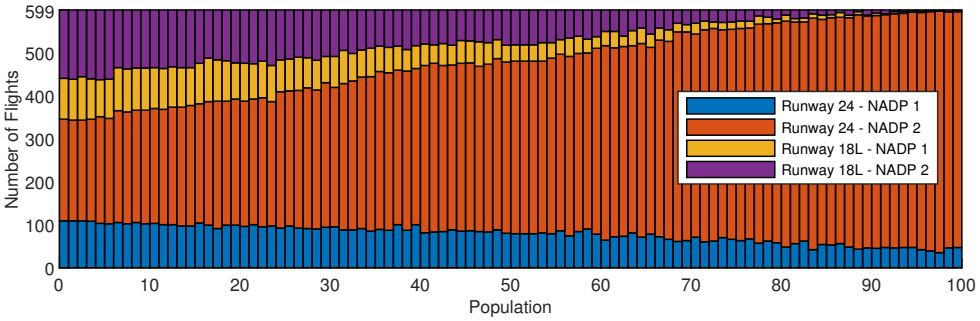

Figure 4.19: Distribution of flights over the different runways and procedures for each population

Analysis of the allocation of runways, routes and procedures

In the previous sections the entire final solution has been presented, and the different objective values have been elaborated upon. Subsequently the noise contours were analyzed, where it was shown that noise is pushed to lower noise levels in order to decrease the amount of buildings and people affected. The differences in fuel usage and noise annoyance between the solutions in the solution set and the reference solutions are obtained by the reallocation of runways, routes and procedures to the flights in the flight schedule. These paragraphs explain where possible gains are obtained.

Irrespective of waypoint and aircraft type, all seven terminal points can be reached from each of the two runways. Furthermore, each SID can be flown by either performing NADP1 or NADP2. Figure 4.19 shows the distribution of flights over the four possible runway and procedure combinations, for all 100 solutions. The solutions are sorted from fuel-optimal on the left to fuel-worst (or noise-optimal) on the right. Several patterns can be obtained from this figure. First, the number of flights that depart from runway 18L decreases from left to right. During this decline, the ratio between NADP1 and NADP2 stays more or less equal. The flights that do not depart from runway 18L, have to take-off from runway 24. Hence, the number of flights that depart from runway 24 increases from left to right. It is however noticeable that the ratio between NADP1 and NADP2 does not stay constant, but decreases from left to right. Departing from runway 24 with NADP2 can be considered the most noise avoiding runway and procedure combination.

Besides considering the distribution of flights over the two runways and two procedures, the distribution of flights can be reviewed more in-depth by looking at changes in the distribution over the different waypoints and the different aircraft type. Such an analysis is presented in Figure 4.20, and shows the result for the four solutions that were also used in the noise contour analysis of the previous subsection. The empty locations in the figure result from certain aircraft type that have no flights to that waypoint. For all the different charts in the figure, it has to be noted that the actual number of flights is used on the vertical axis rather than a percentage of the total number of flights. This might present a distorted picture, but gives the opportunity to valuate each graph with respect to other graphs. Waypoint 'Andik' consists of six possible runway and procedure combinations, which is reflected by the two added bar colors for these graphs. It has to be noted

that the two extra runway and procedure combinations also depart from runway 24.

First of all, considering the totals on the left side of each subfigure. By comparing the different aircraft type with the total distribution of the four chosen solutions, most aircraft type follow the same pattern. The Boeing 767-300 has a larger share of aircraft that perform NADP1 with respect to the other types. The Boeing 747-400, the only four-engined aircraft, has more flights departing from runway 18L for the first three solutions. This can be explained by the fact that the routes from this runway are shorter and therefore require less fuel and do not add that much extra noise.

The second comparison can be made between the totals of the different waypoints. It can be seen that both 'Arnem' and 'Rendi' have a higher portion of aircraft that depart from runway 18L. For these destinations the use of this runway is more convenient as the flight paths of these routes are shorter. Also, these waypoint have a higher proportion of aircraft that perform NADP1, which can be explained due to the vicinity of residents at runway 18L. The terminal points 'Bergi' and 'Valko' present the other side of the spectrum, they both have a large share in departures from runway 24. These terminal points lay closer to the end of runway 24 than the end of runway 18L, and therefore this runway is used more often. Waypoints 'Lopik' and 'Kudad' have not necessarily a different number of flights from one of the two runways compared to the totals, but aircraft that depart from runway 24 have a large share of NADP1 departures. The presence of inhabitants underneath the routes from runway 24 to these waypoints explains this tendency.

Most of the graphs of the different aircraft types show the same pattern as their comparable graphs for the totals, with some outliers for terminal points that receive little traffic. Waypoint 'Arnem' shows a lot more aircraft of the largest three types that depart from runway 18L compared to the smaller Fokker 100 and Boeing 737-800. This can be explained by the fact that the latter two require less fuel and cause less noise annoyance, so it is more convenient to shift larger aircraft to runway 18L instead of the smaller ones. The terminal points 'Bergi' and 'Valko' are approached by the smaller two aircraft type more often from runway 18L compared to the larger three aircraft type, of which almost all aircraft depart from runway 24. This is due to the fact that the flight path from runway 18L is longer, and thus would cause more noise annoyance and require extra fuel.

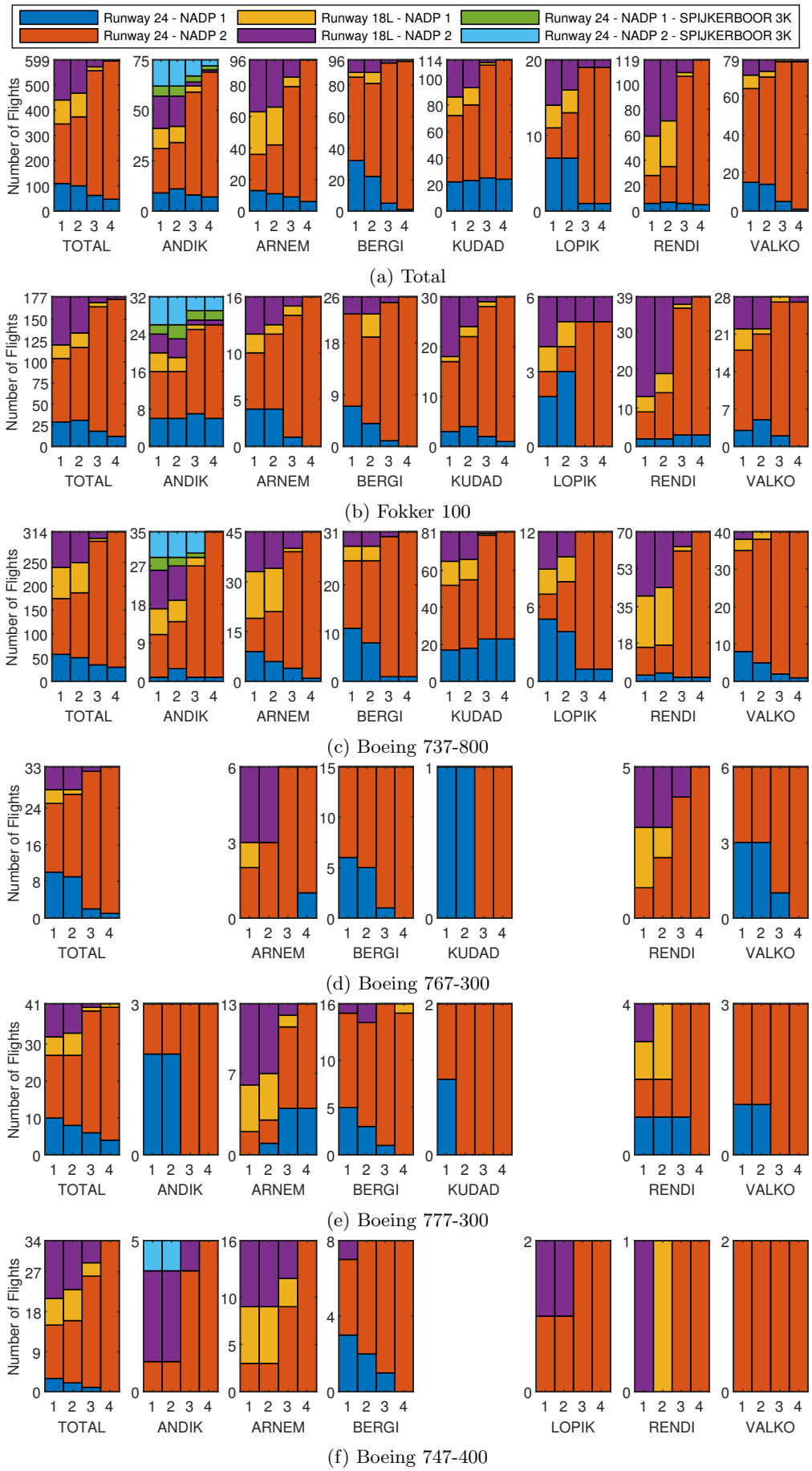

(a) Total

(b) Fokker 100

(c) Boeing 737-800

(d) Boeing 767-300

(e) Boeing 777-300

(f) Boeing 747-400

Figure 4.20: Flight distribution over different runways, routes and procedures. Total, per waypoint and per aircraft type.

Table 4.5: Overview of imposed delay.

	Delay Range [s]	Number of Solutions	Average Max. Delay [s]	Average Flights with Delay
A	0	66	-	-
B	2 - 767	22	205.4	9
C	1441 - 6458	12	3345.0	35

4.3.3 Delay

A set of possible flight distributions has been composed in the optimization process which was presented in the previous subsections. An entire day at Amsterdam Airport Schiphol has been investigated, a day that comprises out of 599 flights. It is assumed that the reference solution is feasible regarding separation requirements and that no delay has to be imposed in order to meet these requirements. The set of possible flight distributions has been researched in order to find out if these solutions are feasible with respect to the separation regulations as well.

A (positive) take-off delay can be imposed that shifts a flight along its flight path over time. The purpose of this is to have enough clearance at the take-off runways, possible crossing points and the terminal point of the flight. In Table 4.5 an overview of the results of this separation feasibility model is presented. As can be seen, 66 solutions require not a single delay over the entire day. These solutions are able to spread their flights over the two runways, as was already presented in Section 4.3.2. 22 solutions need a delay that falls within the range of 2 to 767 seconds, and on average 9 out of 599 flights require such a delay. The last category encompasses 12 solutions, that require a delay between 1441 and 6458 seconds. Of the 599 flights in the schedule, this category requires 35 of those flights to postpone their take-off for a small amount of time. These three categories are also color-coded in Figure 4.15. As one can see the categories are not scattered across the figure, but are nicely grouped together from left to right. It is assumed that the radar based reference solution is executed without any delay, as the ATD is used as departure time and possible applicable delay was already incorporated in these timings. The modelled reference solution is analyzed in a similar manner as the found solution set. A delay of 226 seconds is required for the entire flight schedule of the modelled reference solution, divided over 18 of the 599 flights. The total delay versus the amount of flights with delay of the solution set and reference solutions are plotted in Figure 4.21. Each of the three solution categories follow a comparable pattern. Category A is at the origin, category B follows a more vertical pattern while the solutions in category C are plotted in a more horizontal pattern. From the figure it can be concluded that delays add up almost exponentially. Category C can be regarded as infeasible, but the solutions inside category A and B are feasible.

Figure 4.22 presents the amount of flights that require a delay for the solutions in category B. These box plots show the dispersion between those solutions. In the left most plot (a) the flights with a violation of the separation at departure are presented. The second plot (b) shows delay that is required for a crossing point and the right plot (c) shows the number of flights with a delay due to separation requirements at their terminal point. In Figure 4.23 the solutions that fall within category C are presented. Again the plots show the delay that is required for flights due to departure separation, crossing separation and terminal separation requirements, respectively.

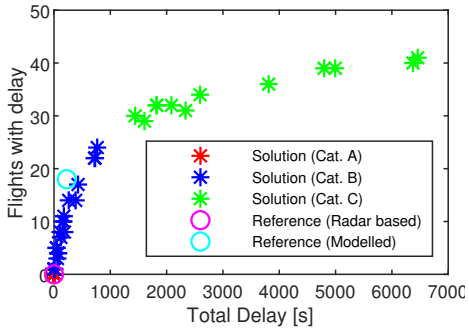

Figure 4.21: Relation between total delay and number of flights with delay.

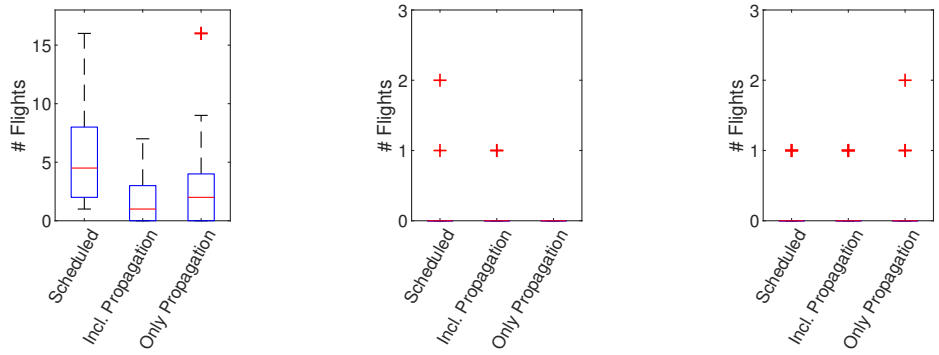

(a) Departure (b) Crossing (c) Waypoint

Figure 4.22: Box plot of delay required for solutions of category B presented per delay range.

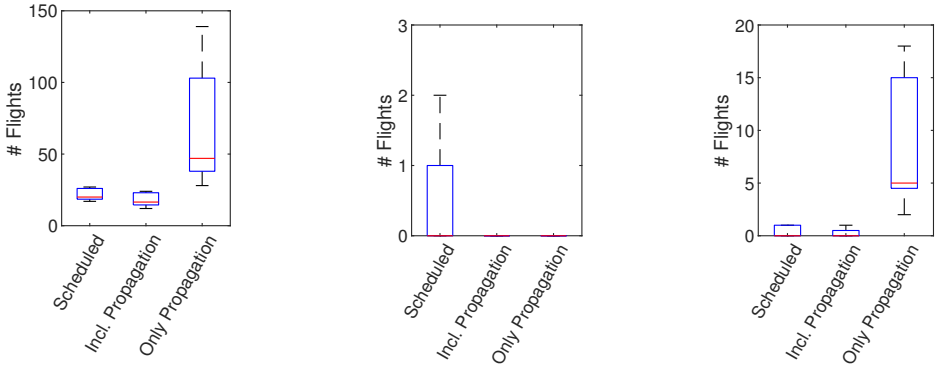

(a) Departure (b) Crossing (c) Waypoint

Figure 4.23: Box plot of delay required for solutions of category C presented per delay range.

Chapter 5

Discussion

In this chapter the results found for the integrated optimization framework will be discussed, together with a discussion on the working principle of the framework itself. The first section of this chapter presents the verification and validation of the framework, which is done by means of two test cases. These test cases are performed in order to check if all component parts of the framework behave how they are supposed to behave. The second section discusses all the results of the case study. This section is subdivided in line with the previous chapter. First the reference and initial solutions will be discussed, followed by the optimization for fuel and noise and after that the feasibility check with respect to the separation requirements.

5.1 Verification and Validation

This section discusses the verification and validation of the integrated optimization framework. These processes are required to check the usability of the model. The first subsection discusses the verification and the validation process is discussed thereafter. Results coming from the two test cases are used for both these processes.

5.1.1 Verification

The verification process is in place in order to evaluate whether or not the integrated optimization framework meets the design requirements and shows the desired behaviour. This evaluation is performed for each individual part of the framework separately.

The calculations of noise and fuel of a flight distribution are performed with the help of the database with routes and a Geographic Information System (GIS). In these calculations the fuel of all flights are summed, and also the L_{DEN} and L_{night} contours are calculated. Subsequently these contours

are used to relate them to the four noise equivalence criteria. In order to verify the working principle of this part of the framework, several steps are taken. For the calculations of the fuel and noise contours, dummy flight schedules are inserted that create the opportunity to track all calculations. The expected outcomes of these dummy flight schedules are also calculated manually so that these can be compared with the model. The noise contours encompasses a wide area of land that consists of a large number of grid-coordinates. The buildings and inhabitants within these contours are required for the calculations of the four noise equivalence criteria. Given the amount of data points, the contours are plotted on a map and for verification purposes the encompassed grid-coordinates are marked with a color. With the help of this visual interpretation it is verified that the model uses the right grid-coordinates and number of buildings and inhabitants located at those coordinates.

The 'popMaker'-function is used to convert the continuous variables of each population into a flight distribution that consists of integers. Dummy variables are used to verify the behaviour of this function. Also the correction factor that is required because of the rounding of the integers is verified using these dummy variables.

With the two parts discussed above, the NSGA-II algorithm is set up. By tweaking the objective function of the optimization the behaviour of the multi-objective algorithm is checked. For example, in order to find a solution where the fuel objective is more important than the noise objective, a correction factor can be inserted. In this way it is verified that the optimization model makes a proper consideration between the objectives. Furthermore, some of the solutions, that represent a flight schedule, are reviewed in detail by which it was shown that certain runway, route and procedure combinations were given the preference for a more fuel optimal solution or a more noise optimal solution. As already discussed in the methodology chapter, the settings of the optimization algorithm have been chosen through a small iterative study. By changing one setting while keeping the other settings constant, a group of settings have been composed that is a best fit for this optimization problem.

The separation feasibility model checks the feasibility of a flight distribution with respect to the flight schedule and imposes a delay to mitigate any separation problems. The behaviour of the constraints of this model are checked one-by-one with the help of a small dummy flight distribution and flight schedule. In this way the expected behaviour can be monitored in a confined area. If no feasible solution can be found a large delay is added to all flights that propagates from earlier flights. This behaviour is also seen in the results of Test Case 2, where category C of the solution set even shows a solution with a total delay of 55702 seconds and almost all flights of the test case flight schedule receive a delay.

The test cases are also used to verify the working principle of the entire framework. It has been shown in the previous chapter that the framework can alter between fuel-efficient and noise optimal runways, routes and procedures in order to find a good balance between those two.

5.1.2 Validation

In the validation process an evaluation is performed to check how the model relates to actual data, in order to tell if the results are realistic or not. Two parts are considered in this subsection: the values for the fuel usage and the values that form the noise contours.

A database has been assembled that consists of all different departure runway, departure route and flight procedure combinations for each of the five aircraft type. The modelling of these combinations has been explained in detail in the methodology chapter. To fly from the runway towards the terminal point of the flight a procedure is followed that indicates the altitude profile of the flight. At several points along this flight path the thrust setting and flight path angle change in order to reach the desired final altitude. By making use of the thrust setting, flight path setting and the length of the flight trajectory the total required fuel for that flight is calculated. For each of the five aircraft type these numbers have been compared with fuel flow reference data of aircraft that performed a departure. In this way it is validated that the numbers found are realistic.

For the noise metrics it is harder to validate the numbers. Comparing the results of the optimization with the reference solutions, it can be seen from Test Case 1 that the amount of grid-coordinates are within comparable range to each other. Furthermore the number of people that are heavily annoyed or disturbed while sleeping are also comparable. However, this comparison is made with respect to the reference solutions which are also modelled using the same method. Another way of validating the noise metrics is to compare them with the real prognosis and maximum amount of the equivalence noise criteria presented in Table 2.7. The flight schedule that is considered is composed out of 599 departures, which is slightly lower but almost similar with the average number of departures at Amsterdam Airport Schiphol. However, since in the proposed framework only departures are considered, the noise equivalence criteria should be multiplied by a factor in order to compare them equally. Given the slightly lower amount of departures than average in the reference flight schedule, and the fact that arrivals tend to cause less noise annoyance compared to departures, for this comparison it is safe to say that the found numbers should be around half of the numbers in the regulations. In this way it is said that the noise metrics are valid.

5.2 Case Study Results

In this section the results of the case studies will be discussed that were presented in the previous chapter. The focus will be on the the final case study that encompasses a full day at Schiphol. The section is composed just like the previous chapter. First the reference solution and initial population will be discussed, followed by the fuel and noise optimization. Subsequent the feasibility of the flight distributions is discussed and the section is ended with a conclusion.

5.2.1 Reference Solution and Initial Population

In order to compare the results of the optimization, a reference is required and for this two reference solutions are calculated. The main reference that is used in the model is the fuel burn and noise annoyance based on radar data. The radar tracks of the flights in the flight schedule are used as ground tracks, and by making use of departure procedure NADP2 the flights are modelled in 3D. Subsequent the total required fuel and noise annoyance is calculated. This reference is uses as the main reference solution as the radar tracks form the real flight paths that were flown on October 22th, 2010.

The second reference solution is based on the modelled flight paths. From the radar data it is known what runways were used and which direction the aircraft were heading to. Based on this information the flights were assigned one of the modelled Standard Instrument Departure routes. Comparing the values of these two reference solutions as presented in Table 4.4, shows that they perform almost equal in terms of fuel usage but the noise annoyance lie a little apart from each other. In reality flights are vectored through the airspace by ATC rather that they are forced to follow the SID in a strict manner. The reason for this is mainly to mitigate separation issues and to differentiate the traffic in the air. The flights that are based on radar data are almost equal in length compared to the modelled SIDs, which explains that the fuel use of both reference solutions is more or less equal. Vectoring results in a wide spread of flights over the entire area, and therefore less flights fly over the same region, which explains the lower noise annoyance levels for the reference solution based on radar data.

The initial population is composed out of the minimum fuel and minimum noise annoyance solutions. Comparing both, it can be seen that the possible gain in noise annoyance is a lot larger than the possible gain in fuel usage. It is also clear that both objectives are adverse: a gain in one of the objectives has a negative effect on the other objective. Relating the initial population to the reference solutions, it can be seen that the numbers of the fuel usage of the reference solutions falls midway in between the initial population. This also holds for the noise annoyance values based on the L_{DEN} contour. Looking at the values for the L_{night} contour, almost no gain can be made compared to the reference solutions. This can be explained by the fact that departures at night time are very much restricted and are therefore already operated in a noise optimal sense.

5.2.2 Fuel and Noise

With the reference solutions and initial populations available, the optimization process has been initiated. After 500 generations of evaluation, the final results have been presented in Figure 4.15 for the entire population of 100. The figure features a vertical part above the radar data based reference solution, and a diagonal part from that point downwards. From the figure it can be obtained that only little to no gain can be made in the fuel objective, which would only cost up to 13% loss with respect to the noise objective. A wide range of solutions form a diagonal strip from the reference solution towards a point that presents a possible gain in the noise objective of 31%, only at a cost of 4% more fuel usage. Altogether there is a lot of potential in terms of noise annoyance, while few benefit can be obtained from less fuel usage. The main explanation that can be given to this fact is that flights already operate the shortest and thus most fuel efficient

routes, and that changing to another route will only benefit for a small discrete amount of fuel. Differentiating the flights spreads the noise annoyance whereby several grid-coordinates will fall in a lower noise level range, resulting in less noise annoyance.

The second objective of the optimization model consists of a composition of the four noise equivalence criteria, and although the objective value itself says something about the gains in noise annoyance, an additional elaboration has been presented in Figure 4.16. As already noticed in the previous subsection, not much gains can be made regarding the L_{night} contours. This is also reflected in the figure where the plots that include L_{night} show an almost horizontal behaviour. Only on the left side of both plots a variation is visible, which relates to the vertical part in the Pareto front discussed in the previous paragraph. An interesting thing is noticeable on the plots for the L_{DEN}. Although both of them show an ongoing change throughout the different solutions, the amount of people heavily annoyed show a gain for the entire solution set while the amount of houses affected both present a loss and a gain. That same plot shows a horizontal part from solution 20 up to population 50, while the plot for the people heavily annoyed shows a downward pattern. This can be explained by the fact that houses within the contour only count above $L_{DEN} \geq 58dB(A)$, while the count of people heavily annoyed already starts from $L_{DEN} \geq 48dB(A)$. For the range of populations from 20 to 50, no difference is being made in the inner contour while there are still gains in the area between the inner and outer contours.

A further analysis of the noise contours has been performed. In order to make the results more tactile, the noise contours have been grouped in several noise level ranges. These ranges are subsequently plotted against the number of grid coordinates affected by these noise levels and also the number of people annoyed and disturbed. Comparing the two reference solutions with the entire set of optimal solutions, several interesting facts can be noticed. First of all, the model disperses the noise in such a manner that noise is higher at grid-coordinates that fall outside the threshold noise levels of $L_{DEN} \geq 48dB(A)$ and $L_{night} \geq 40dB(A)$. Noise levels below these will not be considered in any of the noise equivalence criteria, which means that this is a way the model tends to lower the noise annoyance. On the other side of the spectrum, the noise annoyance in the higher noise level ranges tends to increase a little. At these grid-coordinates the noise is concentrated even more than it already was for the reference solutions. This can probably be explained due to the fact that out of the four noise equivalence criteria, only two have a direct relation to the noise level itself (the people heavily annoyed and people sleep disturbed). The other two criteria just count the number of houses within a certain contour. As few people live in the direct vicinity of the runways, the model tends to shift noise to these locations, resulting at a high noise load. The tendency of the model in terms of the noise contours is what is expected from it. The two tools the framework has to lower the amount of noise annoyance, is flying routes that are optimal noise-wise and try to disperse flights in such a way that the entire noise stays as low as possible. All of this by keeping the fuel consumption low. The noise is only considered inside the noise equivalence criteria threshold levels, and the model tries to keep this contour as small as possible.

The analysis of the runways, routes and procedures showed that shifting flights towards runway 24 and by using NADP2, the noise annoyance is lowered. This is something that would be expected, as runway 24 is one of the main runways of Schiphol and is mainly used that frequently because of the noise-friendly nature of this runway. Internationally NADP2 is known for alleviating noise, which is reflected by the model. The framework is also able to make a distinction between the different aircraft type and the different waypoints. Heavy aircraft generally fly shorter routes and

the routes and procedures to the different terminal points show the circumvention of noise sensitive areas.

5.2.3 Separation Feasibility

The optimization algorithm presented a wide range of solutions of which each have a specific noise and fuel objective value. Although much gain can be obtained in specifically the noise objective, it is not yet known if the flights can be fitted in the flight schedule. A separation feasibility check has been set up in order to find if the solutions are feasible or not.

In Table 4.5 an overview of the imposed delay for the entire set of 100 solutions was presented. 66 Flights require not a single delay and the flights can be fitted such that no separation issues are present. 12 Flights however require an average total delay of 3345 seconds, which is almost 56 minutes. The flights have been categorized according to their required delay, and those three categories are color coded in Figure 4.15. What is noticed is that the categories are nicely grouped and are related to their objective values. This can be explained due to the fact that the solutions that score best at the noise objective tend to direct all flights over the same noise optimal routes, where few people live. As these flights are lined up directly after one another, too little time separation is available at the departure and arrival at the waypoint. This was also reflected in the analysis of the allocation of runways, routes and procedures. The more noise optimal solutions shift all the flights towards runway 24, that cannot handle the entire flight schedule on its own.

This effect can also be seen in the analysis of the imposed delay. It has been investigated where the delay that is imposed originates from: the departure runway, a crossing point or the terminal point. For the second delay category not very much delay is required and almost all of this delay is required at the time of departure. This in comparison to the third delay category, which not only requires a delay at the time of departure but also at the arrival of the terminal point. Furthermore, much of the imposed delay originates from earlier delay and is therefore propagated over the schedule.

5.2.4 Conclusion

In this section the results from the optimization framework were discussed. The results that were found show the desired behaviour and show good potential. As has been discussed, a lot of gain can be obtained in the noise objective compared to the fuel objective. Noise optimal solutions tend to show worse behaviour in terms of the separation requirements, resulting in the fact that not all noise optimal solutions are feasible. However the solutions that are proven to be feasible still show a large possibility to alleviate noise annoyance.

Chapter 6

Conclusions and Recommendations

This research is based on the growing conflicts between the rise in demand of air travel and the annoyance these flights entail to the residents around the airports. Previous research focused on individual objectives like the optimization of the ground track of flight paths or the sequencing of departures for example. The operational effectiveness of these researches became less relevant because all the operational procedures are interconnected. This research will therefore focus on the connection between these procedures. In this study a framework is proposed that integrally optimizes the allocation of runways, departure routes and procedures. This framework was proposed in extension of the research question:

What are the benefits of using a combinatorial optimization of airport and airspace operations in terms of noise annoyance, fuel usage and capacity?

The proposed integrated optimization framework consists of two steps. In the first step, the Non-Dominated Sorting Genetic Algorithm II (NSGA-II) is applied. The advantages of this algorithm are the integration of multiple objectives and the non-linearity that is used for the calculations. In this step a possible allocation of runways, departure routes and flight procedures over the departures in a schedule is given an objective value. The genetic process of the algorithm alters this allocation over subsequent generations in order to find a better objective value. In this application of the algorithm two different contradicting objectives are used: fuel usage and noise annoyance. In the last generation of the optimization a set of solutions is presented that are all found to be optimal with respect to these two objectives. The second step of the framework processes the solutions found in the first step. An Integer Linear Programming (ILP) algorithm is used to check if the different distributions of runways, routes and procedures are feasible with respect to the separation requirements. The ILP allocates a take-off delay to specific flights if these otherwise would violate separation constraints with other aircraft. The delay can be used to mitigate possible separation conflicts at the take-off runway, a crossing point of flight paths and at the arrival at one of the terminal points. Flights with a delay above a certain threshold value are regarded as infeasible. These infeasible solutions will reduce the size of the solution set, but are unavoidable yet acceptable

outliers given the applied modelling approach that consists of two steps.

A case study has been performed to prove that the concept of the integrated optimization works. For this case study a day of operation at Amsterdam Airport Schiphol was used as a benchmark, and the results of this study show promising results. A set of solutions was presented with a trade-off between the fuel usage and a metric for the noise annoyance. It has been shown that the reference solution, that consists of the flight distribution that was actually used on the day of the reference schedule, is located on the Pareto front and can therefore be considered as one of the optimal solutions. An improvement in the usage of fuel seem unlikely, as this would cost a significant downturn of the noise metric. A lot of the presented solutions show a reduction in the noise annoyance, even up to a significant reduction of 31%. This decrease comes only at a cost of almost 4% extra fuel required to fly the routes and procedures of that particular solution.

The benefit of using the framework in terms of fuel usage is that the integrated allocation of runways, departure routes and procedures shows that a shift in any of these not necessarily leads to a significant change in fuel usage. The difference between the fuel-optimal and fuel-worst solution is only 4%, and although all reduction in fuel usage would be beneficial, such a small variety shows airlines, airports, residents and other stakeholders that changing operational procedures will have little influence on fuel usage and thus costs and emissions. Using the framework is beneficial in terms of noise annoyance as it leverages the potential of aircraft specific capabilities by allocating the right runway, route and procedure to each flight in such a way that an optimum noise contour is formed. Large gains can be obtained, mostly for the number of people highly annoyed and sleep disturbed. As these noise equivalence criteria are directly related to the well-being of residents around the airport and their opinion of the operations of the airport, this can only be considered as beneficial.

The second step of the framework, consisting of the separation feasibility model, proved that a large part of the solutions can be considered to be feasible, with not a single delay required. A small amount of solutions require little delay, however 12 solutions require an average delay of 56 minutes, and can therefore be considered infeasible. The three categories of imposed delay are nicely grouped with respect to their objective values, and the infeasible solutions all lay on the noise optimal side of the Pareto front. Still, the remaining solutions present a great possible improvement in terms of noise annoyance in exchange for a small increase in fuel usage. By accepting a little extra noise annoyance, extreme delays can be overcome through shifting a couple flights to other runways.

The integrated optimization framework presents a flight distribution, and the feasibility of this distribution is checked in terms of the separation requirements. The benefit of using this framework capacity wise is that it shows all possible distributions and their feasibility. It is shown that a lot of distributions are feasible and that by utilizing the two different runways a lot of capacity is available. With this capacity it is possible to change the allocation of certain procedures, which can ultimately lead to a significant reduction of noise annoyance. In other words, the available capacity is deployed to alleviate noise annoyance.

With the use of the proposed integrated optimization framework, authorities such as the ATC are presented a tool that gives them the flexibility to distribute flights over different runways, departure routes and flight procedures in order to find a balance between the use of fuel by the aircraft and the noise annoyance of residents implied by these operations. The presented distributions gives

room to choose for a solution that scores higher in one of the two objectives at the cost of the other. Capacity is also included as a measure to check if the separation requirements are met. If these requirements are violated a delay is imposed which would indicate a downturn in capacity.

6.1 Limitations

The presented research has several limitations which are discussed in this section. These limitations also form a starting point for the recommendations for future research.

The departure routes that are used in this research are modelled according to the prescribed Standard Instrument Departure chart. This means these flights are modelled up to an altitude of 6000 ft as above this altitude a clearance of ATC is required. In reality this clearance is given frequently, and therefore flights do not have to fly at such a low altitude for a long period of time. Flying at such altitudes results in extra noise annoyance.

In this research only departures are included and a case study has been performed that makes use of two different runways. This is a limitation since the results that originate from this research are only valid for this specific runway combination which does not even take the arrivals into account. As Amsterdam Airport Schiphol is very much dependant on the direction of the wind, the runways that are used throughout the year and even on a single day changes regularly. In this research only the areas towards the south of the airport are investigated, while the houses and inhabitants in the north and east also have to deal with the noise annoyance. Including arrivals and altering runway usage would present a more holistic view of the situation and usability in a practical setting of this research.

6.2 Recommendations

During the time of this research several choices were made in order to bound the subject. In this section several suggestions are presented that can be used for further improvements of the proposed integrated optimization framework. These suggestions can also be used for future research on this topic.

In the proposed framework the current Standard Instrument Departures at Amsterdam Airport Schiphol are included. These are modelled according to the prescribed charts, which results in a conservative flight path that is only allowed to fly up to 6000ft. It would benefit the method and the results if new routes were introduced, in order to have a broader set of route options to choose from. In line with the possibility of new routes, the addition of new flight procedures would contribute to the usability of the framework. Not only gives this room to utilize the capabilities of each aircraft type even more, this also introduces the possibility to directly couple the ground track of a trajectory with the flight procedure to circumvent certain inhabited areas. A third point that could be introduced is the incorporation of the capability to vector the departures in a diverging manner. The procedure to vector a flight is used frequently by ATC, and also the reference solution

of this research was based on vectored flights. Although the incorporation of vectoring would look a lot like the incorporation of new routes, this would give the opportunity to deviate from strictly determined routes in order to adhere the separation requirements and spread the noise even better.

This research proposed an optimization process that consists of two steps. In the second step the results of the first step were checked in order to know if these solutions were feasible in terms of separation requirements. A delay would be imposed so that flights would satisfy the necessary mutual distances. In an early stage of the framework this check was included as one of the objectives of the first step, but it was found that this method did not satisfy the desired optimization time and quality. Including a feasibility check would improve the solution quality.

Looking at the operations around an airport, departures cause the most noise annoyance and consume the most fuel relative to arrivals. This research therefore only focused on departures as the largest gains could be made with these. In order to provide a more complete solution set and a more complete picture for the user, including arrivals seem a good addition to the framework. Furthermore the addition of arrivals would give room for less strict departure procedures as in this case it would be known if a flight can continue its climb towards their desired en-route altitude.

From a practical side towards the implementation of the optimization framework, a different use of the variables and constraints might have resulted in faster results and also much more manageable data. Considering the limited time for this research the use of continuous variables was chosen and held on to, however the use of predefined integer arrays for the route and procedure selection might give the opportunity to remove some constraints, lower the amount of decision variables and manage the data more clear.

Bibliography

C. Borst. Avionics - lecture 13. University Lecture AE4-393, 2014. Delft University of Technology.

CBS. Hoeveel passagiers reizen via nederlandse luchthavens? `https://www.cbs.nl/nl-nl/faq/luchtvaart/hoeveel-passagiers-reizen-via-nederlandse-luchthavens-`, 2018.

K. Deb and J. Sundar. Reference point based multi-objective optimization using evolutionary algorithms. In *Proceedings of the 8th annual conference on Genetic and evolutionary computation*, pages 635–642. ACM, 2006.

K. Deb, A. Pratap, S. Agarwal, and T. Meyarivan. A fast and elitist multiobjective genetic algorithm: Nsga-ii. *IEEE transactions on evolutionary computation*, 6(2):182–197, 2002.

Eurocontrol. Recat-eu. `http://www.eurocontrol.int/sites/default/files/content/documents/sesar/recat-eu-released-september-2015.pdf`, 2015.

S. Hartjes. Inmtm v3 noise calculation tool specification. Technical report, TU Delft, 2010.

S. Hartjes and H. Visser. Efficient trajectory parameterization for environmental optimization of departure flight paths using a genetic algorithm. *Proceedings of the Institution of Mechanical Engineers, Part G: Journal of Aerospace Engineering*, 231(6):1115–1123, 2017.

V. Ho-Huu, S. Hartjes, H. G. Visser, and R. Curran. An efficient application of the moea/d algorithm for designing noise abatement departure trajectories. *Aerospace*, 4(4):54, 2017.

ICAO. Icao doc 8168 appendix to chapter 3. Technical report, International Civil Aviation Organization, 2006.

ICAO. Icao - aircraft noise. `https://www.icao.int/environmental-protection/Pages/noise.aspx`, 2018.

A. D. Y. C. P. B. H. t. H. J.A.J. van Engelen, R. de Jong. Evaluatie schipholbeleid, trends milieueffecten schiphol. Technical report, NLR, 2006.

Kadaster. Rijksdriehoeksstelsel. `https://zakelijk.kadaster.nl/rijksdriehoeksstelsel`, 2019.

S. Lin. Ngpm – a nsga-ii program in matlab v1.4. `https://nl.mathworks.com/matlabcentral/fileexchange/31166-ngpm-a-nsga-ii-program-in-matlab-v1-4`, 2011.

LVNL. Integrated aeronautical information package, June 2018. URL http://www.ais-netherlands.nl/aim/2018-06-07-AIRAC/html/index-en-GB.html.

LVNL. Separation of aircraft. https://en.lvnl.nl/safety/achieving-safety/separation-of-aircraft, 2019.

K. B. Marais, T. G. Reynolds, P. Uday, D. Muller, J. Lovegren, J.-M. Dumont, and R. J. Hansman. Evaluation of potential near-term operational changes to mitigate environmental impacts of aviation. *Proceedings of the Institution of Mechanical Engineers, Part G: Journal of Aerospace Engineering*, 227(8):1277–1299, 2013.

Schiphol. Gebruiksprognose amsterdam airport schiphol 2015. Technical report, Schiphol Group, 2014.

B. A. Schiphol. Banenstelsel. https://www.bezoekbas.nl/, 2019.

Worldbank. Air transport, passengers carried. https://data.worldbank.org/indicator/IS.AIR.PSGR, 2017.

D. S. Zachary, J. Gervais, and U. Leopold. Multi-impact optimization to reduce aviation noise and emissions. *Transportation Research Part D: Transport and Environment*, 15(2):82–93, 2010.

D. S. Zachary, J. Gervais, U. Leopold, G. Schutz, V. S. T. Huck, and C. Braun. Strategic planning of aircraft movements with a three-cost objective. *Journal of Aircraft*, 48(1):256–264, 2011.

Appendix A

Aerodrome Charts

The aerodrome charts indicating the Standard Instrument Departures of Amsterdam Airport can be found on the next four pages. The first chart presents an overview of the departure routes of all runways, while the other three indicate the routes for runway 24 (Kaagbaan) and runway 18L (Aalsmeerbaan) in detail.

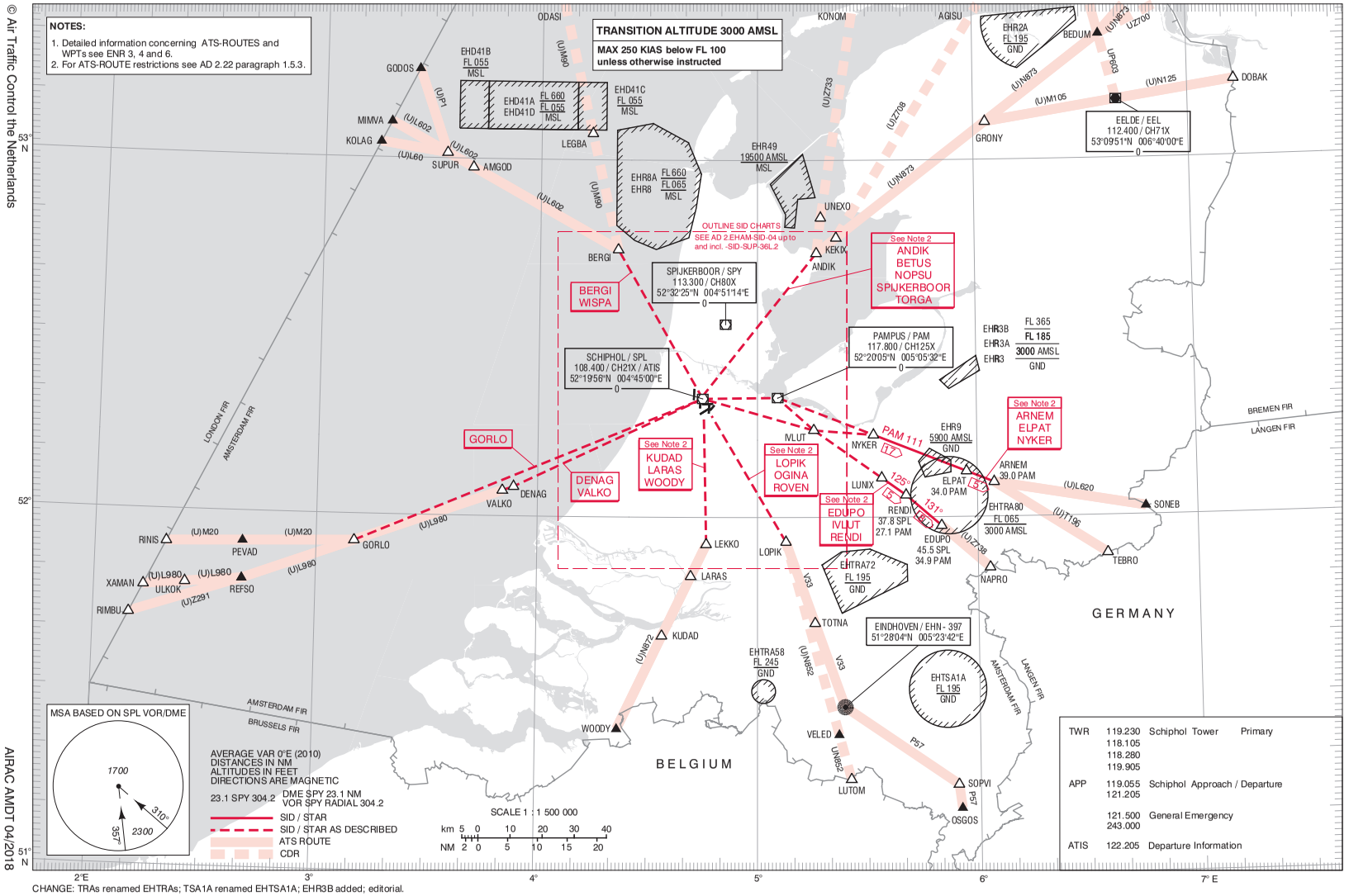

CHANGE: TRAs renamed EHTRAs; TSA1A renamed EHTSA1A; EHR3B added; editorial.

Figure A.1: Overview of SIDs of Amsterdam Airport Schiphol (LVNL [2018])

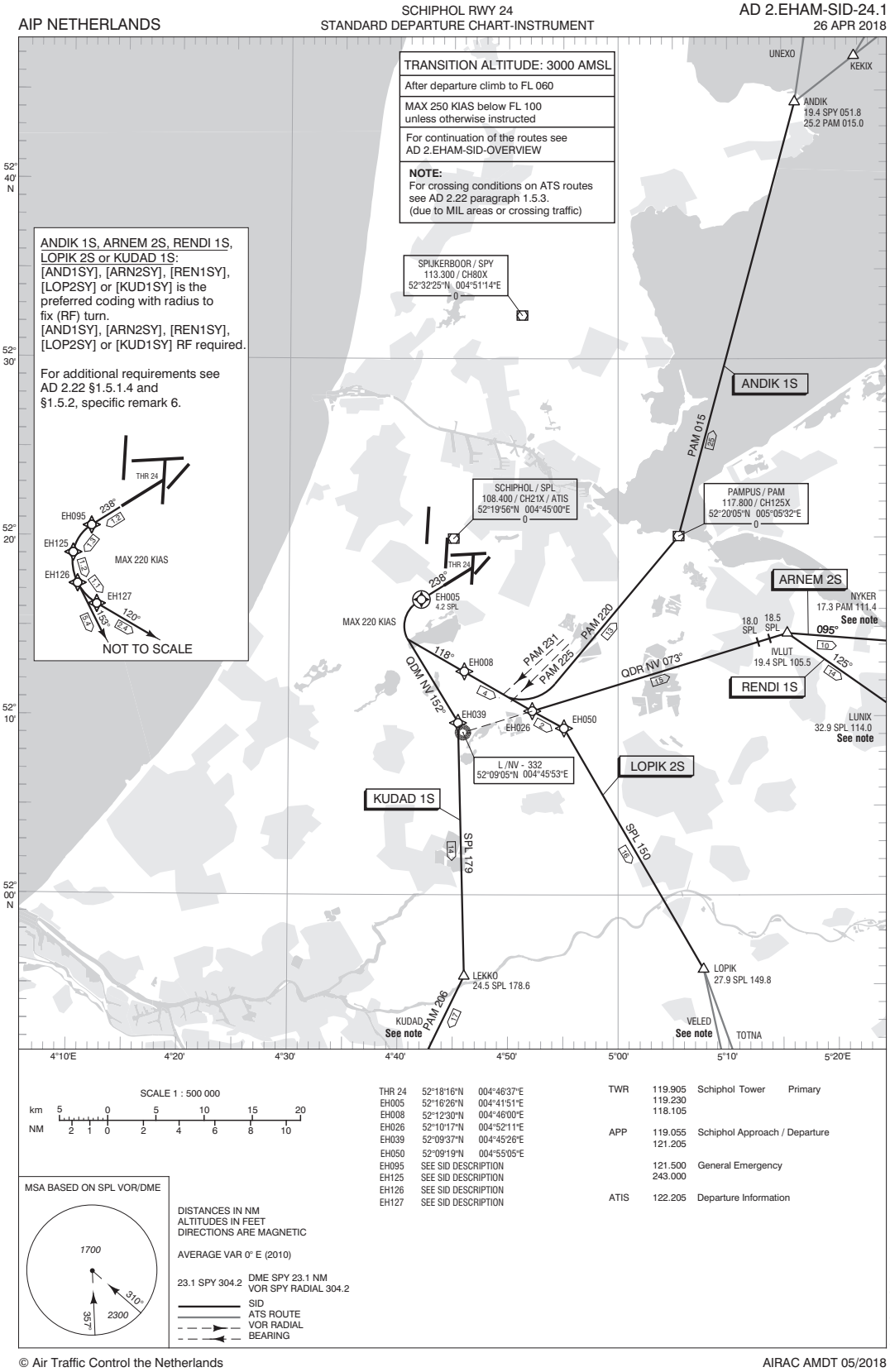

Figure A.2: Standard Instrument Departure chart RWY 24 of Amsterdam Airport Schiphol - Part 1 (LVNL [2018])

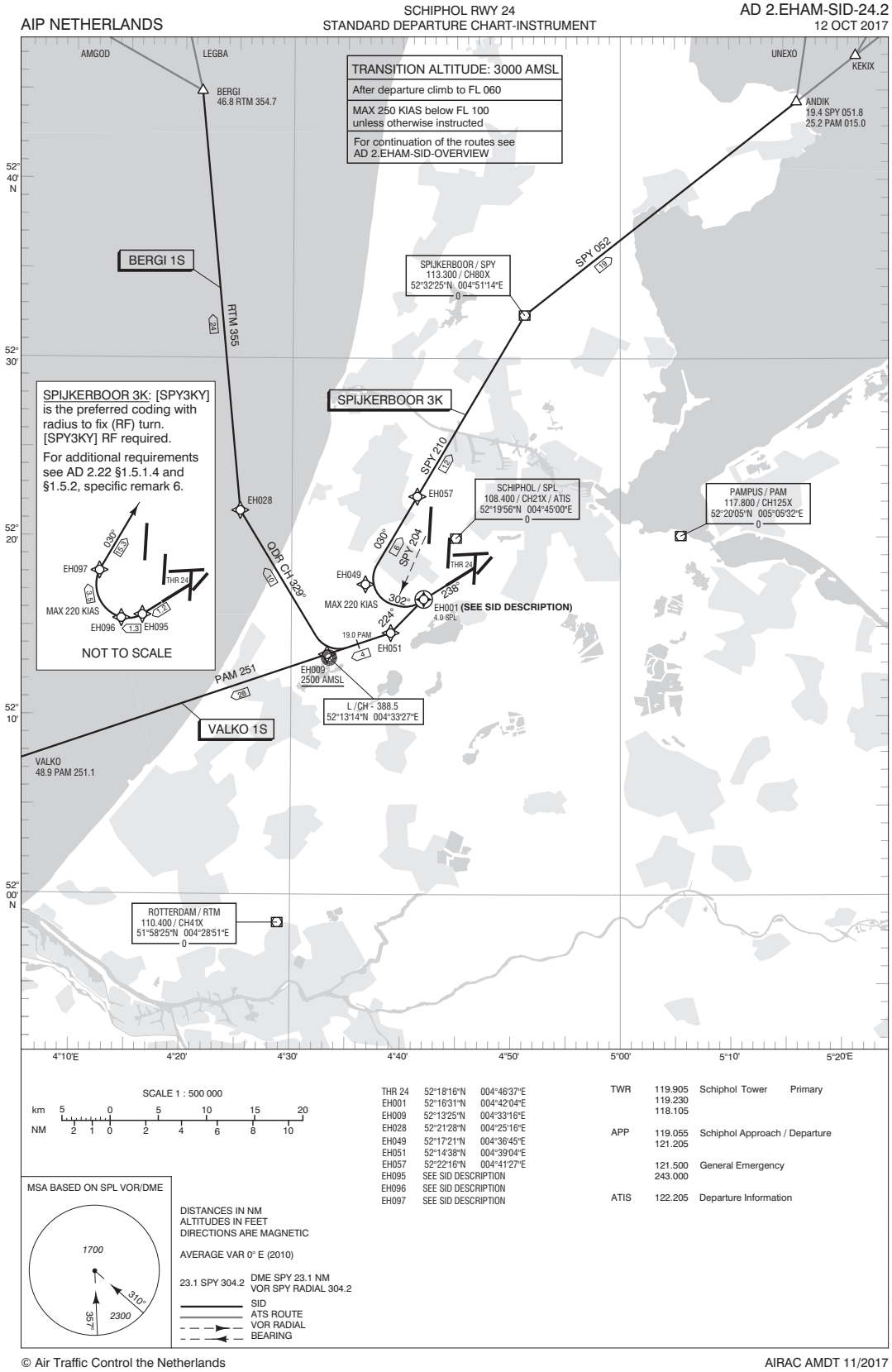

Figure A.3: Standard Instrument Departure chart RWY 24 of Amsterdam Airport Schiphol - Part 2 (LVNL [2018])

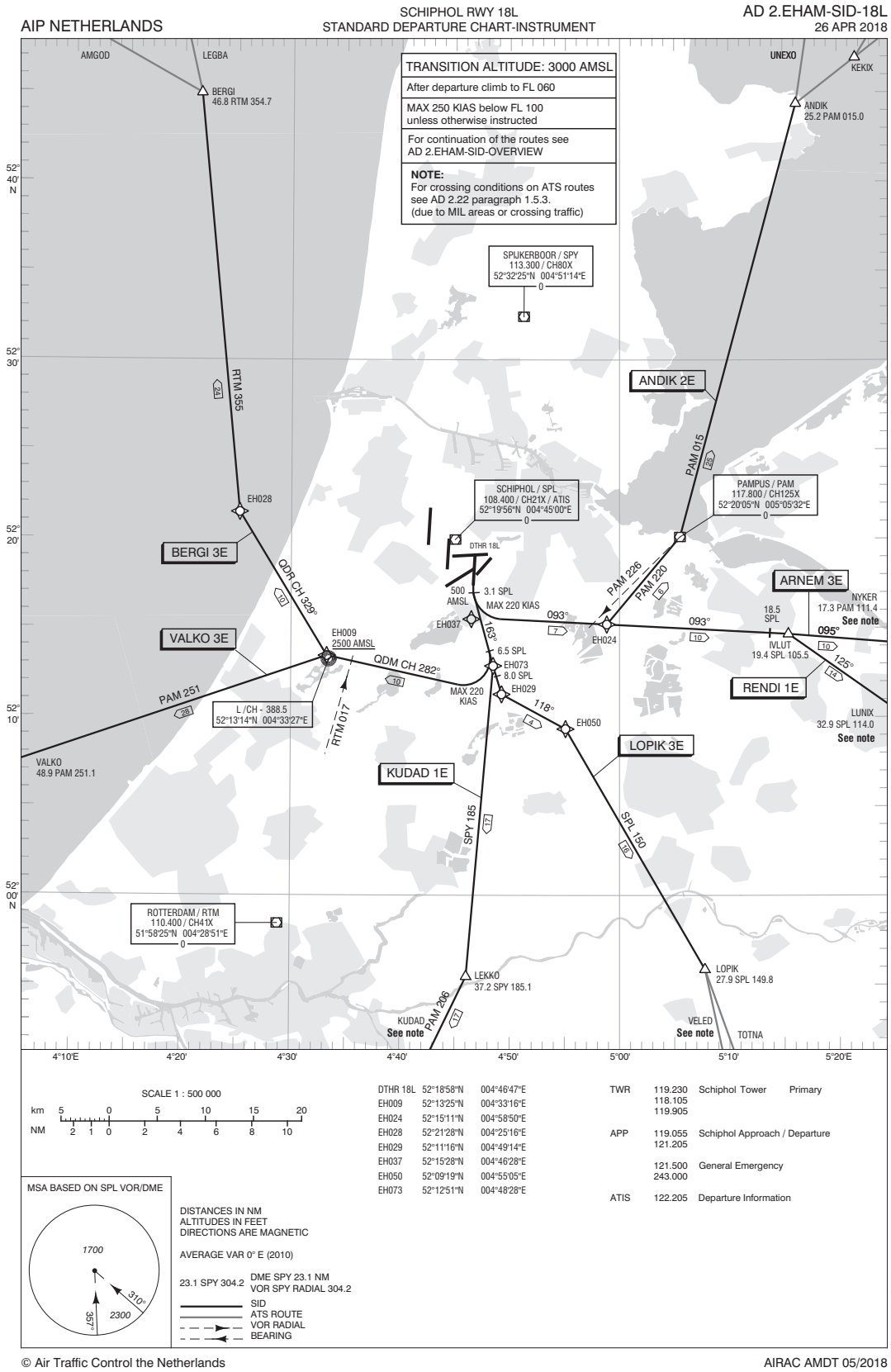

Figure A.4: Standard Instrument Departure chart RWY 18L of Amsterdam Airport Schiphol (LVNL [2018])

Appendix B

Reference Flight Schedule

Table B.1: Reference Flight Schedule (day/evening/night)

SID	**F100**	**B738**	**B763**	**B773**	**B744**
ANDIK 1S	2/0/6	6/1/3	0/0/0	0/0/0	2/1/0
SPIJKERBOOR 3K	19/4/0	19/3/0	0/0/0	1/1/0	0/1/0
ANDIK 2E	0/1/0	0/3/0	0/0/0	0/1/0	0/1/0
ARNEM 2S	2/0/3	12/1/7	2/1/0	3/0/1	7/0/2
ARNEM 3E	10/1/0	20/5/0	2/1/0	6/3/0	3/4/0
BERGI 1S	19/4/3	23/4/1	15/0/0	15/0/1	8/0/0
BERGI 3E	0/0/0	0/3/0	0/0/0	0/0/0	0/0/0
KUDAD 1S	8/0/1	27/0/23	0/0/0	0/0/0	0/0/0
KUDAD 1E	18/3/0	23/8/0	1/0/0	2/0/0	0/0/0
LOPIK 2S	1/0/1	3/0/1	0/0/0	0/0/0	2/0/0
LOPIK 3E	3/1/0	6/2/0	0/0/0	0/0/0	0/0/0
RENDI 1S	13/0/4	24/0/14	0/1/0	2/0/0	1/0/0
RENDI 1E	16/6/0	28/4/0	2/2/0	1/1/0	0/0/0
VALKO 1S	21/3/4	31/3/4	4/1/1	3/0/0	2/0/0
VALKO 3E	0/0/0	0/2/0	0/0/0	0/0/0	0/0/0

Appendix C

Optimization Solutions

In this appendix the different generations of the optimization processes are presented. The two test cases and the case study are presented consecutively.

C.1 Test Case 1: A single waypoint

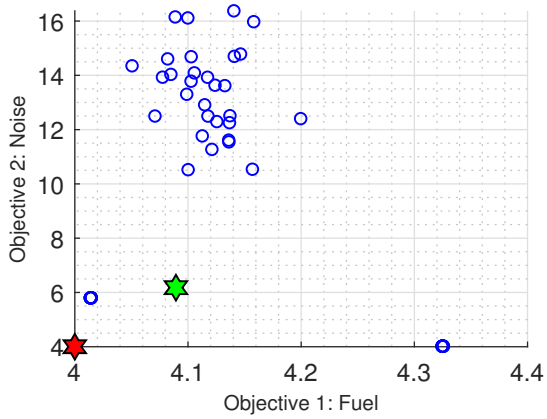

Figure C.1: Generation 1/250

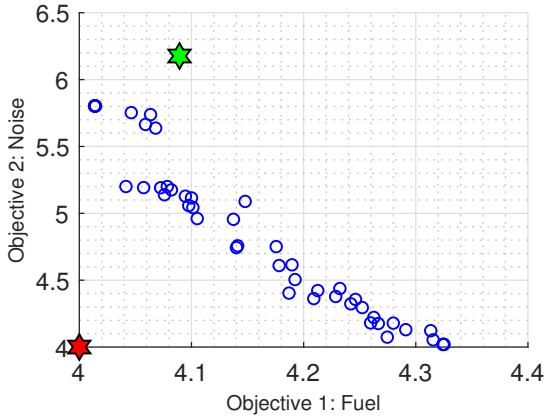

Figure C.2: Generation 50/250

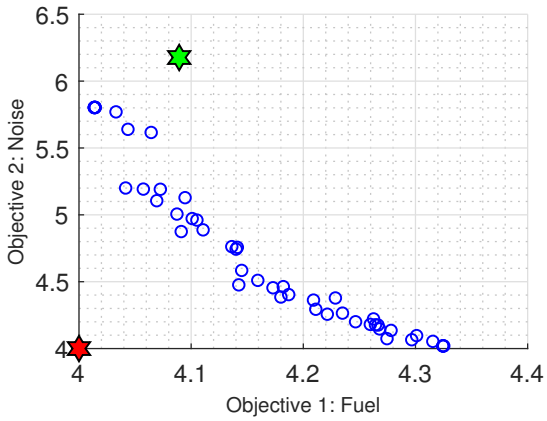

Figure C.3: Generation 100/250

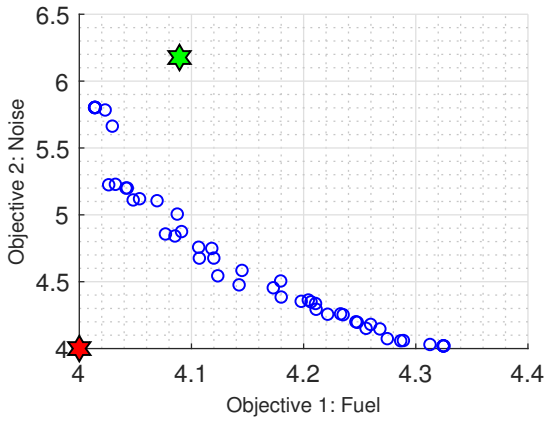

Figure C.4: Generation 150/250

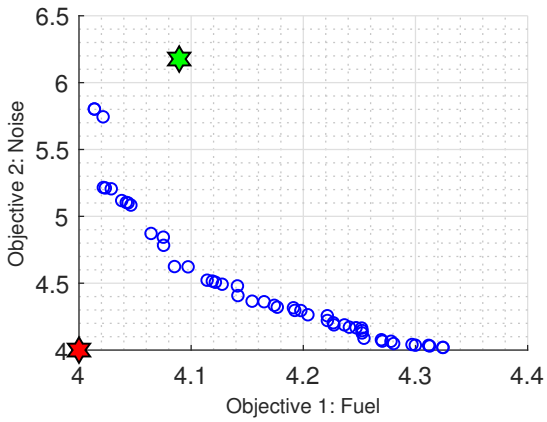

Figure C.5: Generation 200/250

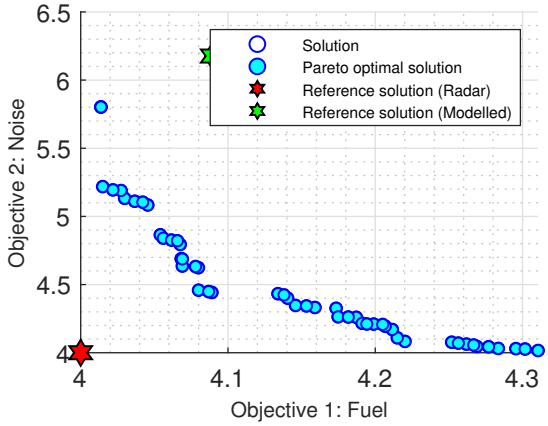

Figure C.6: Generation 250/250

C.2 Test Case 2: A single bank

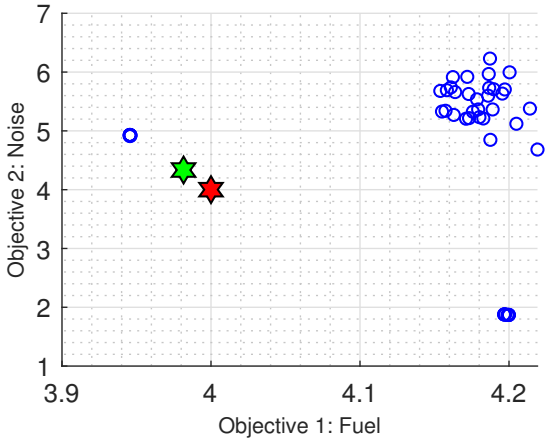

Figure C.7: Generation 1/250

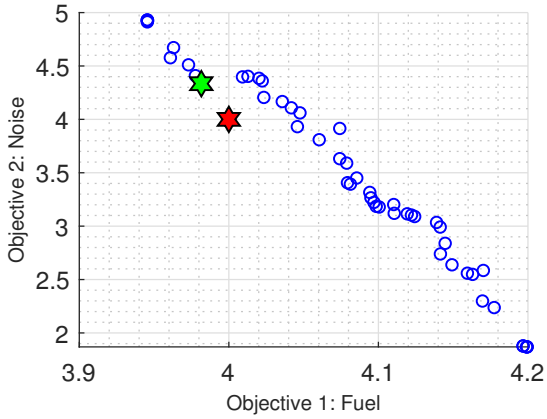

Figure C.8: Generation 50/250

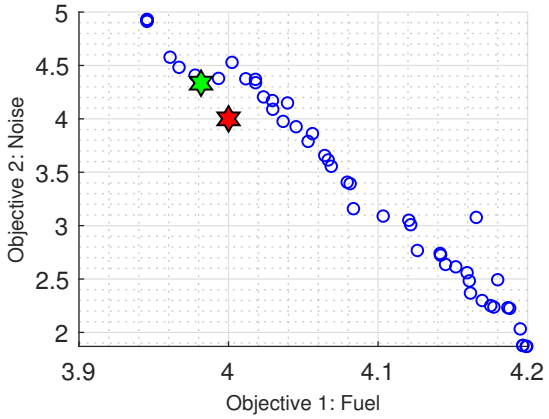

Figure C.9: Generation 100/250

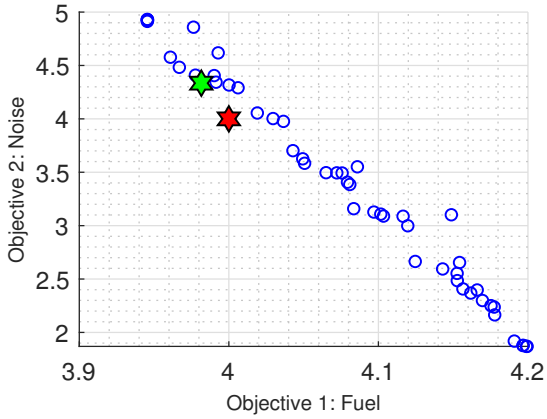

Figure C.10: Generation 150/250

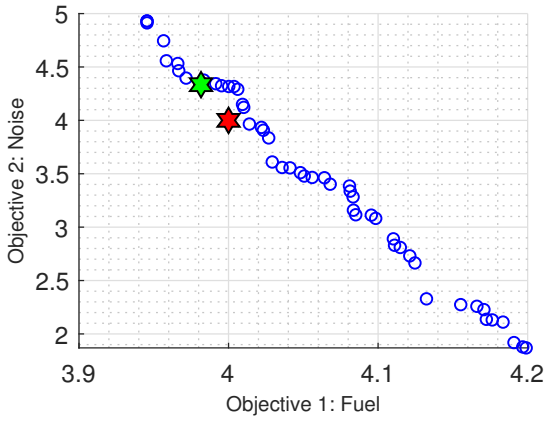

Figure C.11: Generation 200/250

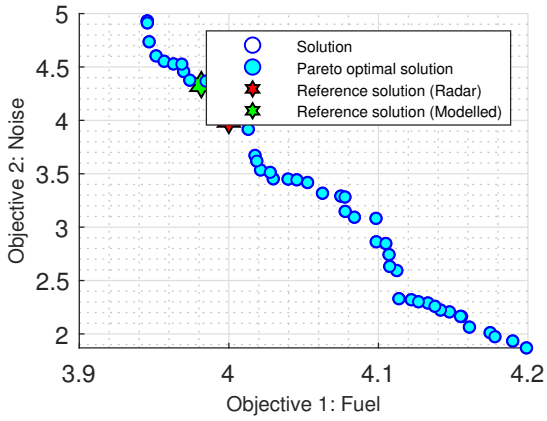

Figure C.12: Generation 250/250

C.3 Case Study: A full day at Schiphol

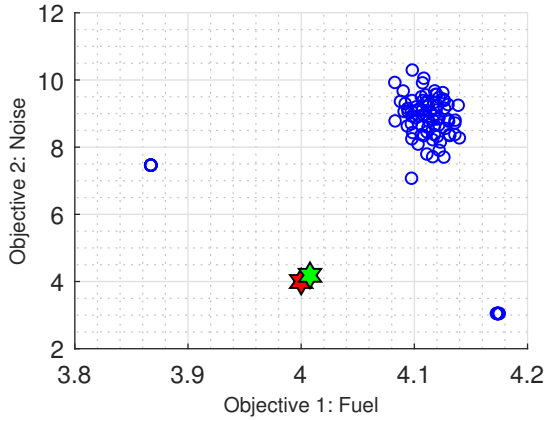

Figure C.13: Generation 1/500

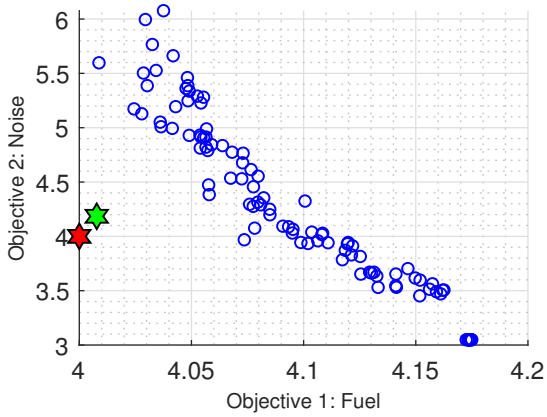

Figure C.14: Generation 100/500

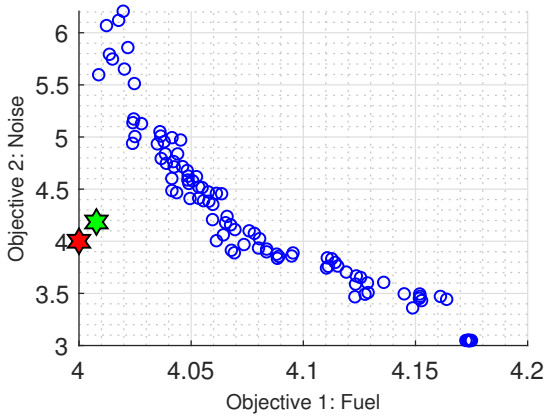

Figure C.15: Generation 200/500

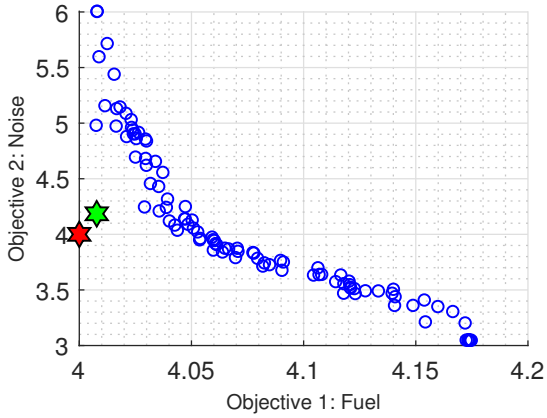

Figure C.16: Generation 300/500

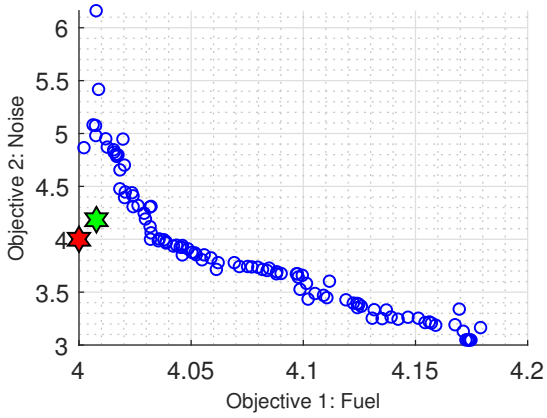

Figure C.17: Generation 400/500

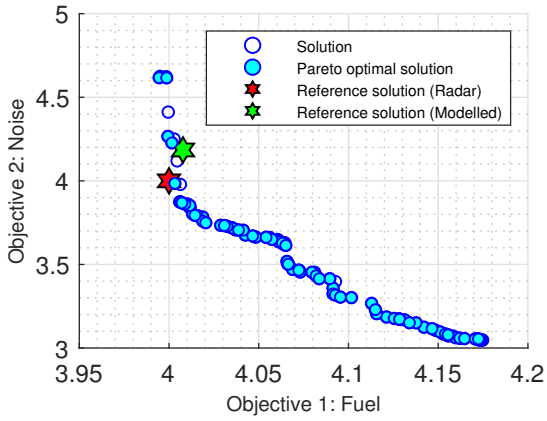

Figure C.18: Generation 500/500